THE EFFECTS OF FROST ACTION ON A PREVIOUSLY UNFROZEN TYPICAL WINNIPEG CLAY

A Thesis

Presented to

The Faculty of Graduate Studies and Research

The University of Manitoba

in Partial Fulfillment

of the Requirements for the Degree of

Master of Science in Civil Engineering

by

Fethullah Aysan

ABSTRACT

Equipment was designed and fabricated, and instrumentation provided, to determine the engineering properties (stress-strain-time relation and relaxation) of Lake Agassiz clays which had not been subjected to natural, annual freezing and thawing cycles because of their depth below the ground surface. During this investigation, the soil specimens were frozen to predetermined constant temperatures, either uniaxially or from all directions, and then tested. External water (over and above natural soil moisture) was provided for some test conditions. The reduction in strength caused by one freezing and thawing cycle of remolded and undisturbed clay samples was also investigated. Of special interest was the study of heaving phenomena caused by the supply of external water during the freezing process.

ACKNOWLEDGEMENTS

The author wishes to thank Professor A. Baracos (Dept. of Civil Engineering, University of Manitoba), Professor M. Mindess (Soil Testing of Minnesota Inc., Bloomington, Minnesota, U.S.A.), Professor A. K. Y. Loh (Dept. of Civil Engineering, University of Manitoba) and Professor G.A. Russell (Dept. of Geological Engineering, University of Manitoba) for guidance and advice regarding the research work and for a review of the manuscript.

The author is also indebted to Professor A. J. Carlson, Assistant Dean, Faculty of Engineering, for his encouragement.

Funds for the study were available from the National Research Council of Canada.

TABLE OF CONTENTS

	Page
ABSTRACT	ii
ACKNOWLEDGEMENTS	iii
LIST OF FIGURES	vi
LIST OF PHOTOGRAPHS	ix
LIST OF TABLES	xi
LIST OF SYMBOLS	xii
CHAPTER I - INTRODUCTION, PURPOSE AND SCOPE	1
CHAPTER II - DESIGN AND FABRICATION OF EQUIPMENT AND INSTRUMENTATION	3
2.1 Design of equipment	3
2.2 The function of equipment	3
2.3 Features of the equipment	4
2.4 Detailed description of test equipment	8
CHAPTER III - GEOTECHNICAL PROPERTIES AND TYPE OF MATERIALS USED	21
CHAPTER IV - SAMPLE PREPARATION	29
CHAPTER V - LITERATURE REVIEW	35
Part 1 Frost action	35
A. Heaving of frozen soils due to redistribution of moisture and ice segregation in frozen soils	35
B. Shrinkage of clays caused by ice segregation	37
C. Penetration of freezing plane	37

Page

D. Thickness of ice lenses 39

E. Frost susceptibility 39

F. Volumetric expansion and contraction of frozen soils 44

Part 2 Stress-strain-time relation and stress release of frozen soils 47

CHAPTER VI - OBSERVATION OF TESTS AND EXPERIMENTAL TEST RESULTS AND DISCUSSION 68

Part I Data and results of freezing process 68

Part II Data and test results of stress-strain-time and strength behavior 87

CHAPTER VII - CONCLUSIONS 136

BIBLIOGRAPHY 140

LIST OF FIGURES

Figures		Page
2.1	Freezing cell	5
2.2	Heat exchange chamber	6
2.3	Proposed freezing cell	7
2.4	Diagram of loading frame	18
3.1	Location where the sample soil blocks were obtained	22
3.2	Approximate boundaries of the Red River Valley plain	23
3.3	Grain size distribution graph of soil sample	28
4.1	Detail of external water supply strips	33
5.1	Frost susceptibility chart of Nielsen and Rauschenberger	41
5.2	Frost susceptibility determination chart	42
5.3	Schematic creep curve of frozen soil	52
5.4	Instantaneous deformation	61
5.5	Retarded deformation	61
5.6	Irreversible deformation	62
5.7	Burger's body: Combination of three basic mechanical models	62
5.8	Stress relaxation	63
5.9	Relaxation time curve	63
5.10	Unfrozen water content during freezing of Winnipeg clay (after Williams)	65
5.11	Water film explanation of structural bond (according to Terzaghi)	67

Figures

		Page
6.1	Ice segregation caused by slow uniaxial freezing	71
6.2	Temperature-percent heaving-time relation of frozen soil samples	79
6.3	Temperature-percent heaving-time relation of frozen soil samples	80
6.4	Maximum shearing stress in terms of principal compressive stress	92
6.5	Strain-time relation of samples OC-N-27-114, 115, 116 at 27°F	100
6.6	Triaxial diagram of stress-time-strain of the samples in 6.5	101
6.7	Stress-time-strain relation of samples OC-N-27-128 A, B and C at 27°F	102
6.8	Triaxial diagram of stress-time-strain of the samples in 6.7	103
6.9	Strain-time relation of samples OC-N-17-124 A, B and C at 17°F	104
6.10	Triaxial diagram of stress-time-strain relation of samples in 6.9	105
6.11	Strain-time relation of samples OC-N-7-125 A, B and C at 7°F	106
6.12	Triaxial diagram of stress-time strain relations of samples in 6.11	107
6.13	Strain-time relations of samples OC-R-27-118, 121 and 123 at 27°F	108
6.14	Triaxial diagram of stress-time-strain relations of samples in 6.13	109
6.15	Young's Modulus of elasticity of frozen soil	112

Figures

		Page
6.17	Duration of strain at decelerating strain rate vs. temperature	114
6.18	Strain at decelerating strain rate vs. temperature	116
6.19	Strain-rate-temperature relations	123
6.20	Stress-time and strain-time relations for sample OM-N-27-126 at 31.5°F	124
6.21	Unconfined compressive strength of thawed soil samples following one cycle of all directional freezing and unconfined compressive strength of non-frozen, undisturbed or remolded soil samples	125
6.22	Stress-strain relation for given time of samples OC-N-27-114, 115 and 116 at 27°F. No external water supply	126
6.23	Stress-strain relation for given time of samples OC-N-27-128 A, B and C at 27°F. No external water supply	127
6.24	Stress-strain relation for given time of samples OC-N-17-124 A, B and C at 17°F	128
6.25	Stress-strain relation for given time of samples OC-N-7-125 A, B and C at 7°F	129
6.26	Strain-stress relation for given time of samples OC-R-27-118, 121 and 123 at 27°F with external water supply	130
6.27	Strain-stress time and stress release relation of sample OM-N-27-127 at 27°F	131
6.28	Stress release-time relation of sample OM-N-17-131 at 17°F	132
6.29	Rigid zone buildup by all around freezing	134

LIST OF PHOTOGRAPHS

Photographs		Page
2.1	Components of freezing cell	10
2.2	Sample assembly of soil sample	10
2.3	Installation of flexible insulation and loading piston	10
2.4	Insulation hood	10
2.5	Heave measurement of soil sample during freezing	11
2.6	Component of freezing cell	11
2.7	Loading frame for constant stress	11
2.8	Equipment and instrumentation for measurement of stress-strain	11
2.9	Heat exchange box	17
2.10	Complete set-up of freezing equipment	17
2.11	Complete set-up of freezing equipment	17
2.12	Detail of the loading frame for constant stress	20
2.13	Transducer	20
2.14	Sample assembly with provision of water by means of supply strips	20
2.15	Sample assembly for freezing in heat exchange box for heave measurement	20
4.1	Trimmed soil sample	33
4.2	Preparation of soil samples for freezing process	33
4.3	Placing a soil sample inside of the freezing cell	33
6.1	Horizontal ice segregation caused by slow uniaxial freezing	71
6.2	Uniform horizontal ice segregation due to rapid uniaxial freezing	71

Photographs

		Page
6.3&6.4	Cross-sectional view of polygonal patterns of vertical cracks	71
6.5&6.6	Ice segregation caused by external water supply	76
6.7	External water supply strips	76
6.8&6.9	Ice crystallization at the location of water supply zone and ice sheet buildup in the shrinkage cracks above water supply zone of sample OC-R-27-119	77
6.10	Failure plane of sample OC-N-27-126 at 31.5°F	118
6.11 & 6.12	Failure plane and vertical shrinkage cracks of sample OC-N-27-126 at 31.5°F ice buildup in the vertical shrinkage cracks of sample OC-N-27-126	118
6.13	Squeezing out of ice to the free surface due to application of cyclic stress to frozen soil specimen	122

LIST OF TABLES

		Page
5.1	Theoretical and practical classification of frost susceptibility according to Schaible	46
6.1	Heave vs. time of soil-sample OC-N-27-116	81
6.2	Heave vs. time of soil-sample OC-N-17-124	82
6.3	Heave vs. time of soil-sample OI-N-17-132	83
6.4	Heave vs. time of soil-sample OC-R-27-119	84
6.5	Heave vs. time of soil-sample OC-R-27-122	85
6.6	Experimental and computed frost heave results	86
6.7	Program No. I for testing sample	95
6.8	Program No. II for testing sample	96
6.9	Program No. III for testing sample	97
6.10	Program No. IV for testing sample	98
6.11	Young's Modulus, duration at decelerating strain rate and slope of constant strain-time	111
6.12	Relaxation time-released stress due to cyclic strain of sample OM-N-27-131	122

LIST OF SYMBOLS

A_o	initial area of cross-section of a sample
A_c	area of cross-section after application of stress at any time of deformation at any stage
E_o	Young's modulus of instantaneous deformation
E_1	Young's modulus of decelerating strain
E	Young's modulus of elasticity
F_o	no frost damage to the soil due to freezing temperature
F_1	light frost damage to the soil due to freezing temperature
F_m	sensitive frost damage to the soil due to freezing temperature
F_s	strongest frost damage to the soil due to freezing temperature
h_o	height of soil sample before application of stress
h	height of soil sample after application of stress at any time of deformation at any stage
G	Modulus of rigidity
h_h	frost heave
i_o	relative ice content of frozen soil in percent
ℓ	initial length of mechanical model
$\Delta\ell$	expansion of mechanical model
Q	volume of external water supply

t	time
T_T	transition time
T_r	retardation time
ω	water content in percent
ω_s	weight of dry soil
ω_u	unfrozen water content in frozen soil
γ_{12}	maximum elastic shearing strain
γ^o_{12}	rate of maximum viscous shearing strain
$\bar{\varepsilon}_1$, $\bar{\varepsilon}_2$, $\bar{\varepsilon}_3$	principal logarithmic strain
$\bar{\varepsilon}^o_1$, $\bar{\varepsilon}^o_2$, $\bar{\varepsilon}^o_3$	rate of principal logarithmic strain
ε_o	instantaneous strain
ε_1	creep strain at decelerating rate of strain
ε_2	creep strain at constant rate of strain
ε_x, ε_y, ε_z	compressive elastic strain
ε^o_x, ε^o_y, ε^o_z	rate of compressive viscous strain
η	coefficient of shearing viscosity
η_1	coefficient of shearing viscosity at decelerating rate of strain (Reversible Deformation under creep)
η_2	coefficient of shearing viscosity at constant rate of strain (Irreversible Deformation under creep)
μ	Poisson's ratio
$\tan \theta$	slope of strain vs time plot
Ψ	coefficient of compressive viscosity
Ψ_1	coefficient of compressive viscosity at decelerating rate of strain (Reversible Deformation under creep)

Ψ_2	coefficient of compressive viscosity for constant rate of strain (Irreversible deformation under creep)
σ_x, σ_y, σ_z	compressive principal stress
σ_o	constant stress
τ_{12}	maximum shearing stress

CHAPTER I

INTRODUCTION, PURPOSE AND SCOPE OF WORK

CHAPTER I

INTRODUCTION, PURPOSE, AND SCOPE

1.1 The investigation was carried out in the laboratory of the Department of Civil Engineering of the University of Manitoba. It is a development of qualitative tests begun in the Geological Engineering laboratories of the University of Manitoba.

1.2 One of the original objectives was to determine what happens to typical Glacial Lake Agassiz clays when frozen for the first time. Sealed Shelby tube samples were available. These samples had been stored at room temperature. The samples were obtained at a depth of 40 feet. The samples were trimmed and were frozen in rubber membranes surrounded by ethyl alcohol. Prior to freezing, the clay was extremely firm. Manual squeezing produced very little impression. When thawing had taken place, the previously frozen samples were soft, with the approximate consistency of butter when compressed between the fingers.

1.3 In conversations with the Materials and Research Division, Manitoba Department of Highways, this change in the physical properties of the clay was mentioned. The remark precipitated discussion of some subgrade fill failures that had taken place. The Highways Department had been considering whether excavated materials or cuts for subgrade should be "left for a winter". One subgrade had functioned well during the winter but with the spring thaw, had failed completely. The

following conjecture was suggested for discussion. Had the freezing and subsequent thawing altered the properties of the clay, and in what manner? Did freezing alter the structure of the clay? Did moisture in the clay become re-distributed?

1.4 It was decided that a quantitative engineering analysis was required. With the assistance of funds available from the National Research Council for study of the urban geology of Metropolitan Winnipeg, work was started to design and manufacture instruments to test and investigate the properties of freezing, frozen, and thawed soils in the laboratory in undisturbed or remolded conditions.

CHAPTER II

DESIGN AND FABRICATION OF EQUIPMENT AND INSTRUMENTATION

CHAPTER II

DESIGN AND FABRICATION OF EQUIPMENT AND INSTRUMENTATION

2.1 Design of equipment:

Equipment was designed and manufactured in the laboratory that would permit controlled freezing of soils, with or without water supplied to the sample. In addition, allowance had to be made for application and measurement of either constant or varied axial stress or strain.

2.2 The function of the equipment:

a) to provide uniaxial freezing or thawing of samples under controlled temperature.

b) to supply water under controlled head, when and where required, according to the type of test performed.

c) to permit control of the rate of freezing or thawing of the sample.

d) to apply constant or variable axial pressure to samples and measure sample deformation.

e) to apply a controlled rate of axial deformation and to measure the corresponding pressure. (A special case is the measurement of stress release when axial deformation is not allowed.)

f) to measure heaving

g) to measure adfreezing of soil to other materials inserted in the soil before or after freezing.

h) to permit repeated cycles of freezing and thawing under the above conditions.

i) to permit automatic or manual recording of temperatures at any desired location in the sample.

2.3 Features of the Equipment

A. Special features of the Freezing Cell (Fig. 2.1)

a) controlled uniaxial freezing from the bottom. This reduced vertical loads on sample and eliminated need for counterbalance. (initially designed to reduce the vertical load on samples) Counterbalancing could have been used to permit top freezing by direct contact of the samples with the heat exchange plates. Alternatively, the eliminating of direct contact with the heat exchange plates, but permitting atmospheric heat transfer, as in nature, inside the freezing cell could be used. (See Fig. 2.3)

b) the provision of cooling coils around bushing and upper plate to minimize possible heat flow to the sample for external sources.

c) ability to freeze individual samples (rather than using cold room). This also allows quick changes in temperature if so desired.

d) ability to handle samples up to 2.78 inches in diameter by 6.0 inches in length.

e) control of amounts of water to be supplied to the sample.

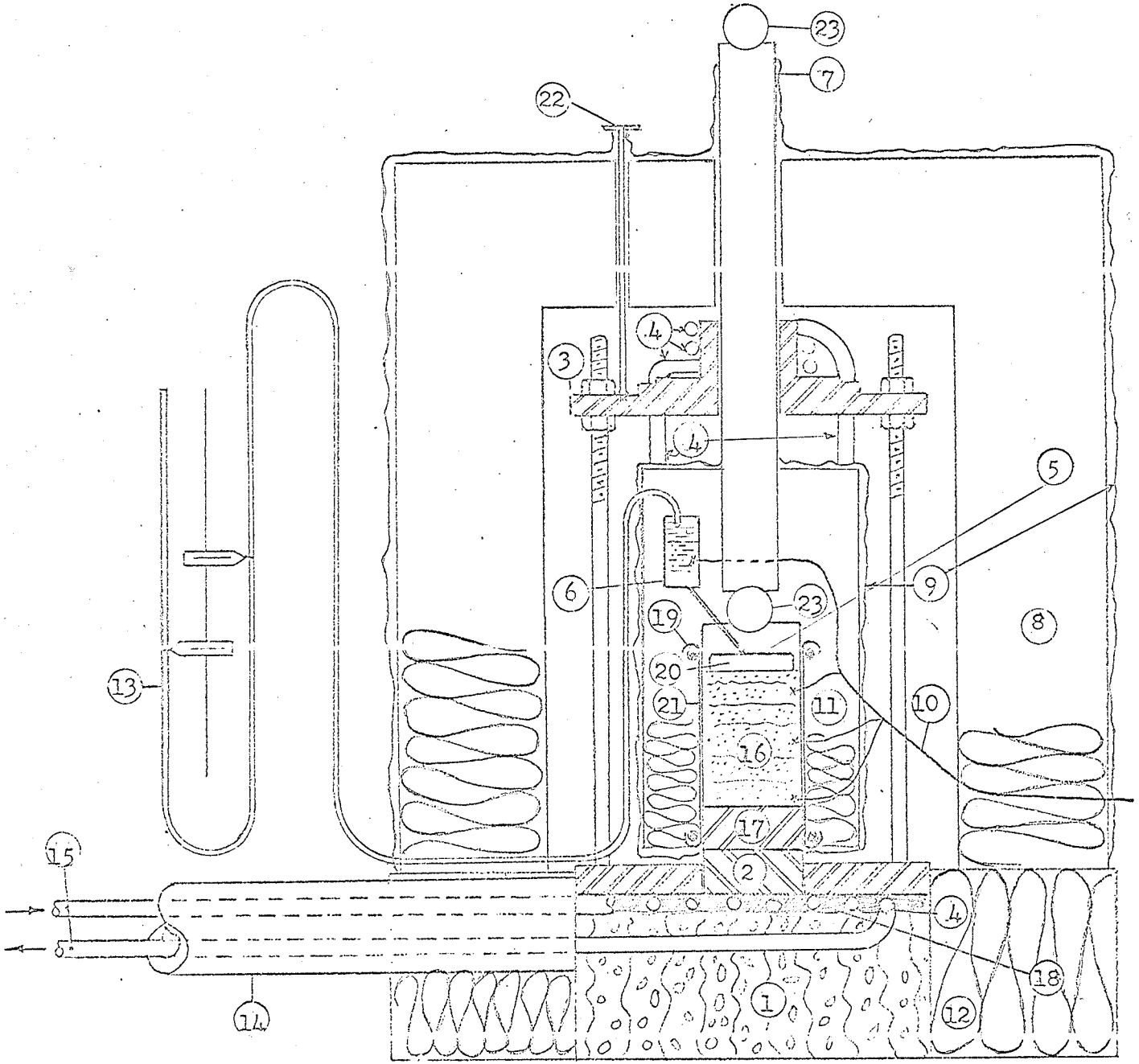

1. Base Plate
2. Heat Exchange Pedestal
3. Upper Plate
4. Cooling Coil
5. Loading Cap
6. Water Reservoir
7. Loading Piston
8. Insulation Hood
9. Vapor Barrier
10. Thermocouple
11. Flexible Insulator
12. Rigid Insulation
13. Manometer
14. Foam Rubber Insulation Conduit
15. Circulating Tube
16. Soil Sample
17. Freezing Plate
18. Zinc Plate
19. "O" Ring
20. Bauxilite Filter
21. Rubber Membrane
22. Strain Measurement Pin
23. Stainless Steel Ball

FIGURE 2.1 FREEZING CELL

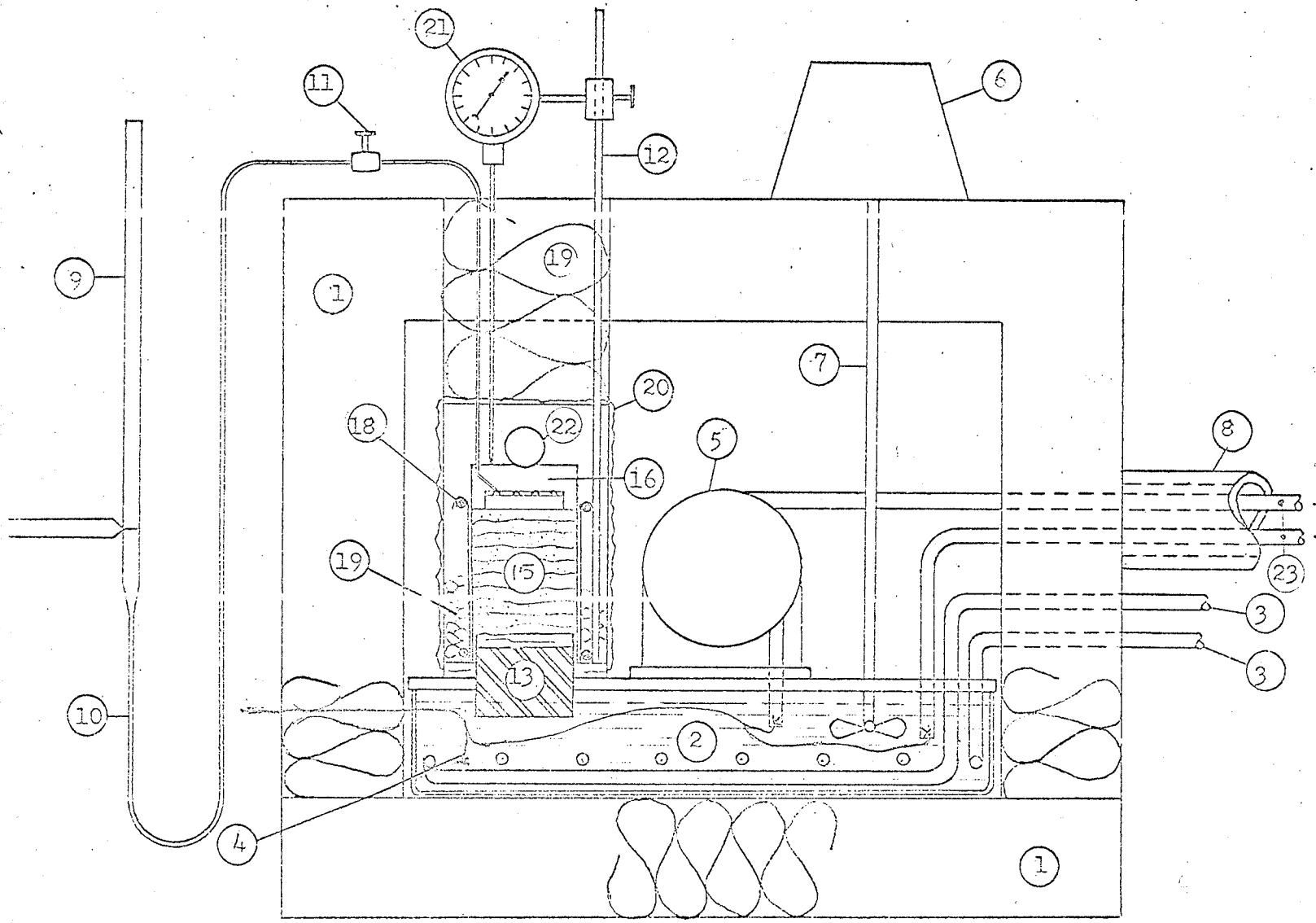

1. Insulation Box
2. Cooling Liquid
3. Copper Tube to Heat Exchange Unit
4. Thermostat
5. Circulating Pump
6. Agitator
7. Agitator Shaft
8. Foam Rubber Insulation Conduit
9. Burette
10. Nylon Tubing
11. Valve
12. Studd
13. Cooling Plate
14. Thermocouple
15. Soil Sample
16. Loading Cap complet with Bauxilite Filt
17. Rubber Membrane
18. "O" Ring
19. Flexible Insulation
20. Vapor Barrier
21. Dial Gauge
22. Stainless Steel Ball
23. Coolant Circulating Tube

FIGURE 2.2 - HEAT EXCHANGE CHAMBER

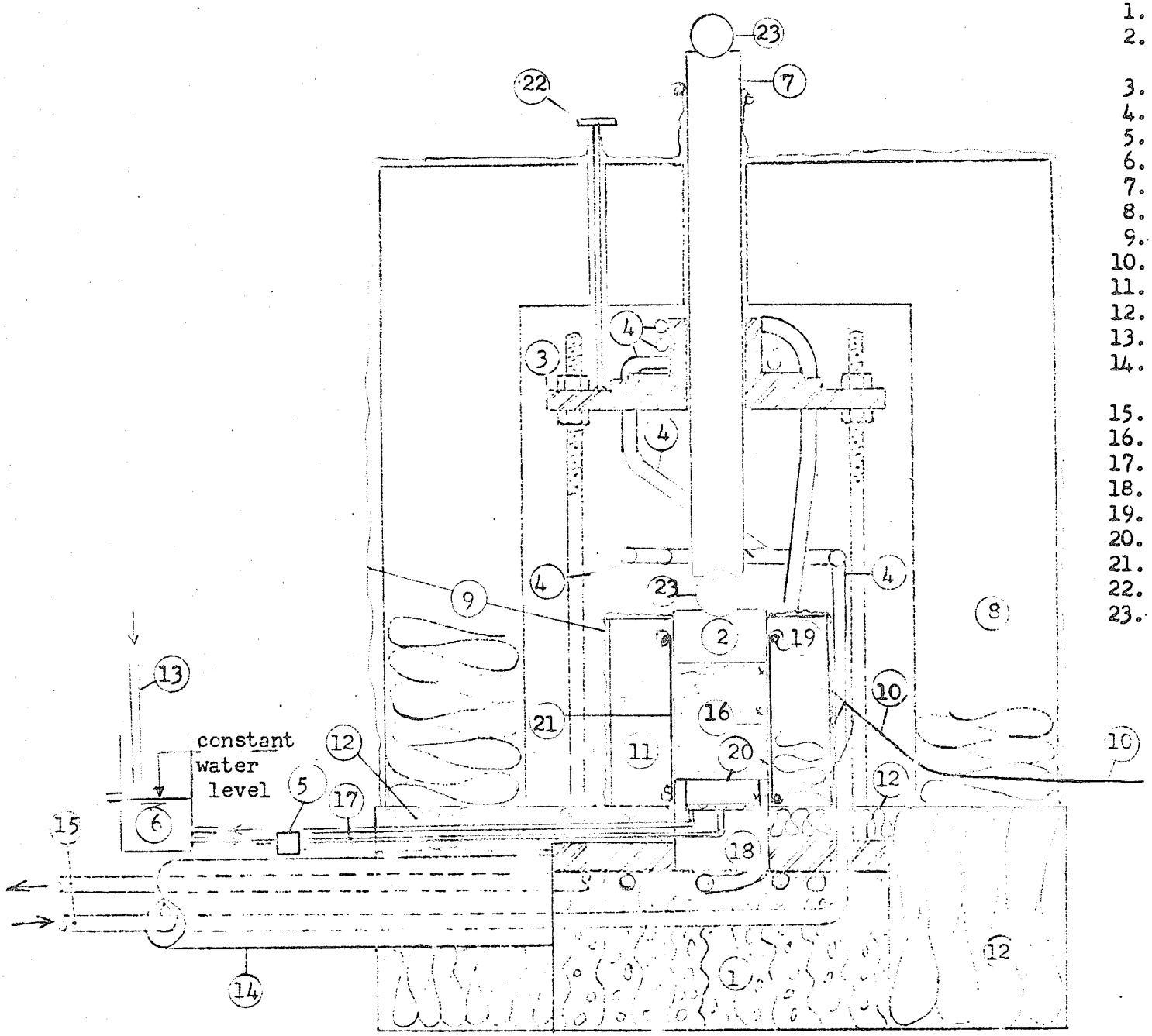

1. Base Plate
2. Aluminum Cooling Plate and Loading Cap
3. Upper Plate
4. Cooling Coil
5. Circulating Pump
6. Water Reservoir
7. Loading Piston
8. Insulation Hood
9. Vapor Barrier
10. Thermocouple
11. Flexible Insulator
12. Rigid Insulation
13. Water Supply
14. Foam Rubber Insulation Conduit
15. Coolant Circulating Tube
16. Soil Sample
17. Water Circulating Tube
18. Acrylic Pedestal
19. "O" Ring
20. Filter
21. Rubber Membrane
22. Strain Measurement Pin
23. Stainless Steel Ball

FIGURE 2.3 PROPOSED FREEZING CELL

B. Special features of heat exchange chamber (Fig. 22)

a) electric motor (¼ HP) used to drive a refrigeration compressor

b) refrigeration compressor reversible to cool or heat

c) this compressor was used to cool or heat a thermostatically controlled alcohol bath.

d) submersible pump of 18.75 gal./hr. capacity used to circulate either cooled or heated alcohol to freezing cell.

e) an agitator provided to keep bath at uniform temperature.

f) heat exchange chamber designed to permit up to 5 samples to be frozen in the bath itself.

2.4 Detailed description of test equipment

A. Freezing Cell

The freezing cell consists of the following components: (Fig. 2.1)

1) Base plate (see Photograph 2.1)
2) Heat exchange pedestal (see Photograph 3.1)
3) Upper plate (see Photograph 2.1)
4) Cooling coils (see Photograph 2.1)
5) Loading cap (see Photograph 2.2)
6) Water reservoir (see Figures 2.1 and 2.2)
7) Loading piston (see Photograph 2.3)
8) Insulation hood (see Photograph 2.4)
9) Vapor barrier (see Photograph 2.3, 2.5 and 2.15)

1) The base plate was cast together with the heat exchange pedestal. The base plate material used was perforated epoxy resin. The purpose of the perforation was to further reduce the low heat conductivity of the plate, while providing a rigid base.

2) The heat exchange pedestal was made of ½ inch thick by 7½ inch diameter steel plate containing a 1½ inch diameter copper cylinder (see Photograph 2.6). This cylinder was machined flush with the bottom face of the plate and projected ½ inch above the upper face to form the base on which the cooling plate of the sample rested. A ¼ inch I.D. copper coil was placed under the heat exchange plate. To provide a larger contact surface, a zinc plate was cast flush with the heat exchange coil which, in turn, was fastened to the plate (see Fig. 2.1).

3) The upper plate was fabricated of steel and contains a bronze bushing to guide the loading piston. Copper coils were placed around the bushing and horizontally over the upper plate. Three coils were placed vertically between the upper plate and the pedestal (see Photograph 2.1). This minimized possible heat flow to the sample from external sources. The upper plate was supported in its position by three 5/8 inch diameter studs which were welded to the pedestal.

4) All cooling coils were connected to the circulating pump of the heat exchange chamber with 3/8 inch I.D. nylon tubing which was placed within 2½ inch O.D. by 1 inch wall thickness Armstrong foam rubber insulation hose (see Photograph 2.7).

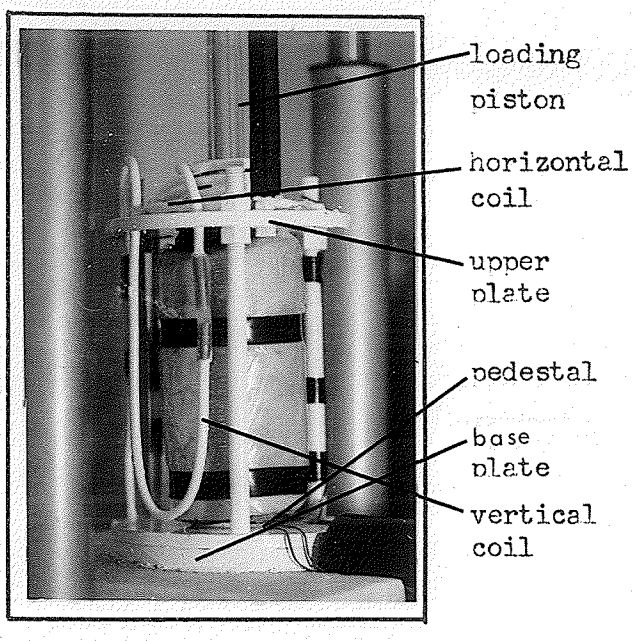

Photograph 2.1

Components of freezing cell

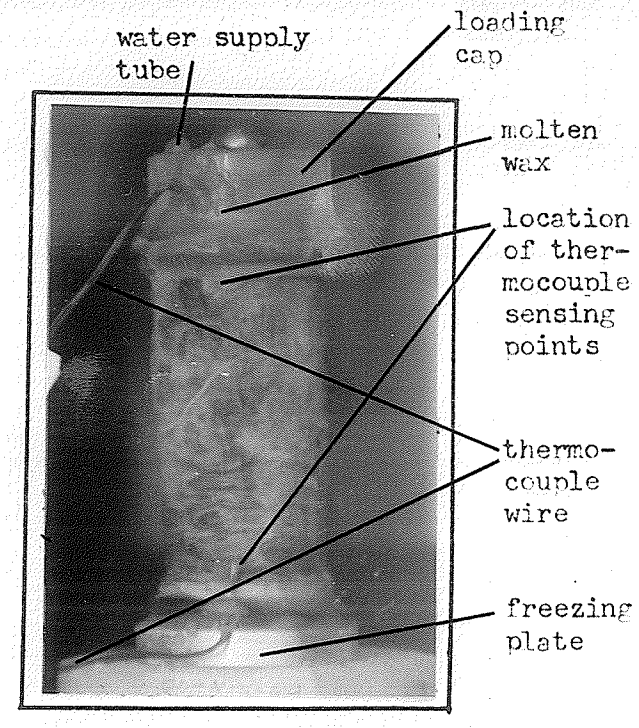

Photograph 2.2

Sample assembly for frozen soil sample taken out of flexible insulation

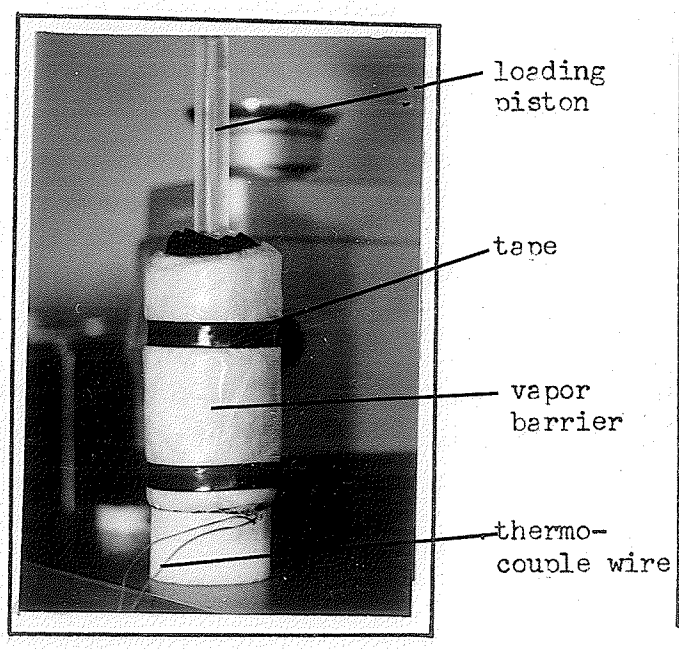

Photograph 2.3

Installation of flexible insulation and loading piston on prepared sample

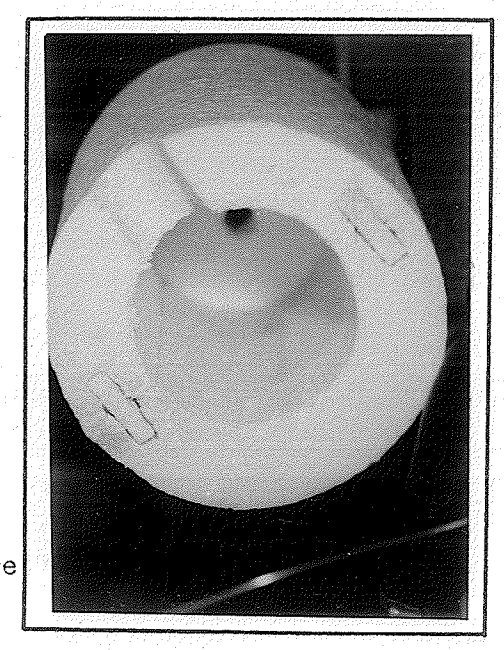

Photograph 2.4

Insulation hood

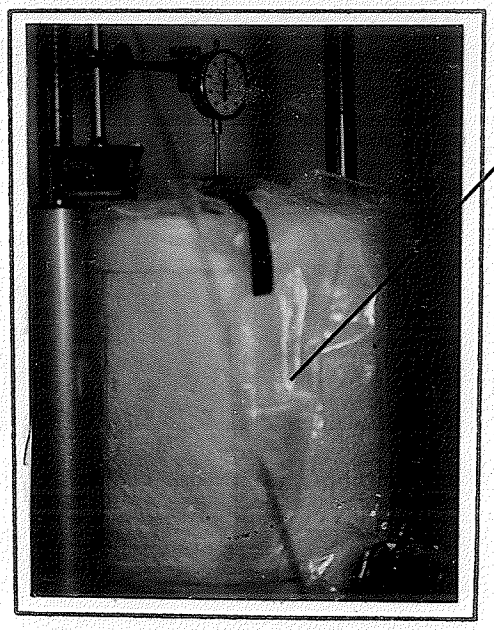

Photograph 2.5

Heave measurement of soil sample during freezing

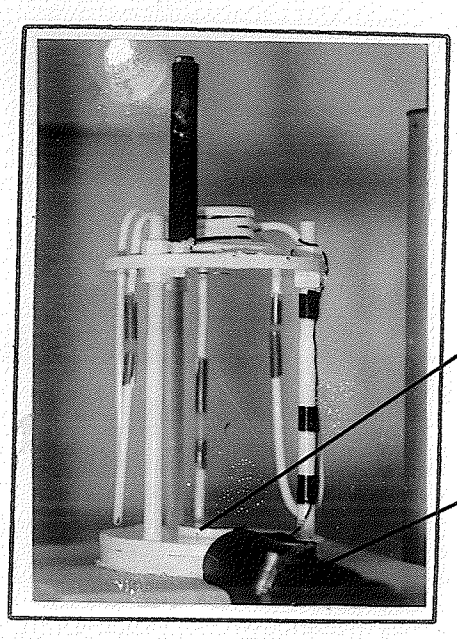

Photograph 2.6

Components of freezing cell

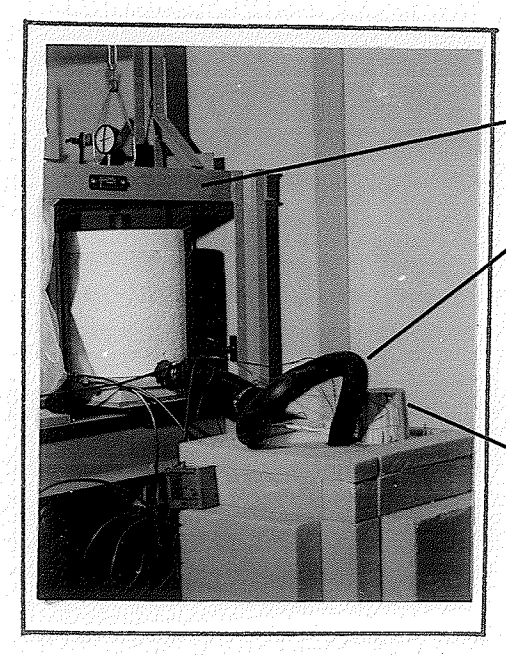

Photograph 2.7

Loading frame for application of constant stress to a soil sample in frozen condition

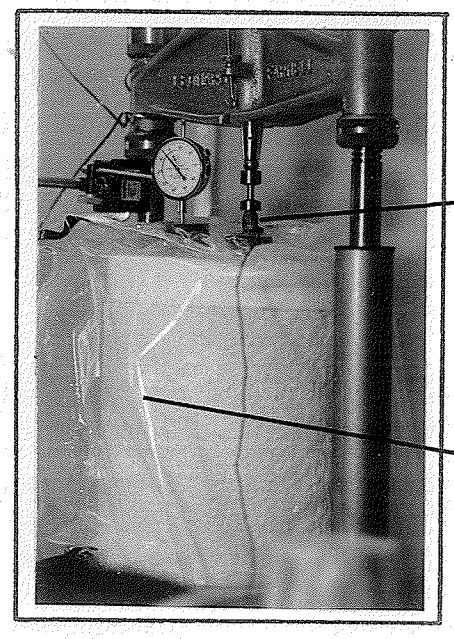

Photograph 2.8

Equipment and instrumentation for measurement of stress-strain-time relation or stress relaxation

5) The loading cap was made of low conductivity acrylic material containing a vitrified bauxilite filter. The filter faced the soil sample and connected with 1/8 inch diameter polyethelene tubing to the water supply reservoir. The upper surface of the cap was machined to hold a 1/2 inch diameter stainless-steel ball. The ball acted to transmit load from the piston which was similarly machined. This ensured that the load was applied axially to the sample during testing. A 1/16 inch spiral groove was machined on the face of the loading cap in contact with bauxilite filter to provide uniform moisture distribution to the filter and consequently to the soil sample.

6) Two kinds of water reservoir were used to supply water to the samples during freezing tests.

a) Water was supplied to the sample while the sample was in the heat exchange chamber,(see Figure 2.2) or,

b) Water was supplied to the sample while the sample was placed for freezing in the freezing cell (see Figure 2.1).

In the first instance,an external graduated burette was connected to the top cap of the sample through the upper insulation using 1/8 inch I.D. nylon tubing. A valve was provided to cut off the water supply to the sample. The water level in the burette could be adjusted to produce any desired head.

In the second instance a reservoir containing a predetermined quantity of water was directly connected to the top cap and was heavily insulated. The hydraulic head for experimentation

was produced by a manometer after the sample was placed in the freezing cell. A thermocouple sensing-junction was placed in the reservoir to determine the temperature of the liquid.

7) A 1 inch diameter acrylic rod was fabricated into a loading piston to apply pressure to the sample. This material was selected because of its low heat conductivity and high compressive strength (See Photograph 2.1 and 2.3).

8) The insulation hood was made of styrofoam 1 1/2 inch in thickness. This hood was placed above the rigid lateral insulation of the base plate to cover the freezing cell completely (see Photographs 2.4, 2.6 and 2.12). Two holes at the top allowed passage of the acrylic piston and of the pin connecting the upper plate for strain measurement (see Figure 2.1). A semi-circular hole was provided for exit of the insulated hose containing the alcohol circulating tubes (See Photographs 2.6 and 2.7).

9) Finally, a 2 mil plastic sheet was used to cover the cell to prevent atmospheric moisture from condensing and freezing around the cell components during cooling operations (see Photographs 2.5 and 2.8)

B. Heat-exchange Box

The heat exchange box consisted of the following components (see Fig. 2.2):

1) Insulation box

2) Cooling liquid (ethyl alcohol) reservoir

3) Heat transfer unit

4) Thermostats

5) Circulating pump

6) Agitator

1) The insulation box was made of 5 inch thick walls consisting of rigid styrofoam, to contain a 12 x 12 x 4 inch alcohol reservoir and circulating pump. The cover of the box was made of 8 inch thick styrofoam insulation with 3 1/2 inch diameter holes to permit concurrent freezing of five samples. These holes can be plugged with flexible insulation materials when not used (see Fig. 2.2 and Photograph 2.9).

2) The cooling liquid reservoir was made of plexiglass containing a spiral copper coil connected to the heat transfer unit refrigeration compressor. Five circular holes were provided in the cover of the reservoir. These permit dipping of the bottom face of the cooling plates of samples to be frozen in the heat exchange box. Other holes were cut to permit installation of the agitator shaft, thermocouple wires, inlet and outlet of the circulating pump, thermostats, and inlet and outlet of the heat exchange coil. A 1/2 inch diameter, flexible, transparent tube was connected from the outside of the box to the alcohol reservoir, allowing observation of the alcohol level. The tube also provided an auxiliary supply of alcohol to the reservoir without necessitating removal of the cover.

3) The heat transfer unit consisted of a 1/4 HP refrigeration compressor. A solenoid valve was used to reverse the compressor from cool to heat or heat to cool, keeping the thermostatically controlled alcohol reservoir within a temperature range of $-55^{o}F$ to $+50^{o}F$ (within $\pm 0.5^{o}F$ accuracy).

4) Two thermostats were installed in the alcohol reservoir and were connected to the circuit of the compressor motor. Only the first thermostat was engaged during freezing, to control the predetermined low temperature. The second thermostat was required simultaneously when the compressor was reversed to heat the alcohol reservoir. This thermostat was in control until the temperature of the alcohol returned to the level at which the first thermostat was re-engaged.

5) A submersible circulating pump of 18.75 gal. per hr. capacity was placed inside the insulation box. It provided circulation of cooled or heated alcohol to the freezing cell through 3/8 inch I.D. polyethylene tubing. At each intake and outlet of the circulating hose, a thermocouple was installed to measure the temperature differential of alcohol being circulated. This enabled calculation of the heat loss in the insulated box and freezing cell, and through the freezing process of the soil sample.

6) To provide a uniform temperature in the alcohol bath, a 1 1/2 inch diameter propeller, consisting of two vanes, was installed inside the alcohol reservoir. It was driven by an electric motor which was placed over the cover of the insulation box and connected

by a 1/8 inch diameter stainless steel shaft. Prior to installation of the agitator recorded temperature differentials were noted of $\pm 3^{o}F$ at different points within the alcohol reservoir. These differentials were negligible after installation of the agitator.

C. Loading System

Two loading systems were used as follows:

1) controlled stress (see Photograph 2.7)

2) controlled strain (see Photograph 2.8, 2.10 and 2.11)

1) For controlled stress load, an axial loading frame supplied with a balancing lever was used. After the freezing cell had been placed under the loading frame, the bracket of the frame was lowered until the groove in the middle of the bar touched the stainless steel ball on the loading piston. A dial micrometer was positioned over the bracket to obtain deformation readings. Predetermined loads were then hung on the weight hanger to load the sample (see Figure 2.4 and Photograph 2.12)

This frame was also used to obtain the magnitude of heave of the soil samples during freezing, without adding weight to the hanger but keeping the balanced bracket in touch with the acrylic piston which was resting on the sample being cooled.

2) Controlled strain - a Farnell electrically driven adjustable variable speed triaxial compression frame was used giving strains ranging between 0. 000013 inch per second to 0.0013 inch per second (see Photographs 2.8, 2.10 and 2.11).

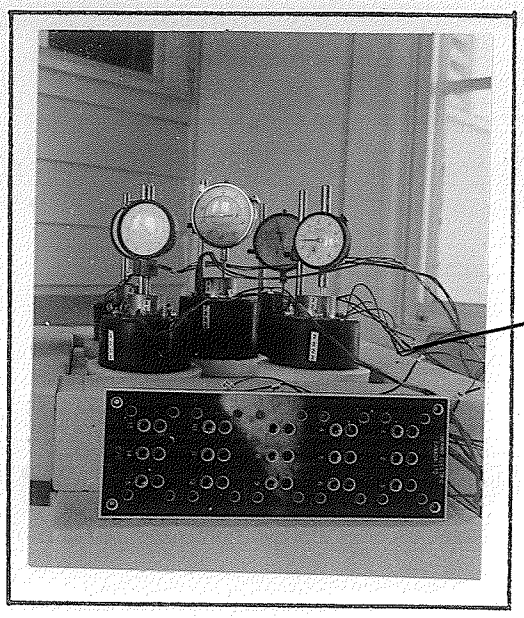

Photograph 2.9 Heat exchange box

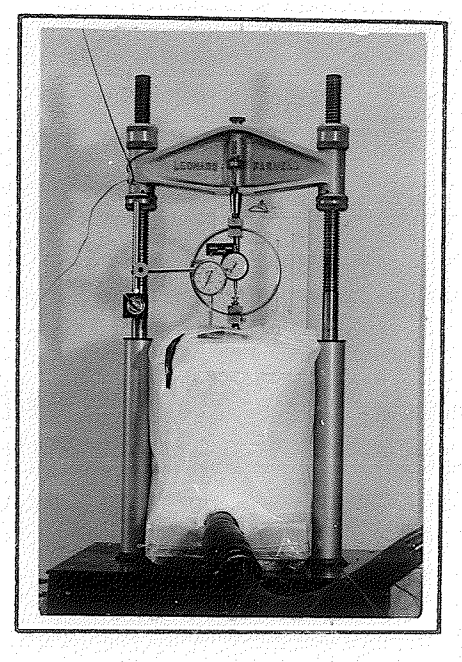

Photograph 2.10

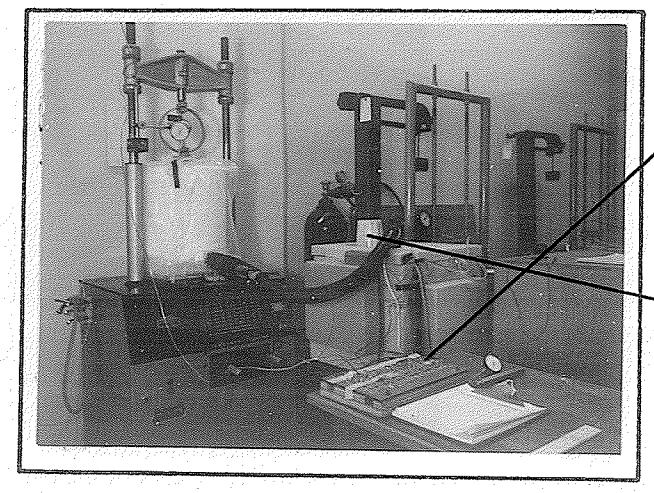

Photograph 2.11

Photographs 2.10 and 2.11 show the complete setup of heat exchange box, freezing cell, compression machine and other instrumentations.

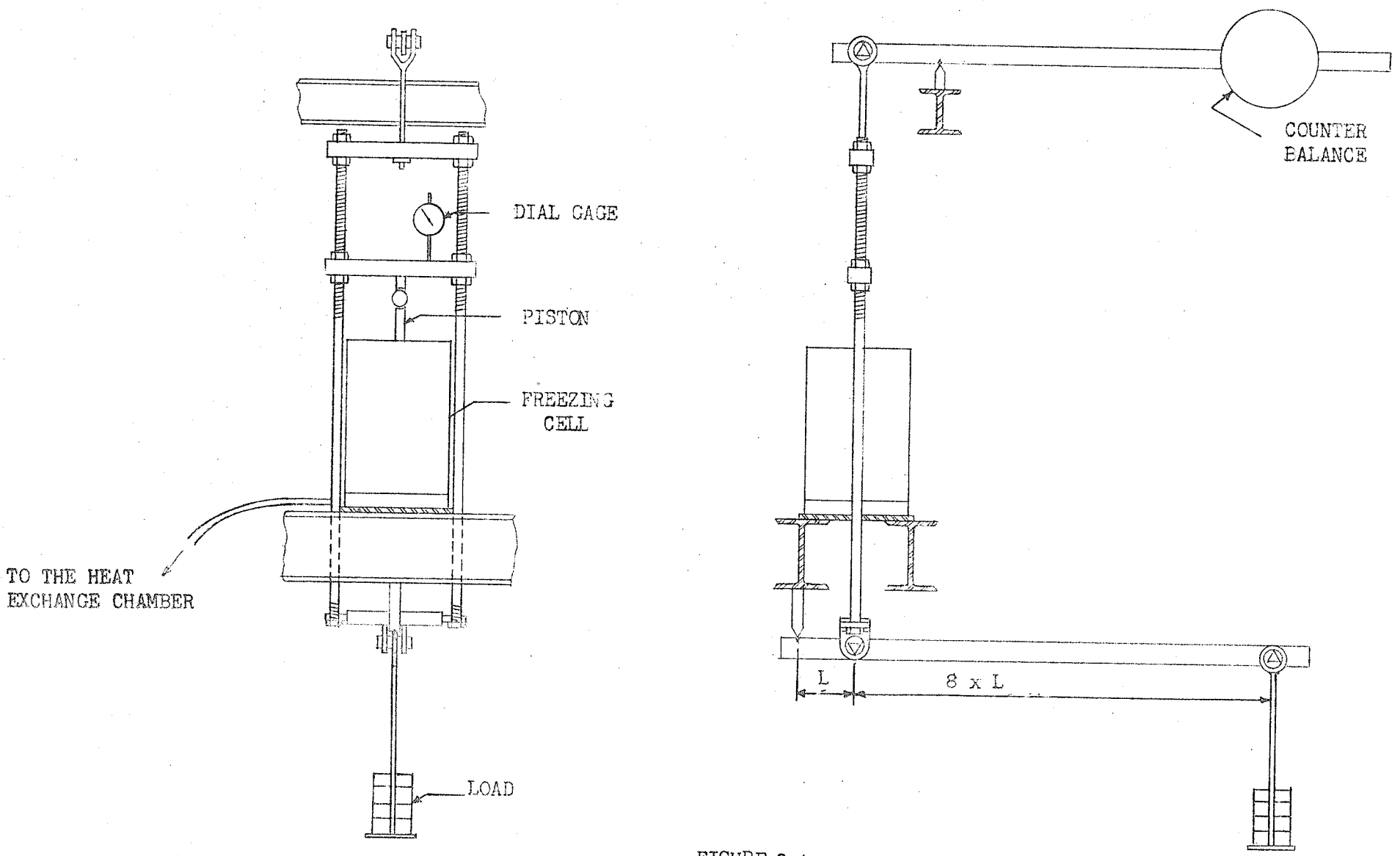

FIGURE 2.4
SUSTAINED OR CONTROLLED STRESS LOADING FRAME

A proving ring (see Photograph 2.10) or transducer was used (see Photograph 2.8 and 2.13), to measure stress applied to the load.

D. Temperature Measurement

The temperatures of the soil sample, alcohol reservoir, and specific locations in the cooling cell were obtained by means of copper-constantan thermocouple temperature sensing points (see Fig. 2.1, 2.2 and 2.3 and Photograph 2.2, 2.14 and 2.15) and potentiometer, or Yellow Springs thermistor probes and telethermometer. The temperature of the thermistor could also be recorded on a temperature recorder if required.

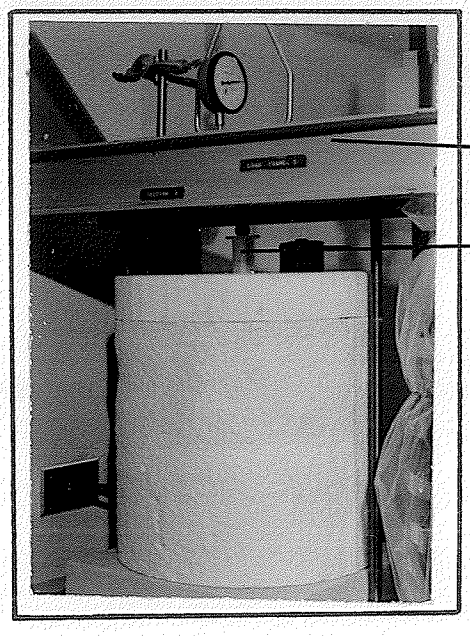

Photograph 2.12

Detail of the loading frame for constant stress

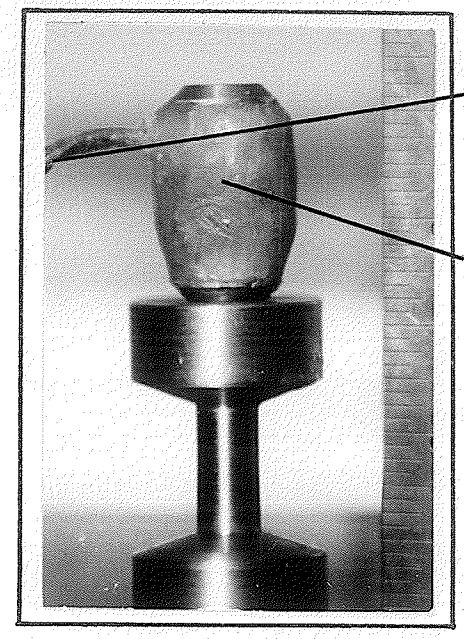

Photograph 2.13

Transducer

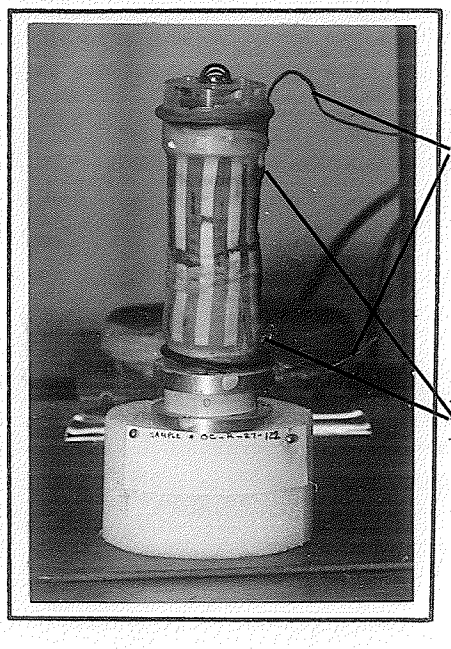

Photograph 2.14

Sample assembly with provision of filter strip for external water supply after completion of freezing process

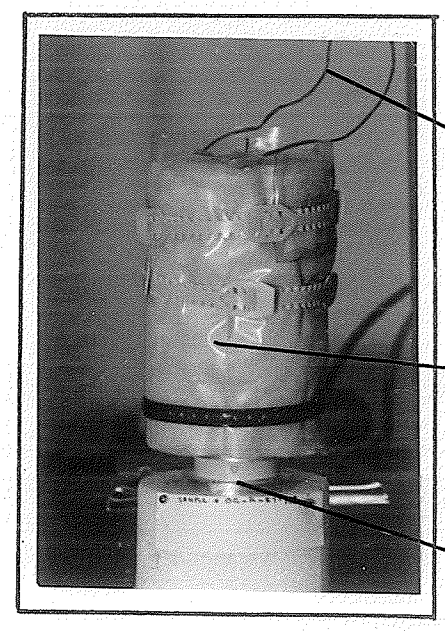

Photograph 2.15

Sample assembly for freezing in heat exchange box for heave measurement

CHAPTER III

GEOTECHNICAL PROPERTIES AND TYPE OF MATERIALS USED

CHAPTER III

GEOTECHNICAL PROPERTIES AND TYPE OF MATERIALS USED

3.1 The materials to be tested were taken in blocks approximately 18 x 18 x 9 inches in dimension. These were obtained in an undisturbed condition from a 24 foot depth during construction of an overpasss structure of the Winnipeg floodway near St. Vital during September of 1966 (see Fig. 3-1). At this depth the clay could be assumed to have remained unfrozen since deposited in Glacial Lake Agassiz.

3.2 Seven blocks were wrapped with a layer of "Saranwrap", a layer of aluminum foil, and a layer of cheese cloth. They were then covered with molten microwax and placed in the humidity room of the Soil Mechanics Laboratories of the University of Manitoba.

3.3 The area from which the material was taken is referred to as the Red River Plain and represents only a small portion of the extent of the Lake Agassiz clay.

As a result of Pleistocene glaciation, a large area was covered by glacial drift or till. As the ice began to melt, the glacial till was modified by geological agents other than ice. The original till, which consisted of cobbles, gravel, sand, silt and

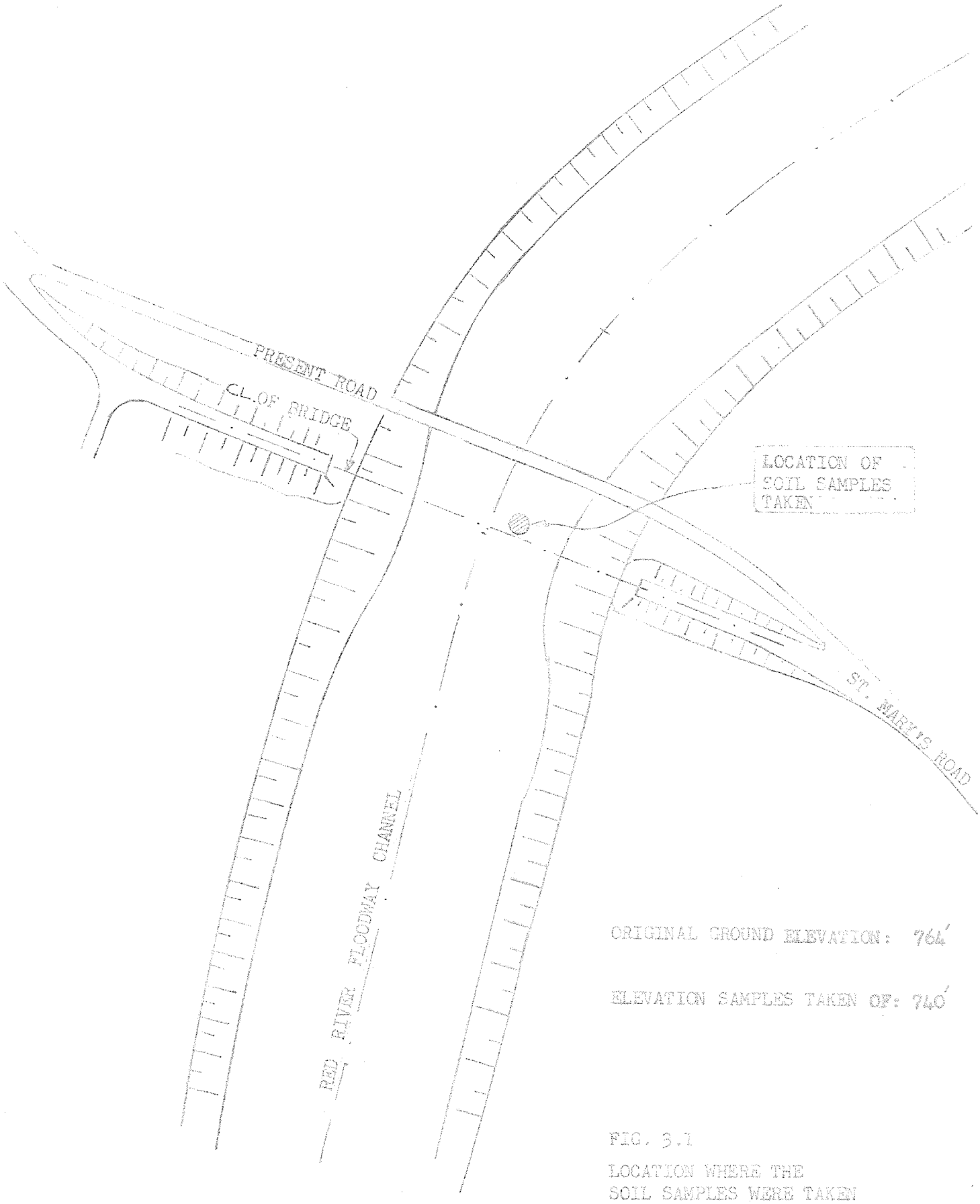

ORIGINAL GROUND ELEVATION: 764'

ELEVATION SAMPLES TAKEN OF: 740'

FIG. 3.1

LOCATION WHERE THE SOIL SAMPLES WERE TAKEN

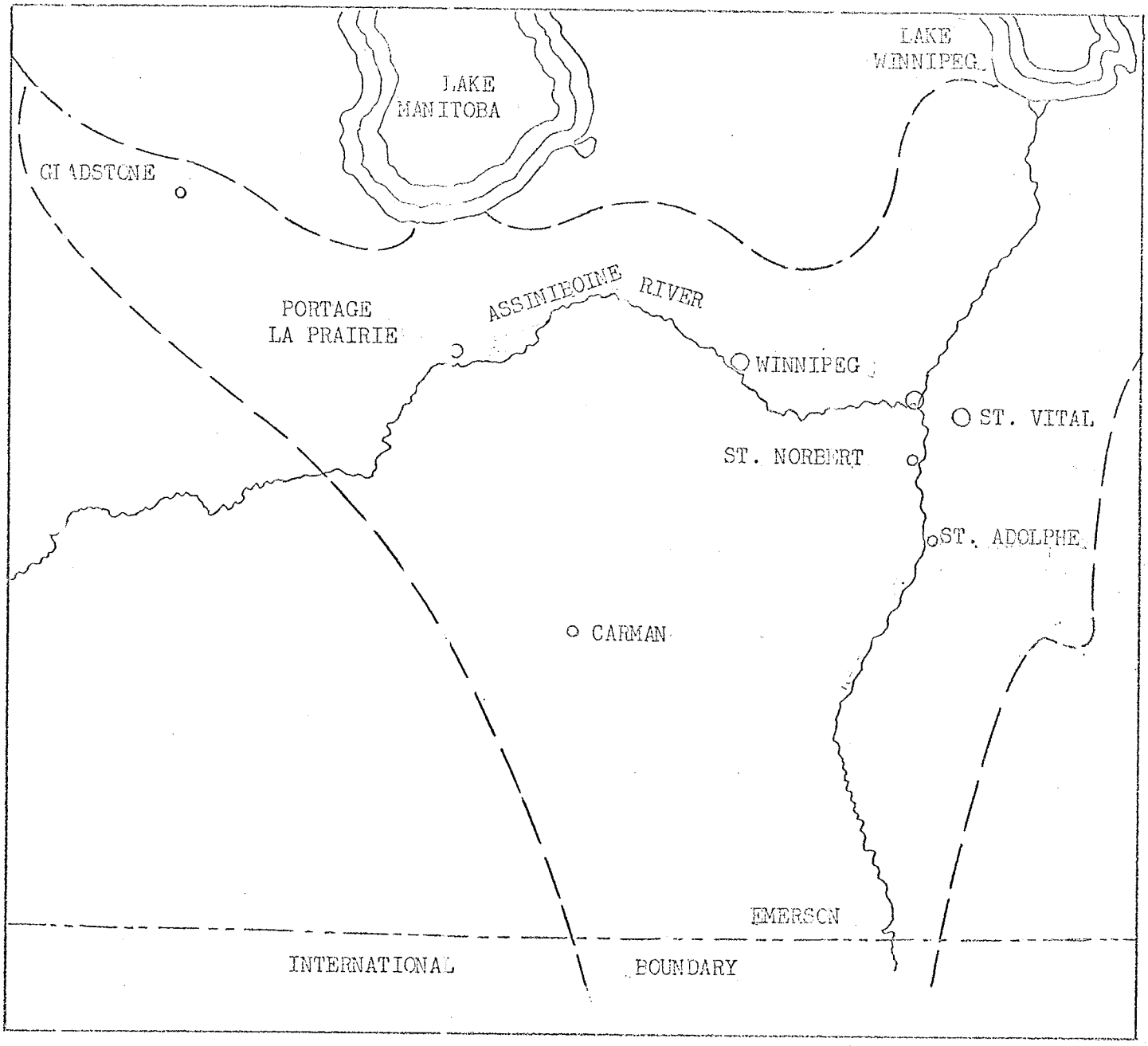

FIG. 3.2

APPROXIMATE BOUNDARIES OF
THE RED RIVER VALLEY PLAIN

clay, mingled indiscriminately in an unstratified mass, was severely modified by the water of the glacial lake. In addition, detritus from the higher lying Cretaceous shales (which included some bentonite and gypsum) was carried into the lowlands as a result of wave erosion, stream transportation and density underflows. (2)

Along the shoreline and shallows, the waves of this gigantic lake, 600 feet in maximum depth, eroded the ice-deposited drift and shale bedrock. The erosive force of the waves removed the finer particles and a density underflow transported them to deeper sections of the lake bottom. The accumulation of these sediments resulted in conspicuous stratification of the lacustrine deposits in many sections of the basin. Varves of colloidal clay were interspersed with thin layers of coarser clay and silt or very fine sand.

As the lake receded, and its depth decreased, wave action diminished. Consequently, materials eroded and transported during this later period were the finer fractions, consisting predominatly of fine sand, silt and clay. When the lake had receded to the central lowlands, very fine materials were brought in by stream action, and were deposited in the quiet water of the Lake Agassiz basin.

As the lake reached its last stage, the lower part of the basin received alluvial sediments. The thickness of water-laid sediments varies widely. The superficial deltaic and lacustrine materials in the central lowlands range up to 60 or more feet in thickness.

3.4 Originally, horizontally varved clays at the bottom of the lake were foliated occasionally by back and forward oscillation of the glacial sheets formed along the western and southern shorelines of Lake Agassiz and due to differential compaction caused by pressure of the overburden in variable height. (3)

3.5 With increasing depth, the clay color changes from brown to olive gray. The depth of the layers varies considerably. The soil making up these different colored layers varies from silt or silty clay to clay, with the silt fraction decreasing with increasing depth. (1)

3.6 The varves themselves vary in thickness from ¼ inch to as little as 1/64 inch. The varves consisted of clay layers with intermediate silt or silty layers. Considerable variation of moisture content is possible within small differentials of depth.

3.7 The dry density of this varved clay varies from 53 lb. per cu. ft. to 102 lb. per cu. ft. The wet density varies from 95 lb. per cu. ft. to 125 lb. per cu. ft. Moisture content of the soil varies from 20% to 63%, based on dry weight. The degree of saturation of most Lake Agassiz varved clay ranges from 86% to 100%. However, soils below depths of 6 to 12 feet show complete saturation, indicating a substantial zone of capillary rise. Free water is also found at times in the thin silt layer overlying the varved clays. The amount of this free water is usually small. It percolates through fissures in the upper layers of soil. However, prolonged dry weather results in its

disappearance. Based upon consolidation test data, these clays have permeabilities in the order of 10^{-9} cm per second to 10^{-11} cm per second.

The soil below the completely saturated level is said to be normally consolidated. The unsaturated soil is generally considered to have been preconsolidated. This is due to desiccation resulting from lowering of the water table as Lake Agassiz receded. Winnipeg varved clays show unconfined strengths varying from 865 lb. per sq. ft. up to 4570 lb. per sq. ft.

The liquid limit of these clays generally varies from 37 to 117; plastic limit varies between 14 and 40. The plasticity index ranges from 20 to 88. (4)

3.8 The samples which were taken from St. Vital showed the following properties obtained according to Procedures for Testing Soils ASTM (5)

Natural water content	48.3% to 49.3%
Degree of saturation	100%
Void ratio	1.25 to 1.32
Specific gravity	2.74
Natural dry density	74.9 lb. per cu. ft.
Grain size	See fig. 3.3

M.I.T. Classification

gravel	0%
sand	1%
silt	28%
clay	71%

See Figure 3

liquid limit	81.2
plastic limit	27.1
plastic index	54.1
shrinkage limit	12.52
water soluble sulfate	0.17%
average unconfined compressive strength	3,200 lb. per sq. ft.

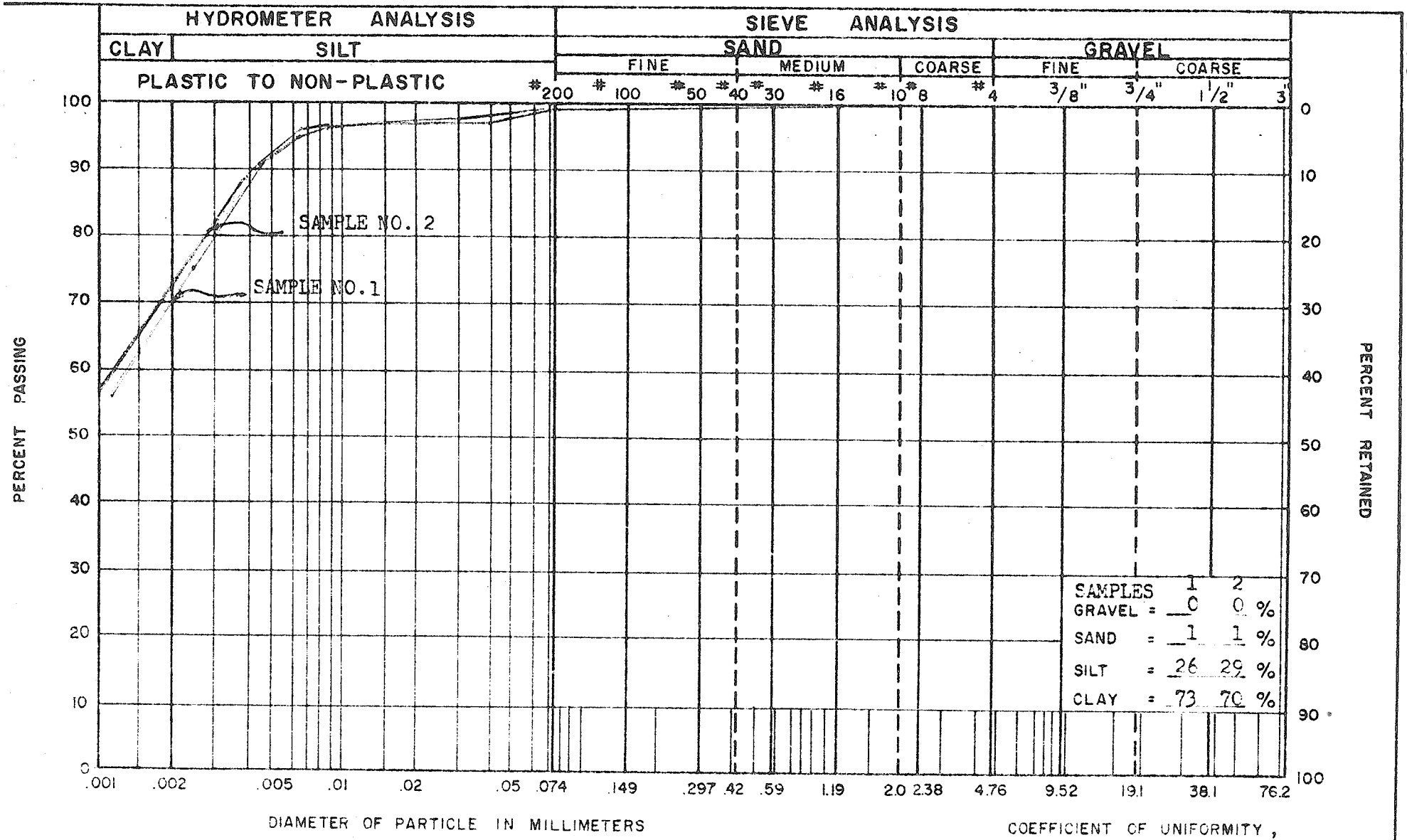

COEFFICIENT OF UNIFORMITY,

$C_u = \frac{D_{60}}{D_{10}} =$ _____

COEFFICIENT OF CURVATURE,

$C_c = \frac{D_{30}^2}{(D_{60})(D_{10})} =$ _____

TESTED BY F.A. DATE Sept. 1967

SOIL MECHANICS LABORATORY
DEPARTMENT OF CIVIL ENGINEERING
UNIVERSITY OF MANITOBA
FORT GARRY MANITOBA

FIGURE 3.3
GRAIN SIZE DISTRIBUTION GRAPH

PROJECT:

SAMPLE NO.	HOLE NO	DEPTH
1 AND 2	BLOCK No. 3 AND 4	24'-0"

I-1016

CHAPTER IV

SAMPLE PREPARATION

CHAPTER IV

SAMPLE PREPARATION

4.1 Cylindrical samples 2.8 inches in length and 1.4 inches in diameter were used in tests for determination of heave, deformation under constant load (creep), stress under constant strain rate, and stress release.

4.2 As pointed out in Chapter III, block samples from the field were stored in the humidity room, Soil Mechanics Laboratories of the University of Manitoba. Square pieces of soil were cut from the block samples and given a rough cylindrical shape with trimming equipment. To ensure square ends and constant diameters and length, a 2.8 inch long by 1.4 inch internal diameter polished brass cutting tube with sharpened edge was pushed over the roughly cut samples. At least ¼ inch of soil was left projecting beyond both ends of this tube. A wire saw was used to trim this soil flush with the ends. The samples were then pushed out with a loose fitting brass piston (see Photograph 4.1)

4.3 For water content determination, only the side trimmings corresponding to the anticipated final length of the sample were used. Top and bottom trimmings gave ± 2 to 3% differences in water contents, due to the varved nature of the clay and were not used in water content determination.

4.4 Three circumferential measurements (top, middle and bottom) and three length measurements were taken to determine sample dimensions. Two or three 1/32 inch diameter by ¼ inch deep holes were drilled at various elevations along the centre line and at right angles to the heat flow direction. Copper-constantan thermocouple sensors of 30 gauge wires were positioned in the holes after the initial weight of the samples had been determined.

4.5 Different methods in the preparation of the soil samples were used for the following cases of freezing and testing.

Case 1 - preparation of samples for uniaxial freezing and testing with no water supply to the sample; testing included;

a) Heave measurement,

b) Creep test,

c) Stress under constant strain rate,

d) Stress release.

In this case, the sample was placed between the freezing plate and loading cap. The bauxilite filter in this case was sealed with aluminum foil to prevent moisture migration to or from both the sample and the filter element. In addition, the sample was covered with an elastic membrane and sealed against the freezing plate and loading cap using vinyl O-rings. The points of exit of the thermocouple wires between the membrane and cooling plates and the O-ring were coated with molten microwax. The elastic membrane was then covered with silicone grease (see Photograph 4.2).

4.6 Case 2 -- preparation of samples for uniaxial freezing and testing with water supply to the samples; testing included:

a) Heave measurement,

b) Creep test.

The sample was placed over the moistened freezing plate after the installation of thermocouple points as described in Case 1. Moistened filter paper strips, ¼ inch wide, were then placed vertically on ½ inch centres, partially overlapping the sample top. The parts of the vertical filter paper strip surfaces facing the soil sample were blocked off with Scotch tape to supply water to any predetermined zone. (See Fig. 4-1 and Photograph 6.7)

The top of the sample was then covered with moistened filter paper. The de-aired filter was placed in the loading cap and sufficient de-aired distilled water was drawn through the filter to the burette. To avoid air trapped between the soil sample and filter, the loading cap was inverted under sufficient head to allow the forming of a meniscus. Then the loading cap was righted and carefully moved over the top of the sample. The membrane was placed over the freezing plate in rolled form and unrolled up over the sample after the addition of several drops of water between the rolled end of the membrane and the soil sample to form a ring of water between the rolled membrane and the soil sample. This would eliminate any air that might have been trapped between the membrane and soil sample.

The membrane was sealed against the freezing plate and loading cap using an O-ring and was coated with silicone grease as described in Case 1.

The sample was surrounded loosely by 1 1/2 inch to 1 3/4 inch thick fiberglass insulation. The water reservoir was insulated together with the soil sample for external water supply. The insulation was covered with a vapor barrier made of Saranwrap. The vapor barrier and insulation were fastened with plastic tape to the side of the cooling plate and acrylic piston. The loosely placed fiberglass insulation allowed the sample to expand or contract without difficulty when the sample was frozen or subjected to any stress. Then the sample was placed over the pedestal and aligned with the bushing of the freezing cell (see Photograph 2.1). The insulation hood was then placed over the cell and covered with an external vapor barrier to prevent icing of the freezing cell by condensation (See Photograph 2.4, 2.5 and 2.8).

4.7 In addition, the sample could be placed in the heat exchange box for freezing and heave measurement for slow freezing after temporary removal of the acrylic piston (See Photograph 2.9). The sample was then transferred to the freezing cell for rapid freezing, which was kept at the same temperature (see Fig. 2.2 and Photograph 4.3).

The acrylic piston was placed back in its former position for further testing.

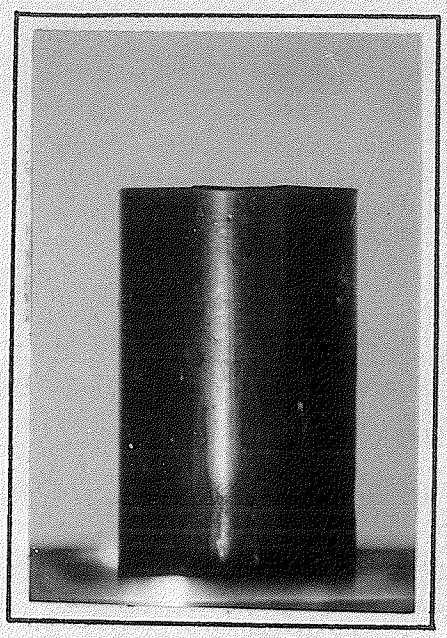

Photograph 4.1

Trimmed soil sample

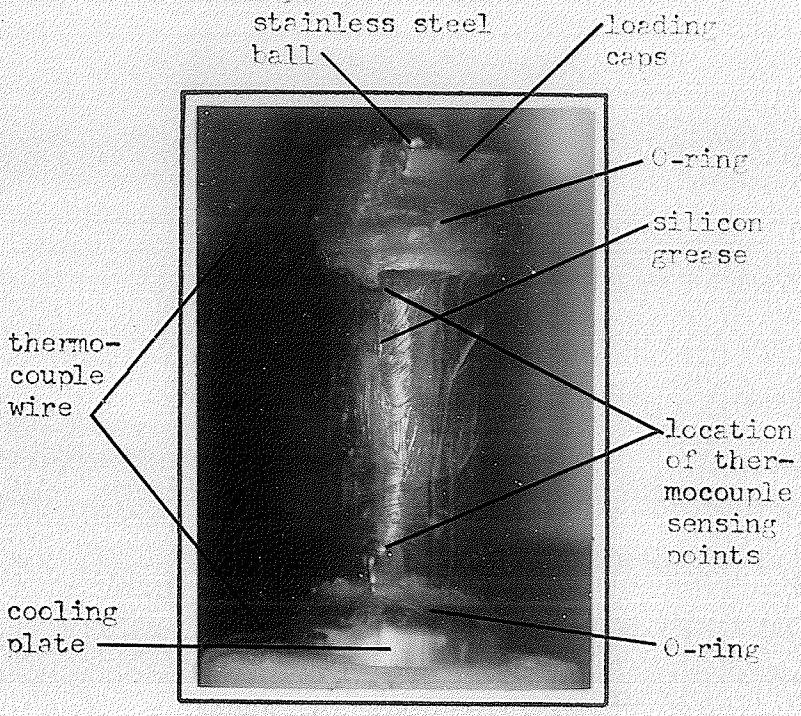

Photograph 4.2

Preparation of soil sample for freezing process

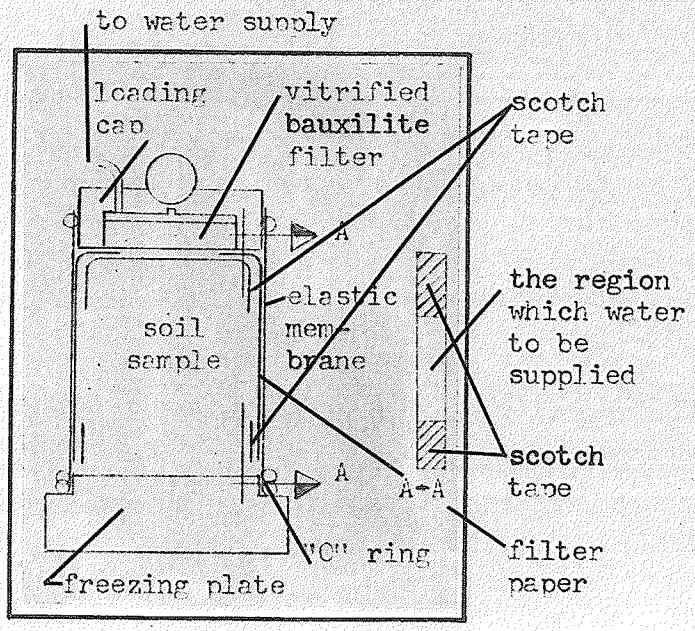

Fig. 4.1

Detail of lateral water supply strips

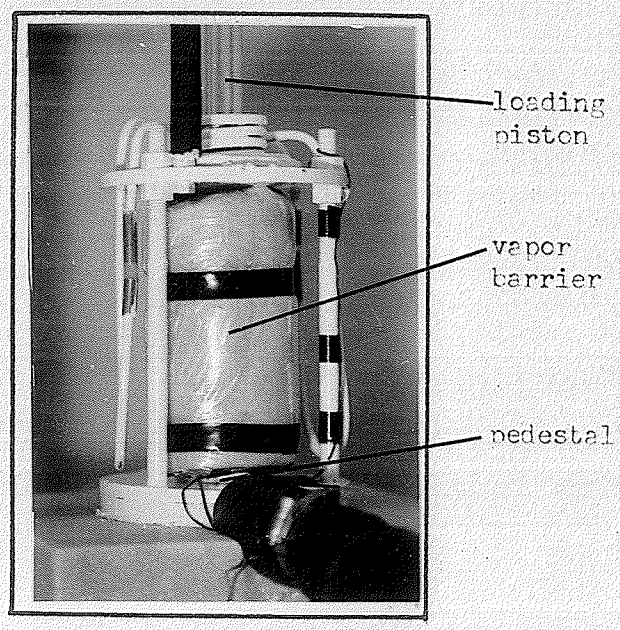

Photogrph 4.3

Placing a sample inside freezing cell

4.8 Case 3 - preparation of samples to be frozen from all around with no water supply to the sample; testing included:

a) Observation of ice crystallization,

b) Unconfined strength of undisturbed soil samples which were thawed out after one cycle of freezing to compare their residual strength with undisturbed or remolded non-frozen soil samples.

In this case, the samples to be frozen were placed between the freezing plate and an aluminum loading cap, and were covered with double elastic membranes and sealed against the freezing plate and loading cap using vinyl O-rings as described in Case 1.

The samples then were placed in the cooling liquid reservoir for rapid freezing at a predetermined temperature.

CHAPTER V

LITERATURE REVIEW

CHAPTER V

LITERATURE REVIEW

The following material is transcribed from the references listed in the bibliography.

PART I - FROST ACTION

A. Heaving of frozen soils due to redistribution of moisture and ice segregation in frozen soils

5.1 Water, upon freezing, increases its volume by approximately 10 percent. Soil layers which contain moisture will therefore show an increase in volume unless the volume of voids is so great that it can hold the moisture content in the frozen state.

In most cases, the increase in volume of the soil layers is sufficient to cause heaving of the ground. (6)

5.2 As the first ice crystals form, they attract moisture and draw it into the crystal lattice by means of the crystallizing force. If the capillary force in the soil is great enough, the moisture drawn into the crystal lattice will be replaced by moisture from a low lying water reservoir (if available). The movement of the water is possible because moisture in narrow capillary tubes will only freeze at temperatures below 32 ^{o} F. If there are no obstructions, the water will flow steadily to the face of the crystal, thus increasing its thickness. As the crystal is enlarged, so called ice lenses, which

vary from a fraction of an inch to a few feet in thickness and several feet in diameter are formed. The volume increase occurs in the direction of the heat flow and in the direction of the least resistance - upwards. (6, 7)

5.3 Because capillary rise is almost negligible in coarse soils (sand and fine sand) crystallization rapidly comes to a standstill due to a lack of water supply.

5.4 In medium-fine soil types (coarse silt and medium-coarse silt) the capillary rise is so great that moisture can be absorbed from depths of as much as 3 to 6 feet or more. The permeability of these soils is also high enough to maintain adequate flows to the freezing zone.

5.5 Fine soil types (fine silt and clay) exhibit large capillary rise but the size of the openings is so small that crystal growth is slight. Freezing advances deeper into the soil.

5.6 It can be seen, therefore, that frost heaving is of the greatest importance for soil layers consisting of coarse silt and medium coarse silt. Severe frost heaving may be expected if the water used in crystallization can be replenished from some source, for example, the water table.(8)

B. Shrinkage of clays caused by ice segregation

5.7 It may be shown experimentally that in cases where additional water is not allowed to enter the system, the withdrawal of water from the lower regions causes shrinkage; and usually, tension cracks. The decrease in volume is an indication of the force which draws the water to the growing ice crystal (8). Terzaghi has shown that the force involved in the shrinkage of clay on evaporation is equal to the external pressure required to produce the same change in volume, and that this force may be very great. (9)

5.8 In very impermeable soils, with high colloid content, tension is set up due to the formation of segregated ice. This stress is uniformly distributed and leads to the development of vertical tension cracks which form a polygonal pattern in the cross section. Clear ice gradually fills and enlarges these cracks. As freezing progresses, these ice filled cracks descend forming a columnar structure or combination with the usual horizontal ice layers; this results in a cellular structure. (8)

C. Penetration of the freezing plane

5.9 If the supply of water to the freezing plane is adequate and the soil is of the proper type, ice lenses may grow almost indefinitely. However, further penetration of the freezing plane into the unfrozen

soil is prevented because of the heat given off by the water as it freezes.

In practice, however, the freezing plane seldom remains stationary for any prolonged period. A decrease in the supply of water or an increase in the rate of heat loss may occur due to a change in conditions. The balance between the heat given off from the freezing water, and the heat loss to the surface is then disturbed. The freezing plane advances until conditions for the growth of a new ice lens are restored. Consequently, a series of ice lenses separated by layers of frozen soil are formed. This commonly occurs under natural conditions. (10)

5.10 Stephen Taber stated (11) that when water is under tension due to the growth of ice layers in clay, the stress is ordinarily greatest at the point where the water molecules are being pulled into the film which separates the growing ice crystals from the lower clay layers. Therefore, breaks would occur at this plane. The breaking of a water filament being drawn toward the ice layer indicates that the molecules are separated beyond their range of attractions; or, in other words, that a gas phase has formed between the water and the ice. However, the gas force could not extend far below the ice layer because the tensile stress in the water just below the ice is due to frictional resistance to the passage of water through the small soil voids. As soon as the upward movement is checked, this passage stops.

The energy required to separate the molecules when converted to gas (the ultimate tensile strength of water) has been estimated at over 1300 atmospheres. A water column of larger cross-section is placed under tension, only with difficulty. When under negative pressure, the water is superheated (even at temperatures below 32°F), and the formation of a gas phase immediately breaks the column. Extremely slender columns of water are more easily held in tension than the larger ones. Water is present in this form in clays. Ice forming gradually in the soil voids below a growing ice layer is a probable explanation for the rhythmic banding due to the development of successive ice layers as freezing extends downward in clays.

D. Thickness of ice lenses

5.11 Taber stated (11) that the layers of segregated ice in undisturbed or artificially consolidated clays are clear and very sharply separated from the frozen clays. Ice layers are not so sharply defined in unconsolidated clay and it is usually impossible to estimate (with any accuracy) the thickness of the segregated ice.

E. Frost susceptibility

5.12 The size of the particles in a soil has a marked influence on its properties. This characteristic is often used to assess the heaving potential of a soil. Although the amount of ice lensing may be predicted quite readily when based on the particle size of the soil, there have been many cases where frost heaving has occurred in soils

considered safe after an examination of particle size. Attempts have been made to use other properties of the soil, such as the height of capillary rise, to predict more accurately the frost heaving potential of a soil. The results from a test of this type provide a more realistic indication of frost heaving characteristics and give an indirect measure of size and distribution of soil pores (10). However, this type of test has the disadvantage of being more difficult to perform than those based solely on particle size.

5.13 By far the most commonly used criterion for frost-susceptibility is that of Casagrande, who worked from field and laboratory studies. It is employed in its present form, by the U.S. Army Corps of Engineers and other large agencies. His criterion is that well graded soils will be frost susceptible if they contain more than 3 percent by weight of particles finer than 0.02 mm. For uniform soils, the amount of material finer than 0.02 mm. can be as great as 10 percent before the soil is considered frost susceptible. (10)

5.14 Penner, 1946 (12) pointed out that although the two factors are obviously related, theory suggests that pore size is more important in establishing frost susceptibility than grain size. In uniformly graded soils, pore sizes are larger and, it is interesting to note, that the Casagrande criterion allows for a large amount of material smaller than 0.02 mm. in uniform soils. This obviously recognizes the influence of pore size.

FIGURE 5.1 FROST SUSCEPTIBILITY CHART
(AFTER NIELSON AND RAUSCHENBERGER)

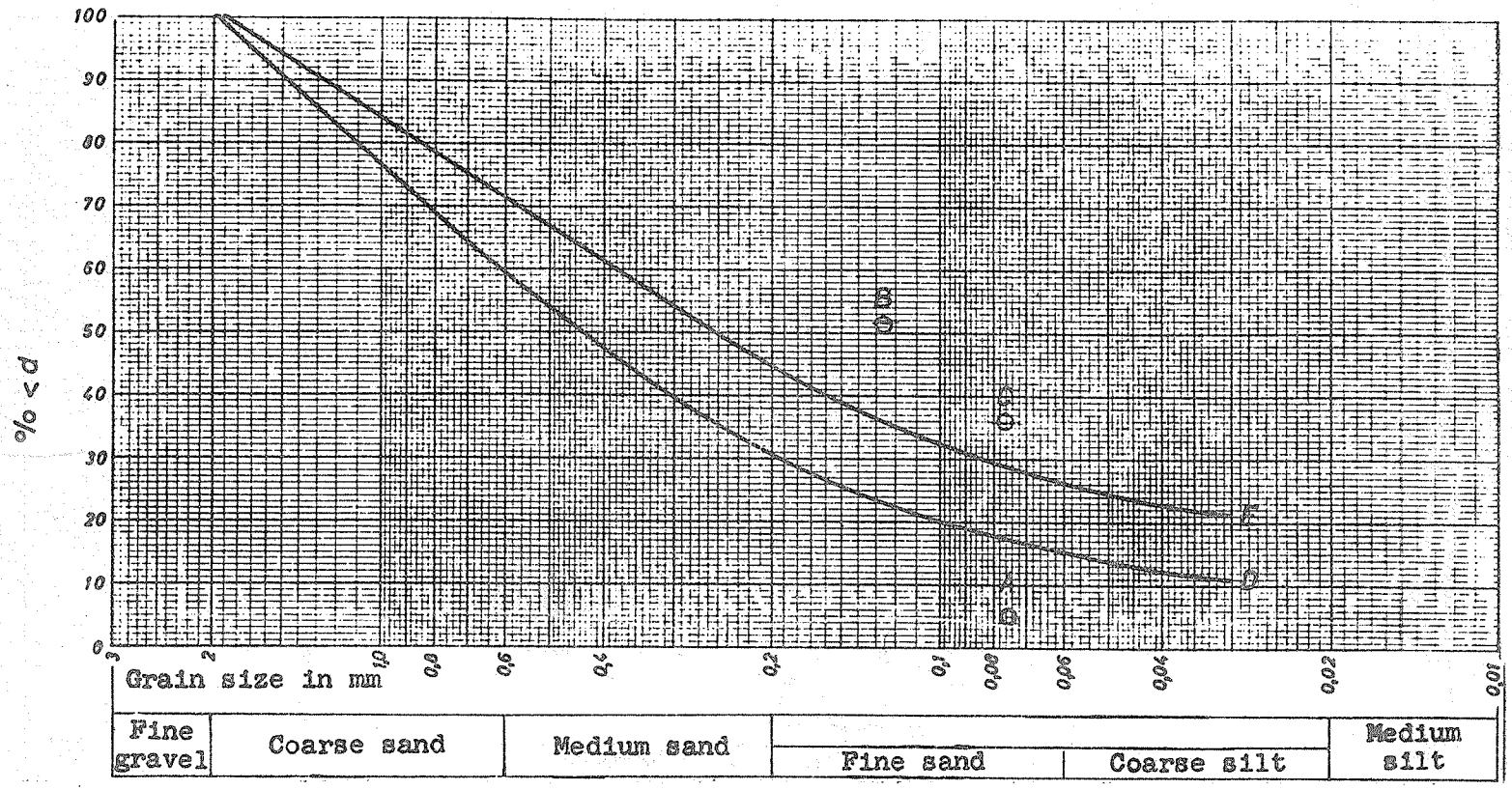

1. All the soil types containing less than 5% with d < 0.075, i.e. soil types in which the grain-size curve drops below point A are not frost-susceptible.

2. The other soil types are divided as follows:
   a. Sediments are not frost-susceptible when less than 50% is smaller than 0.125 mm and at the same time not more than 33% is smaller than 0.075 mm, i.e. when the grain-size curve lies below points B and C. Sediments, the grain-size curve of which lies above points B and C, are frost-susceptible.
   b. Ungraded soil types are not frost-susceptible when the grain-size curve lies below curve D. Ungraded soil types, the grain-size curve of which lies above curve E, are frost-susceptible.

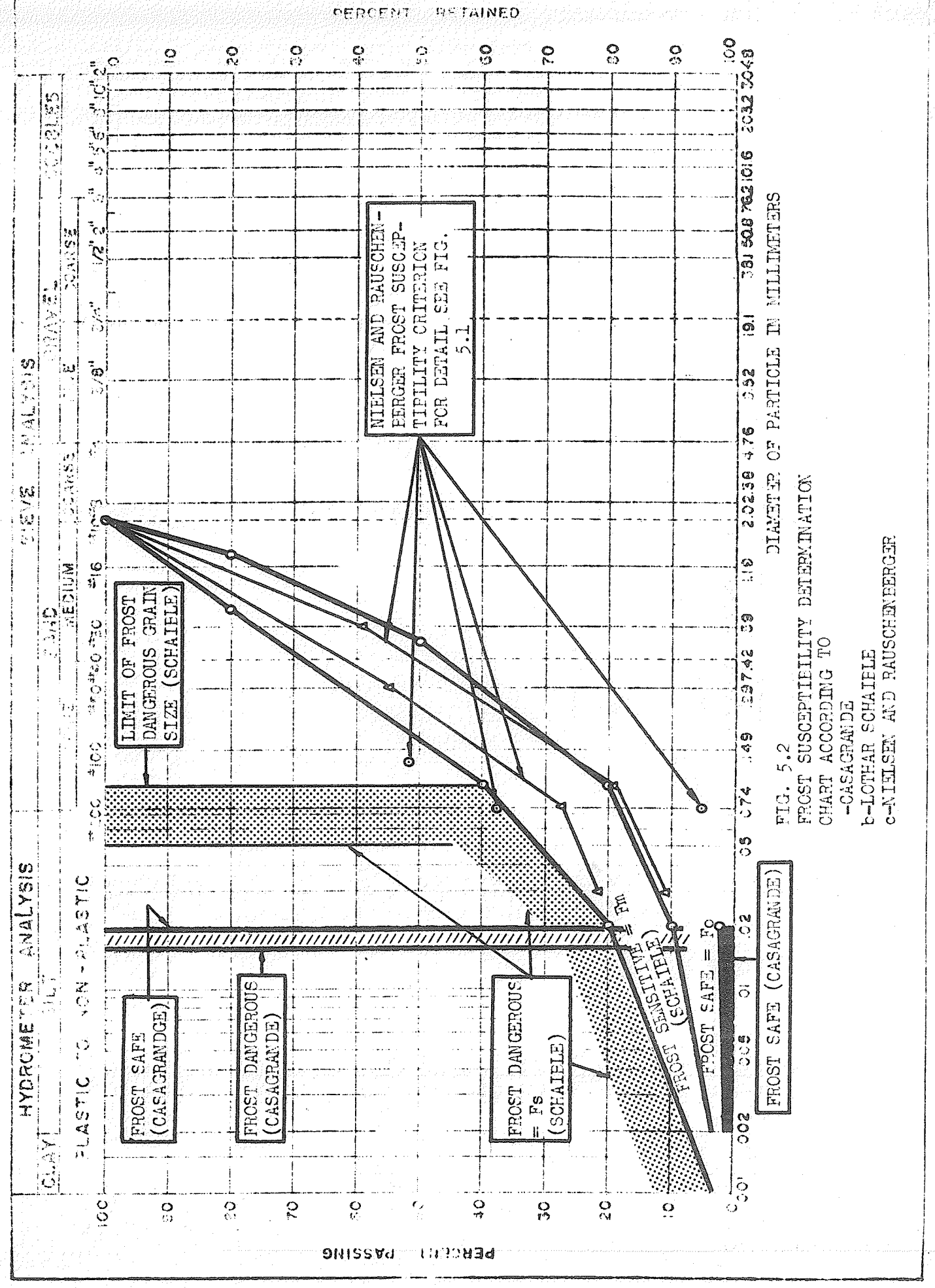

FIG. 5.2
FROST SUSCEPTIBILITY DETERMINATION CHART ACCORDING TO
-CASAGRANDE
b-LOTHAR SCHAIELE
c-NIELSEN AND RAUSCHENBERGER

5.15 The most reliable method of identifying a frost heaving soil at present is to carry out a laboratory freezing test. The test is on the safe side since soils that show frost heaving in the laboratory do not always behave similarly in the field. (10)

5.16 Nielsen and Rauschenberger (7) suggested that the frost susceptibility of soils may be determined by means of curves and notes as shown in figure 5.1.

5.17 After 20 years of thorough observation in central Europe, Lothar Schaible, 1955 (13) came to the conclusion that the grain composition of a soil must play a decisive role in any assessment of the frost danger. Only the fine soil or soil matrix and the grain size components below 2 mm. are considered and a classification of dangerous grain size was suggested. A classification of this type affords the possibility of determining the frost susceptibility of soils on the basis of their percent grain size composition below 2 mm. in the following series:

a) for the clay and silt series.

b) for the clay, silt and very fine sand series

(See table 5.1).

With this new frost criterion (see fig. 5.2) Lothar Schaible suggested that decisions regarding the degree of frost susceptibility can be made on the basis of grain size analysis.

F. Volumetric expansion and contraction of frozen soils

5.18 Water attains its maximum density at a temperature of $4^{o}C$. On further cooling, it begins to expand until it crystallizes. With further decrease of temperature, the ice contracts. Therefore, when moist porous soil freezes, its volume first increases, until most of the water freezes, and then upon further cooling the volume decreases. (14)

5.19 Calculation of frost heave: Frost heaving of soil is the external result of the increase in its volume. The extent of frost heaving depends on the amount of water drawn to the freezing front during migration. The total heave of completely saturated soil, if the average increase in volume of water on changing from liquid to solid state is 9%, is:

$$h_h = \frac{1}{A}\left(0.09 \times \omega \times \frac{\omega_s}{\gamma_\omega 10^4} \times i_o + 1.09Q\right). \qquad \ldots\ (5.1)$$

Q is the volume of water drawn to the freezing front in an open system. In a closed system, where no external water supply is available, however, Q = 0. Therefore:

$$h_h = 0.01\ \omega \times \frac{\omega_s}{\gamma_\omega} \times \frac{0.09}{A} \times i_o \times \frac{1}{100}. \qquad \ldots\ (5.2)$$

Where:

h_h = frost heave, cm.,

ω = water content, percent,

ω_s = weight of dry soil, gm.,

γ_ω = unit weight of water, gm. / c. cm.,

A = cross-sectional area of frozen soil, sq. cm.,

i_o = relative ice content, percent,

ω_u = unfrozen water content in frozen soil,

$$i_o = \left(1 - \frac{\omega_u}{\omega}\right) 100 . \qquad \ldots\ldots (5.3)$$

5.20 According to the definition of K. Terzaghi, 1948 (15), in a closed system, with regard to water supply to the freezing front, water comes only from pore water within the soil. The volume increase associated with freezing of the closed system does not exceed about 3 to 5 percent of the total volume. In an open system, however, with regard to water supply to the freezing front, water comes from a pool of free water located below the ground.

TABLE 5.1 Theoretical and Practical Classification of Frost Susceptibility According to "SCHAIBLE"

Fraction in % of fine soil composed of grain size <2 mm For (a)	For (b)	Theoretical Classification		Practical Classification
0 to 5	0 to 10	No frost damage	= Fo	Safe
5 to 10	10 to 20	Light frost damage	= F1	
10 to 15	20 to 30	Med. frost damage	= Fm	Sensitive to frost
15 to 20	30 to 40	Med. to strong frost damage	= Fm/Fs	Near upper limit; use caution and carry out comprehensive investigation
over 20	over 40	Strong frost damage	= Fs	Dangerous

PART II - STRESS-STRAIN-TIME RELATION AND STRESS RELEASE OF FROZEN SOILS

The problem of establishing the parameters involved in the strength of unfrozen soils is complex and depends on the following factors (19):

a) Types of soil mineral and soil mass composition, including stratification,

b) Prestress history,

c) Soil structure (particle orientation and arrangement),

d) Nature of pore water and degree of saturation,

e) Method of test evaluation.

In the case of frozen soils the situation is more complex because of the following additional factors:

a) Influence of temperature in regard to ice,

b) Ice content and unfrozen water content in frozen soils,

c) Type of ice frozen in soil,

d) History and age of freezing and thawing,

e) Size and number of ice crystals found in frozen soils,

f) Orientation of ice crystals,

g) Rate of freezing,

h) Rate of application and duration of applied load,

i) Transformation of ice to other form of ice or phase transformation of ice during application or duration of load,

j) Quantity of air content in soil mixture or in ice crystals , and

k) Content of soluble salt in soil composition, etc. Therefore, frozen soils in different states may have a different resistance to applied load causing compression, tension, or shear stress.

5.21 The transformation of water to ice alters the internal bonds in the soils, leading to a redistribution of moisture and fine mineral particles. The behavior of ice inclusions, especially if ice forms in thin films, differs from water films, giving rise to frozen soils whose strengths differ substantially from unfrozen soils. The strength of internal bonding (cohesive strength of frozen soil) depends on several factors which, in turn, depend upon interactions between the soil components. Experiment shows that the cohesion of frozen soil decreases gradually with rising temperatures, and falls sharply at the stage of thawing. (16) Also, experience has shown that frozen soils under applied load do not behave as Hookian solids. They have irrecoverable deformation (creep) after initial elastic strain. A stress which is produced under a given strain or deformation decreases as a function of time, if the strain is fixed or locked (stress relaxation or stress release).

The internal bonding of unfrozen soil consists of the following:

a - The natural molecular bond, which depends upon the molecular attraction between the solid particles of soil separated by a film of connecting water. This attraction depends on the surface area of particles and the distance between them. The strengthening of soil is achieved when compression causes a reduction of distance between particles thereby increasing molecular attraction.

b - The structural bond is caused by a variety of physical, physico-chemical, mechanical and other processes, which develop a molding during geological formation. This bond is removed when distortion of the natural structure of soil occurs by thawing or remolding.

c - The cementing bond of ice between the ice crystals and the mineral particles. This bond is produced by a liquid layer, which envelopes the soil particles and the ice crystals. It is dependent on the temperature of frozen soil, the volume of ice and the area of interface of ice and the mineral particles.

Although the above classification is somewhat arbitrary, it is useful in separating the roles of various factors which affect the strength of frozen soil.

5.22 The cementing bond of ice is the least stable and changes with changes in the temperature of the frozen mass. Upon thawing, this bond disappears completely and the strength of the thawed soil, accompanied by textural and structural changes, is reduced in an irregular fashion. These textural and structural changes lead to deformation under relatively low stresses.

5.23 When a load is applied to frozen soil, it produces a stress concentration at the contact between the mineral particles and the ice crystals. Even with a comparatively small applied load, the stress at the contact can reach very high values. A further increase in stress causes plastic deformation of the ice forcing the ice from a high stress region to a region of lower stress. It also gives rise to plastic flow of ice with no phase transition because of the pressure difference at and around the contact area. At the same time, the increase in stress at the contact leads to a disturbance of the equilibrium state between the film of water and the ice in contact with it. This finally leads to a melting of ice. Under the influence of the pressure gradient, moisture, which has changed phase from ice into water film, is moved from a region of high pressure into a region of lower pressure. The water squeezed into this region freezes again and reaches an equilibrium state at same temperature.

5.24 Some of the ice-melt may be squeezed out onto a free surface and freeze there. This ice melting and displacement of water has been confirmed by experiments by Vyalow, 1954. (16) Besides the process already described, a process of squeezing-out of the air contained in the frozen soil also takes place.

5.25 Redistribution of the ice in frozen soil under the action of an external load leads to denser packing of the mineral particles. The displacement of ice, water, and air results in a volume decrease or consolidation of the soil. This gives rise to increased molecular cohesion. The process of ice flow, its melting and the squeezing out in form of supercooled water is accompanied by a structural distortion of the frozen soil which causes the structural and cementing bond to be decreased. Two mutually opposed phenomena occur in frozen ground under pressure. On the one hand is a weakening of structural cohesion and cohesion by cementation, and on the other an increase of molecular cohesion.

5.26 With time, rearrangement of solid particles takes place, resulting in irreversible structural deformation known as creep or visco-elastic flow. If disturbance of the structural bond and a weakening of cementation bond is compensated for by a strengthening of molecular cohesion, a state of equilibrium will be re-established and the rate of deformation will stabilize.

However, if the applied load is larger than a certain magnitude,

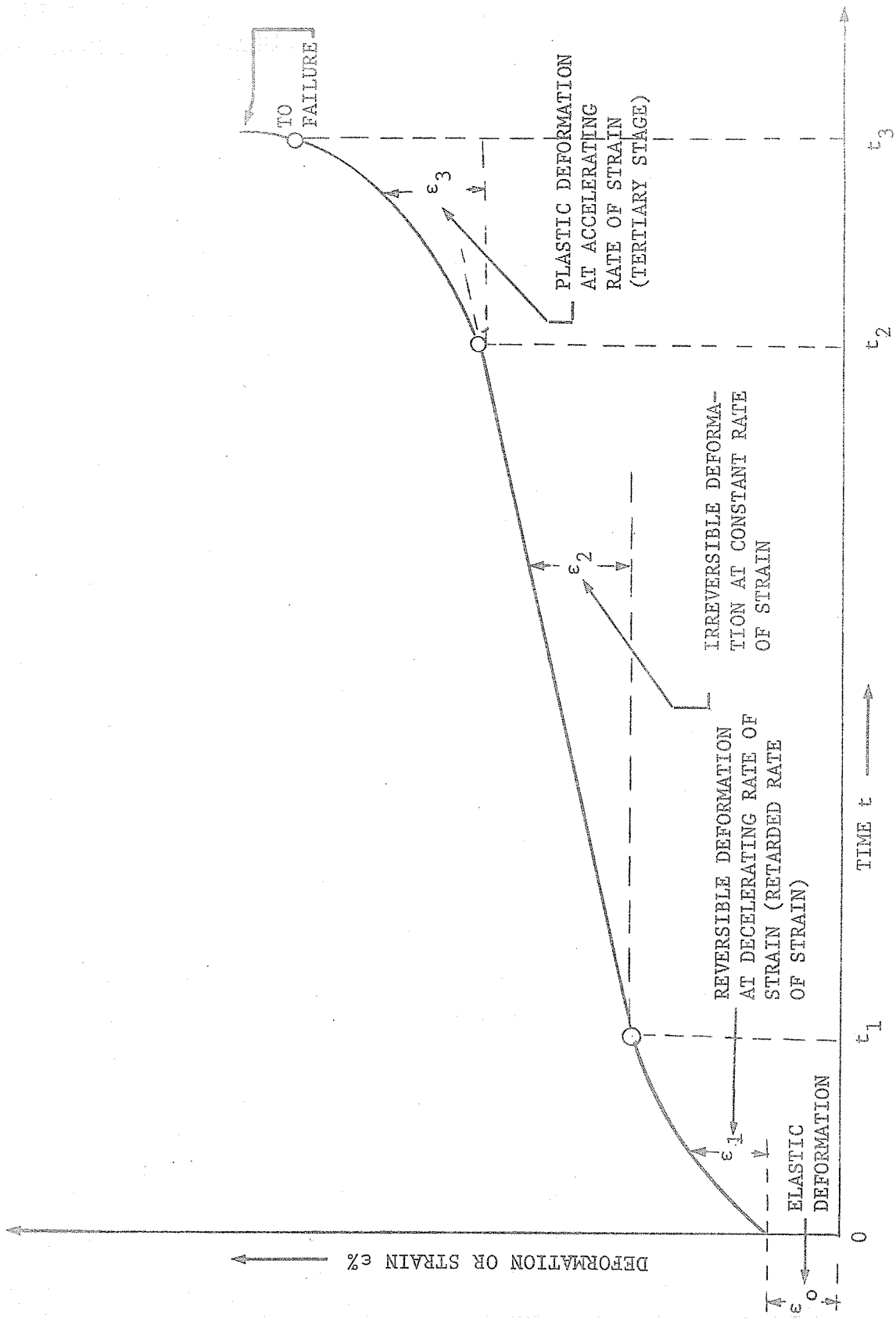

FIGURE 5.3 SCHEMATIC CREEP CURVE OF FROZEN SOIL

the destruction of the internal bonds will no longer be compensated for by strengthening of the molecular bond. Flow would continue and lead to total destruction of internal bonds, commonly called failure.

5.27 The deformation of frozen soils under constant applied stress has been classified by Denisov (1951), Noyabov (1959), and Tsytowich (1954). (16) Throughout the text and with reference to Figure 5.3 all deformations are designated by the symbol 'ε'. The subscripts 0, 1, 2 and 3, designate the stages of deformation of Elastic, Structurally Reversible, Irreversible and Plastic Viscous respectively. The deformations are classified as follows:

a) Elastic deformation 'ε_o' associated with elastic changes in the crystalline lattice of the ice and or minerals, elastic compression of water and any entrapped air contained in the frozen soil - These deformations are instantaneous, occurring immediately upon removal of the applied load. The magnitude of the instantaneous elastic deformation of the frozen soil is comparatively small but may be increased by cycling the load.

b) Structurally reversible deformations 'ε_1' which result from changes in the thickness of the water film at the interfaces of the soilid particles under the action of external pressure, and also as a result of the reversible phase transitions in the ice - This reversible deformation is time-dependent. It can be considered to be a delayed elastic deformation at a decelerating rate of strain.

c) Irreversible deformation 'ε_2' due to phase transition of ice to water and accompanying consolidation under stress - The

squeezing-out of water or any air is accompanied by a decrease in the volume of soil. This is a time dependent deformation and is irreversible.

d) Plastic viscous deformation 'ε_3' that depends on the irreversible displacement of solid particles and flow of ice - This deformation develops with time and may be characterized as visco-plastic. An accelerating rate of deformation terminates in failure (Fig. 5.3). The increase in plastic deformation leads to an irreversible and distorted structure and may lead to a state of progressive flow resulting in complete failure of the soil under load (tertiary stage, "accelerating rate of strain").

5.28 Another manifestation of the rheological properties of a body is stress relaxation under constant strain. The cohesion of frozen soil is not constant and varies with the moisture phase and time. The relaxation (stress release) depends upon ice melting in contact with the mineral particles, dislocations in the mineral aggregates, and upon yield and change of ice structure contained in the soil. In frozen soil subject to relaxation under constant applied strain, most of the high stress produced by the compression is relieved in a short period of time. Further decrease in stress occurs over a longer period of time.

5.29 The above classification of deformations is arbitrary since the occurrence of one or another type depends upon the duration of

the load and, most of all, on the soil temperature.

Mechanical models are often used to express the rheological properties (20), but these are not herewith presented.

5.30 The instantaneous elastic strain shown in figure 5.3 can be compared to a simple mechanical spring (21) (See figure 5.4a and b). The strain for any constant stress can be expressed as:

$$\varepsilon_o = \frac{\sigma_o}{E_o},$$

where:

ε_o = Instantaneous strain,

σ_o = Applied constant stress, and

E_o = Young's modulus of instantaneous deformation.

5.31 The retarded deformation can be illustrated by a mechanical model called a Kelvin-body. It is composed of a spring in parallel with a dashpot (See figure 5.5 a, b and c). The presence of the dashpot, representing an ideal viscous fluid, in a Kelvin-body causes the deceleration of strain rate when a constant stress is applied to the model. The decelerated strain which was caused by the constant stress will recover with time upon removal of the applied stress due to the energy stored in the parallel engaged spring.

The relationship between stress, strain and time for such a model under creep may be expressed as:

$$\varepsilon_1 = \frac{\sigma_o}{E_1} (1 - e^{-E_1 t/\Psi_1}). \qquad \ldots\ (5.4)$$

Where:

ε_1 = Reversible strain at decelerating rate of strain,

σ_o = Constant applied stress,

E_1 = Young's modulus at declerating strain rate,

t = time,

Ψ_1 = coefficient of compressive viscosity,

The coefficient of compressive viscosity Ψ and consequently η_1, the coefficient of shearing viscosity is found to be temperature and stress dependent.

5.32 The irreversible deformation under creep can be illustrated by a mechanical model consisting of a single dashpot (see figure 5.6a, b and c).

The stress-strain-time relationship may be expressed as:

$$\varepsilon_2 = \frac{\sigma_o t}{\Psi_2} . \qquad \ldots\ (5.5a)$$

Where:

ε_2 = irreversible creep strain at constant rate of strain,

σ_o = constant applied stress,

t = time, and

Ψ_2 = coefficient of compressive viscosity at constant rate of strain.

This type of deformation is not recoverable upon removal of the applied stress.

5.33 A combination of these three models illustrated in paragraph 5.30, 5.31 and 5.32 appears to exhibit the ideal behavior of frozen soils. Figure 5.7 a, b and c illustrate the combination of the above mentioned elements in series which, in rheology, is called a Burger's body (21).

5.34 The ratio of relative magnitude of viscous to elastic response $\frac{\Psi}{E}$ is in general, referred to as transition time T_T. If the model is subjected to shearing stresses, $T_T = \frac{\eta}{G}$ in which η and G are the coefficient of shearing viscosity and shear modulus respectively. This ratio, however, is the retardation time, the time interval in which the decelerating strain accrues when the applied stress $\sigma = \sigma_o$. On the other hand, this ratio is called relaxation time, the time interval in which the stress release accrue, when the applied stress σ is reduced to zero (See figure 5.5 b & c). The transition time has a dimension of time (23).

When a Kelvin model is stressed, part of the deformation energy will be stored in the spring while the remainder will be dissipated in the dashpot (See fig. 5.5a and b). If at time t = o, σ = o, the stress-strain-time relationship for a Kelvin model under a constant stress σ_o is given by

$$\varepsilon_1 = \frac{\sigma_o}{E_1} \left(1 - e^{\frac{-E_1 t}{\Psi_1}} \right). \qquad \ldots\ (5.5)$$

Hence, ε_1 increases exponentially with time. When $\frac{\Psi_1}{E_1} = t$, ε_1 approaches $\frac{\sigma_o}{E_1}$, the amount that the spring would have extended in the absence of the dashpot. On release of stress σ_o, ε_i decreases exponentially and approaches zero (See figure 5.5b and c) at time

$$t = T_T = \frac{\Psi}{E}, \text{ or } \frac{\eta}{G} .$$

5.35 The combination of a spring connected to a dashpot in series is called a Maxwell element. The ratio of $\frac{\Psi}{E}$ or $\frac{\eta}{G}$ in the Maxwell model is termed the relaxation time as mentioned in paragraph 5.34. For a Maxwell element under a given constant stress increment,

$$\varepsilon = \frac{\sigma_o}{E_o} + \frac{\sigma_o t}{\frac{\Psi_2}{E_o} \times E_o} . \qquad \ldots\ (5.6)$$

Placing

$$T_T = \frac{\Psi_2}{E_o} ,$$

$$\varepsilon_o = \frac{\sigma_o}{E_o} + \frac{\sigma t}{T_T E_o} . \qquad \ldots\ (5.7)$$

When a Maxwell element is suddenly extended by ε_o, the force required to maintain this extension as a function of time is given by

$$\sigma = E_o \, \varepsilon_o e^{-\frac{E_o t}{\Psi_2}} \qquad \text{or}$$

$$\sigma = E_o \, \varepsilon_o e^{-\frac{t}{T_T}} . \qquad \ldots\ (5.8)$$

The boundary conditions used to obtain equation (5.8) were:

at $t = o$ $\qquad \sigma_o = E_o \, \varepsilon_o \qquad$ and

at $t = t$ $\qquad \sigma = \sigma$

When $t = T_T$ the stress relaxes from its initial value of $E_o \, \varepsilon_o$ to

$$\sigma = \frac{E_o \, \varepsilon_o}{e} , \qquad \ldots\ (5.9)$$

For $\varepsilon = 2\varepsilon_o$,

$$\sigma_{\varepsilon = 2\varepsilon_o} = \frac{2E_o\ \varepsilon_o}{e}$$

In which $\sigma_{\varepsilon = 2\varepsilon_o}$ is the stress produced by an initial compression of $\varepsilon = 2\varepsilon_o$ at $t = T_T$

For $\varepsilon = n\varepsilon_o$

Where n is an integer,

$$\sigma_{\varepsilon = n\varepsilon_o} = \frac{nE_o\ \varepsilon_o}{e} .$$

In which $\sigma_{\varepsilon} = n\varepsilon_o$ is the stress produced by an initial compression of $\varepsilon = n\varepsilon_o$ at $t = T_T$. .... (5.10)

Consequently, at time $t = \frac{\Psi_2}{E_o} = T_T$, any stress σ relaxes from its initial value of $nE_o\varepsilon_o$ or $n\sigma_o$ to $\frac{nE_o\ \varepsilon_o}{e}$ (See Fig. 5.9).

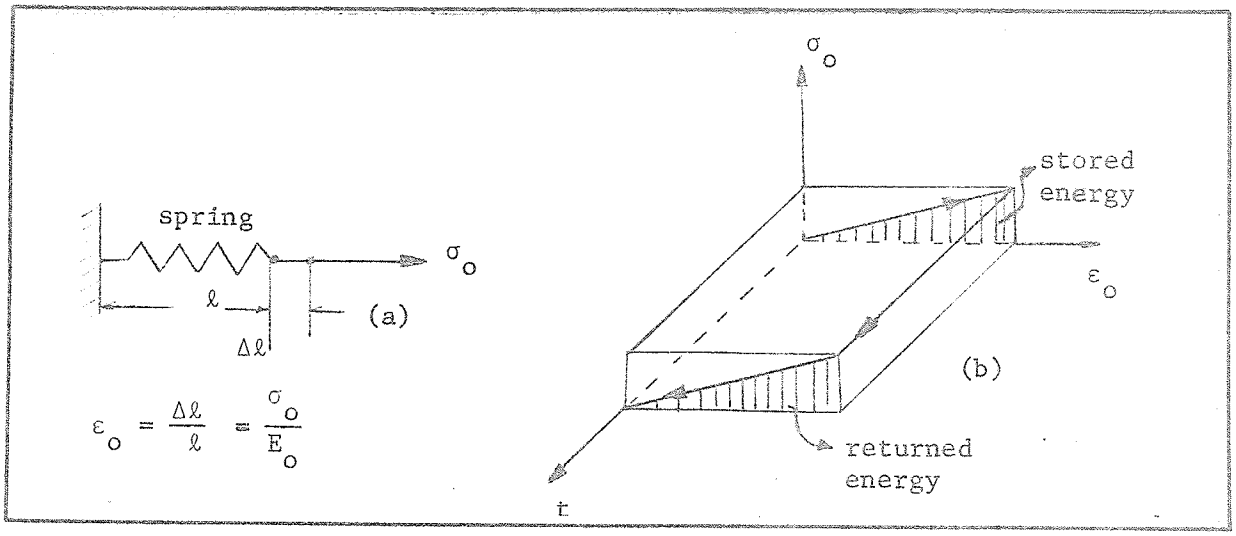

Figure 5.4 Instantaneous deformation: a) Mechanical model illustrating the instantaneous elastic deformation; b) Triaxial diagram of stress-strain time relationship of instantaneous elastic deformation.

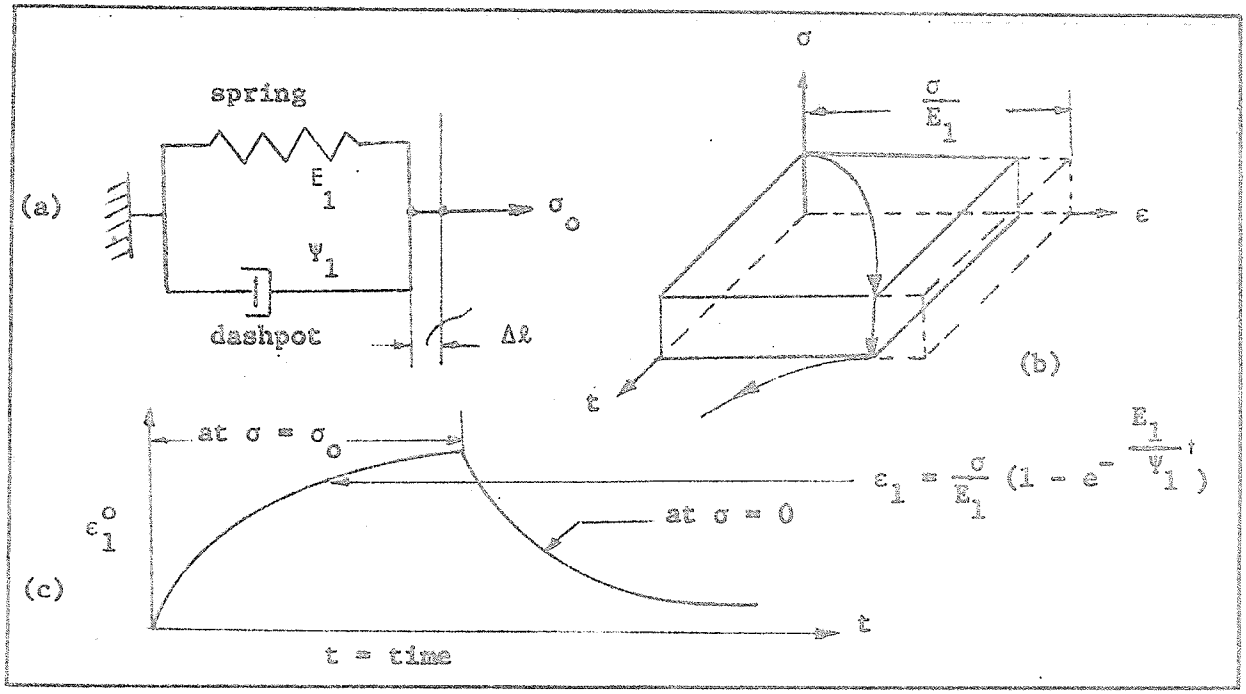

Figure 5.5 Retarded deformation: a) Mechanical model illustrating retarded deformation; b) Triaxial diagram of stress-strain time relationship; c) Strain-time relation.

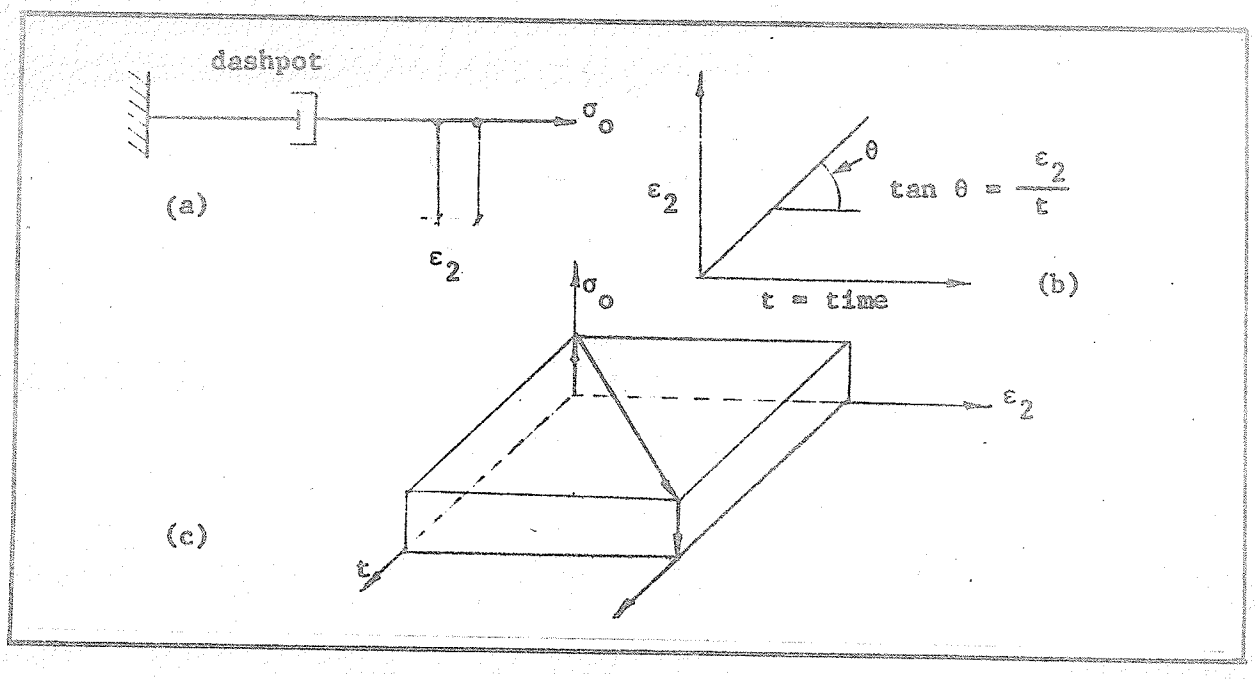

Figure 5.6 Irreversible deformation: a) Mechanical model b) strain-time relationship and c) stress-strain-time relationship.

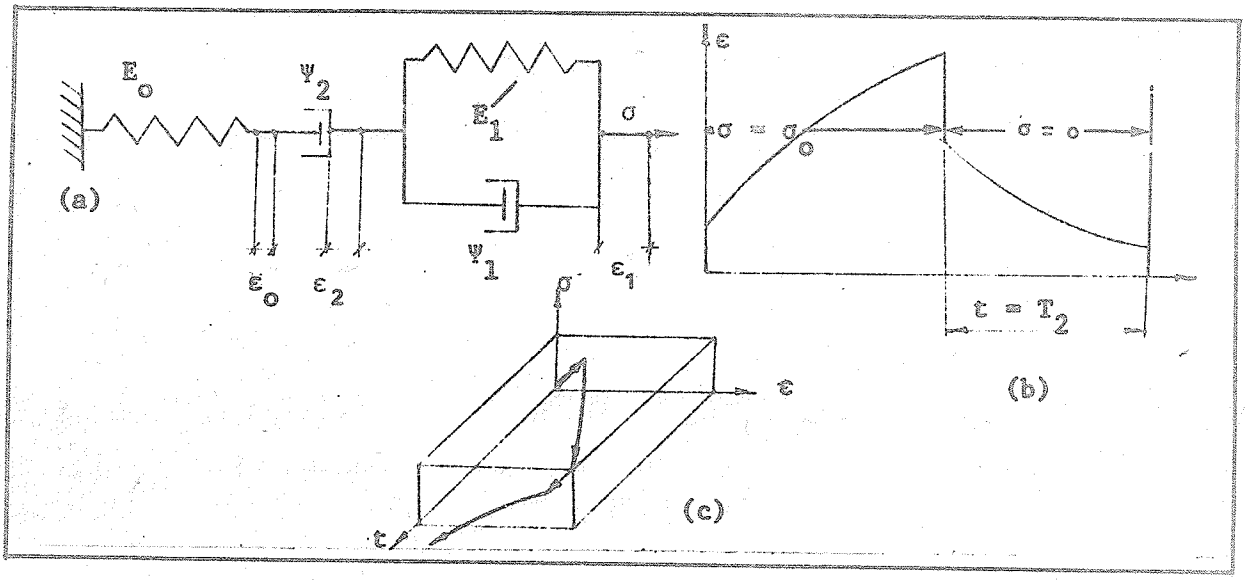

Figure 5.7 Burger's body: Combination of three basic mechanical models to demonstrate the ideal behavior of frozen soil. a) Mechanical model, b) Strain-time relationship and c) Stress-strain-time relationships.

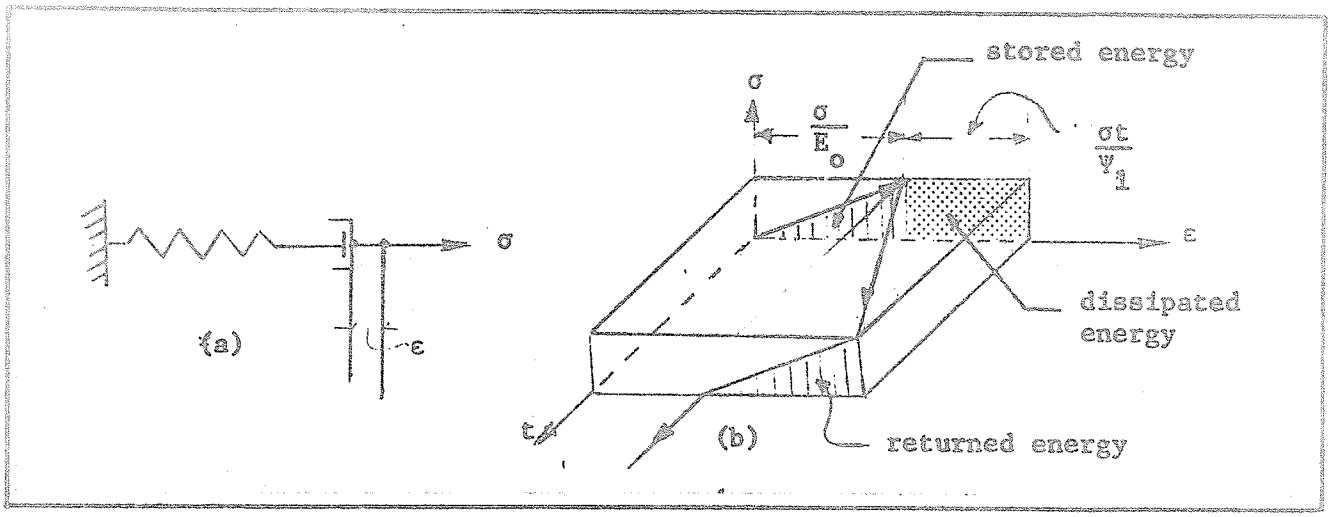

Figure 5.8 Stress Relaxation: a) Maxwell element, b) stress-time-deformation relationship for the element during application and removal of stress.

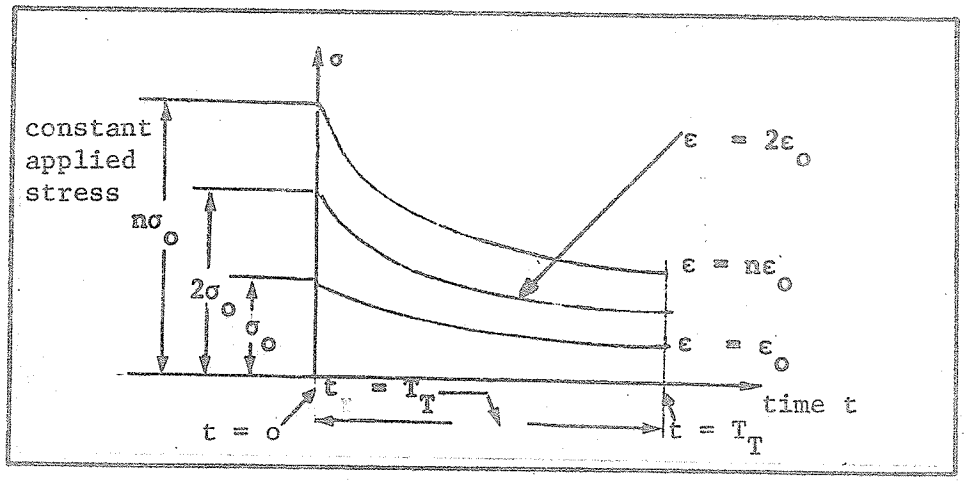

Figure 5.9 Relaxation curve when strain ε is applied at t = o.

5.36 Raymond N. Yong (17) states "From previous investigation and observation of specimen behaviour, it is apparent that ice content and unfrozen water content should also be considered in the evaluation of the strength of the frozen soil-water system.... It would seem that the greater the quantity of water remaining unfrozen, the lower would be the strength of partially frozen soil.... Unexplained is the development of unfrozen water in partially frozen soil, such as double layer water".

5.37 A. A. Nerseovo and N. A. Tsytovich (17) state that "Besides external influences (temperature and pressure), the main factors determining the unfrozen water content in frozen soil are: a) Specific surface area of the mineral solid phase of soil system, b) Chemical and mineralogical composition of soil, c) Physico-chemical characteristics, especially the nature of exchangeable cations, and d) Content and composition of water soluble compounds".

According to N. A. Tsytovich and Z. A. Nerseovo the absorbed water in most soils freezes completely, when the soil temperature is lowered to $-70^{o}C$. No unfrozen water, including absorbed water, can be detected in highly dispersed montmorillonitic clay when it is cooled to a temperature of $-193.8^{o}C$.

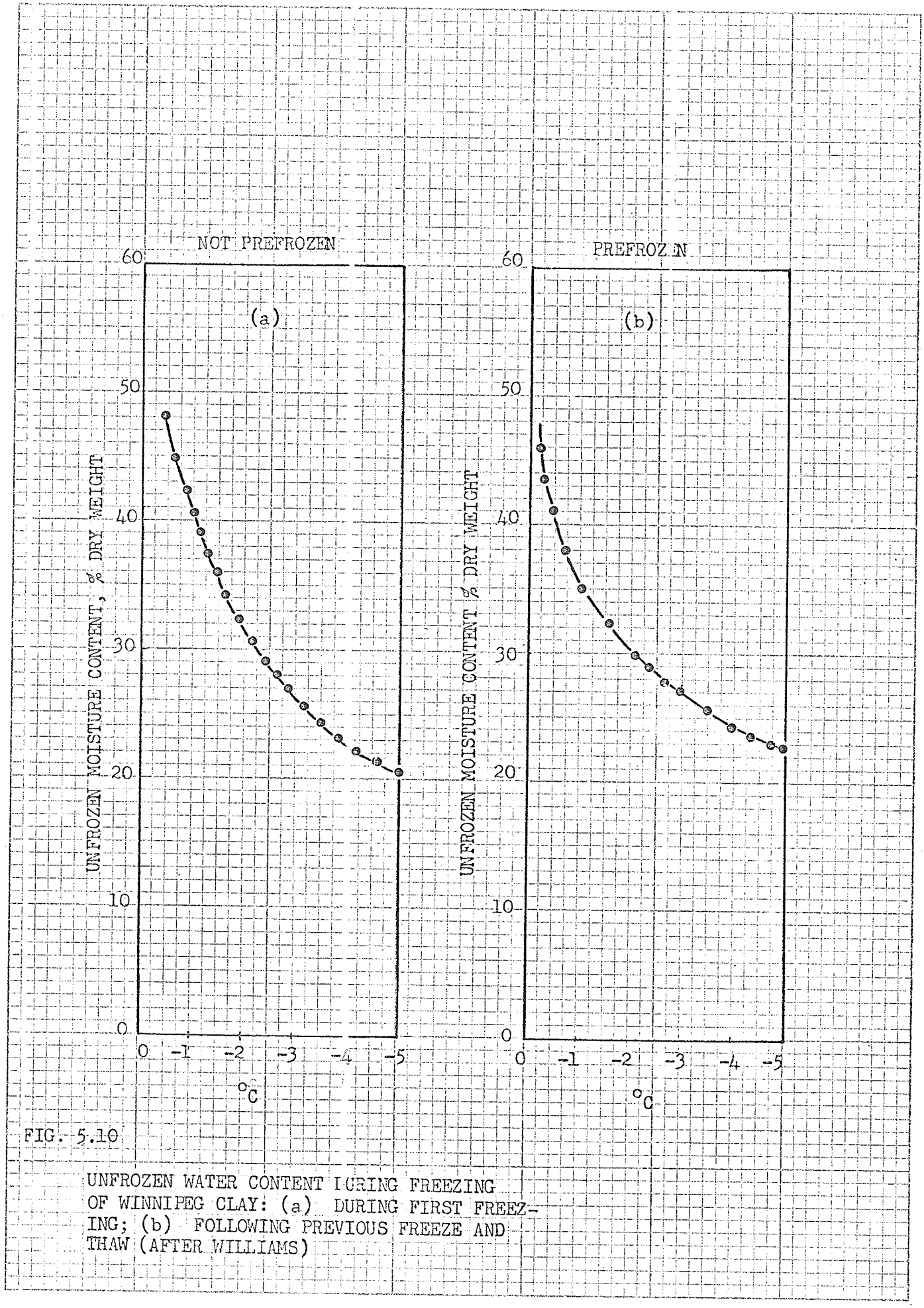

FIG. 5.10

UNFROZEN WATER CONTENT DURING FREEZING OF WINNIPEG CLAY: (a) DURING FIRST FREEZING; (b) FOLLOWING PREVIOUS FREEZE AND THAW (AFTER WILLIAMS)

5.38 P. J. Williams (18) has performed a comprehensive calorimetric investigation to determine the unfrozen water content of various frozen soils and, among them, frozen Lake Agassiz clay. The results of the investigation of Lake Agassiz clay, for unfrozen water content during the first freeze and following a previous freeze and thaw, are shown in Figure 5.10. Williams stated that the greatest depression of the freezing point below $0^{o}C$ presumably occurs in water that is most firmly held and is closest to the soil particles.

5.39 "The phenomenon of loss of strength by remolding has been given by Terzaghi (22) as follows: Each particle may be visualized as coated with a film of water in solid state (adsorbed water), (See fig. 5.11a). The state of this water is such that its viscosity is exceedingly high. If the soil sample is subjected to a pressure over a period of centuries, this water with high viscosity is slowly squeezed from between points of nearest contact of adjacent particles, giving the condition shown in (b). The closer contact which results between particles leads to a higher degree of true cohesional attraction. If the direct pressure is removed, the highly viscous water will flow back, but so slowly in some soils that years may elapse before the loss of strength is appreciable. However, remolding moves the

particles as shown in (c), and as a result the particles are more widely separated and strength is lost."

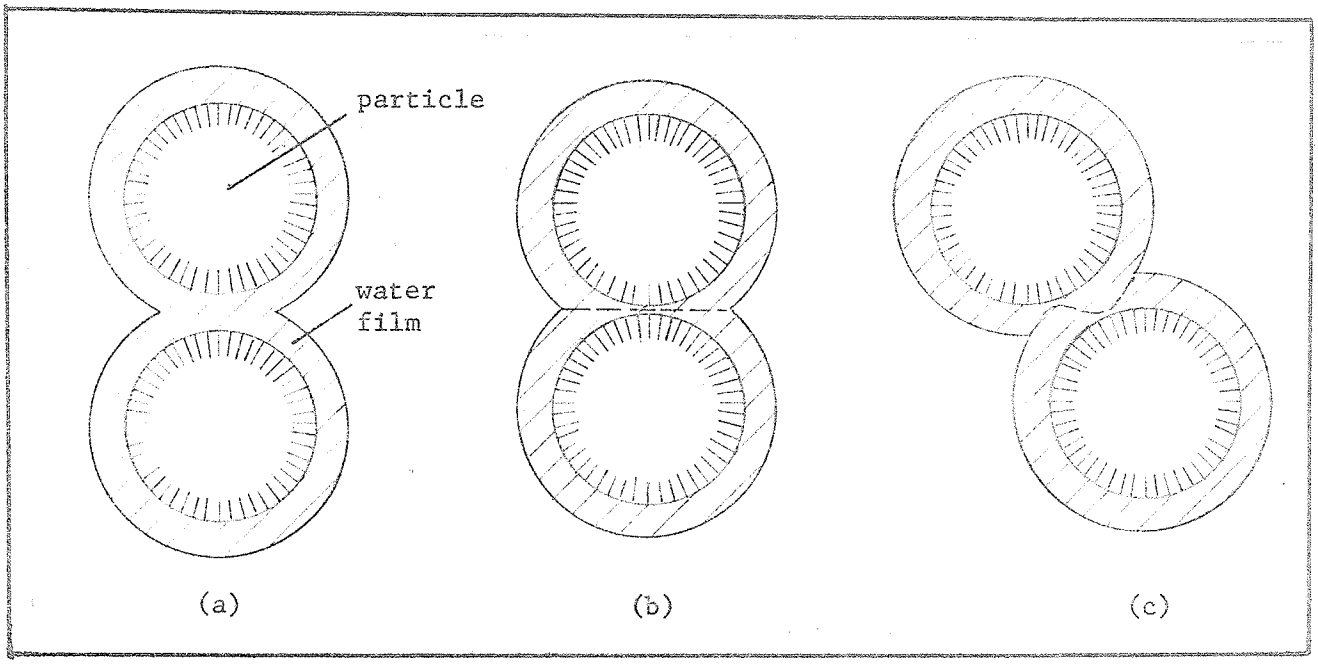

Figure 5.11 Water film explanation of structural bond (according to Terzaghi)

CHAPTER VI

OBSERVATION OF TESTS, EXPERIMENTAL TEST RESULTS AND DISCUSSION

6.1 The experimental test data on Glacial Lake Agassiz clays are presented in two parts. Part 1 deals with the study and observation of the freezing process. Part 2 deals with the study of the stress-strain behaviours under uniaxial loading and stress release (relaxation) of frozen soils. The strength behaviour of several thawed soil samples following one cycle of freezing was also studied. In both cases, undisturbed and remolded soil specimens were used and were frozen uniaxially or from all directions. The test results and findings of each set of tests have been summarized at the end of each part. The design, fabrication of equipment and instrumentation employed and their operation have been presented in Chapter II.

A. Part 1 - Data and Results of Freezing Process:

A total of 28 specimens was frozen in the following groups:

Group No. 1: Three completely saturated samples were frozen without external water being supplied to the samples. The bottom parts of the samples were kept at $27^{\circ}F$ in the heat exchange box for a minimum of 80 hours. The temperature of the top of the samples was kept above the freezing point at approximately $36^{\circ}F$.

CHAPTER VI

OBSERVATION OF TESTS, EXPERIMENTAL TEST RESULTS AND DISCUSSION

The samples were then removed from the heat exchange box in an insulated condition and placed in the freezing cell. The whole sample was allowed to freeze to a uniform temperature of 27 ±0.5F.

Group No. 2: Thirteen completely saturated samples with no supply of external water were placed directly in the freezing cell for uniform freezing as follows:

a 1 sample at 31.5°F,

b 4 samples at 27°F,

c 5 samples at 17°F, and

d 3 samples at 7°F.

The samples under c were cooled initially to 27°F. When heave or contraction had ceased for a minimum of 3 hr., the temperature was reduced to 17°F.

Also, three samples were initially frozen at 27°F, and kept at this temperature until deformation ceased. Then the temperature was reduced to 17°F and maintained at this lower temperature until no deformation occurred for a minimum of three hours. The temperature of these samples was then further reduced to 7°F.

Group No. 3: Six completely saturated samples were frozen in the heat exchange box for a minimum of 300 hr. with a predetermined quantity of external water being supplied laterally to the samples. Filter strips were placed at various heights along each sample (See paragraph 4.6). During the first step of freezing the bottom parts of

the samples were kept at 27°F for 320 to 390 hr., while the tops of the samples were kept at 34°F to 39°F until heaving completely stopped. Then the samples were transferred to the freezing cell for complete freezing at 27±0.5F.

6.2 In order to limit the length of presentation of the observations of Part 1, only five typical test results are discussed.

6.3 The grain size distribution curves for a typical Glacial Lake Agassiz clay indicate that the clay is frost-heave susceptible due to a high percentage of fine materials, according to criteria by Casagrande, Nielsen, and Rauschenberger and Lothar Schaible (see paragraphs 5.15, 5.16, 5.17 and fig. 3.3, 5.1 and 5.2). Consequently a high capillary rise is anticipated. However, because of low permeability in the range of 10^{-9} cm. per sec. (see paragraph 3.7), the heaving potential is minimized. This is due to the crystallization of the pore water caused by freezing and consequent blocking of the fine capillaries of the soil (see paragraph 5.5).

6.4 Photograph (6.1) shows ice segregation in sample OC-N-27-116 of Group No. 1. This sample was put in the heat exchange box for 141 hrs., keeping the temperature of the bottom part of the sample at 27±0.5°F, and the top of the sample at 36±0.5°F. This allowed enough time for migration of the pore water from the unfrozen portion of the sample down to the freezing front where ice crystals could form. In the

Photograph 6.1

horizontal ice segregation caused by slow, uniaxial freezing of sample OC-N-27-116

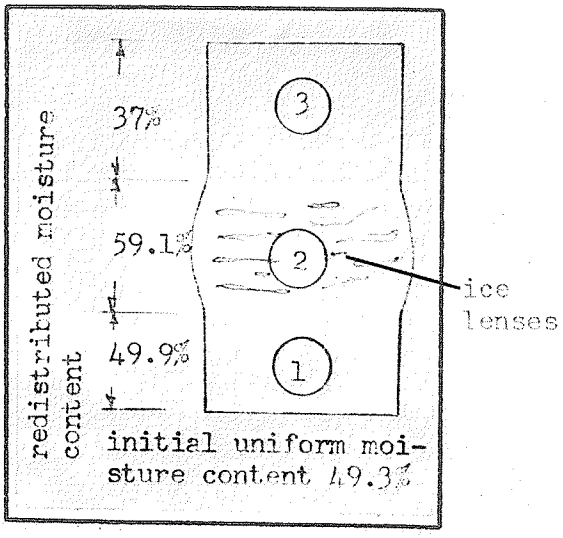

Fig. 6.1

ice segregation caused by slow, uniaxial freezing and moisture redistribution of sample OC-N-116

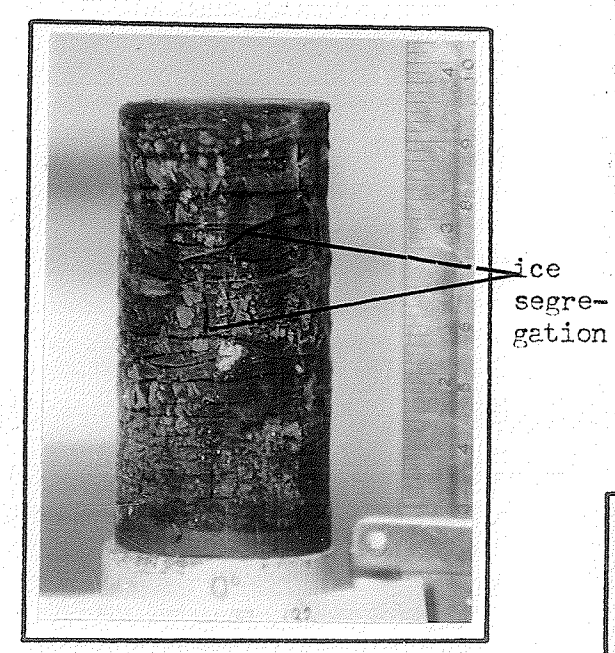

Photograph 6.2

uniform horizontal ice segregation due to rapid uniaxial freezing of sample O1-N-17-132

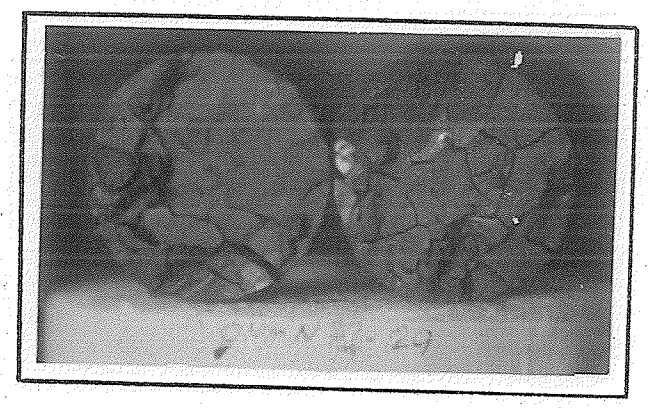

Photograph 6.3

cross-sectional view of polygonal pattern of vertical cracks filled with ice of sample OC-N-27-29

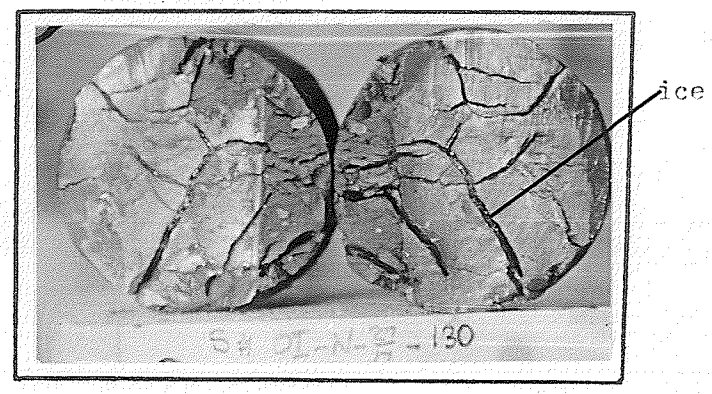

Photograph 6.4

cross-sectional pattern of vertical cracks filled with ice of sample O1-N-17-130

second stage, the sample was transferred to the freezing cell for uniform cooling to 27 $\pm$ 0.5°F. After the transfer, the sample started to contract. Moisture contents, based on the entire sample before commencing freezing and on three portions of the samples as shown in fig. 6.1 after complete freezing, indicated the following:

Before freezing, the moisture content of the entire sample was 49.3%.

After freezing, the moisture content of Portion 1 was 49.9%.

The moisture content of Portion 2 where ice crystallization had taken place was increased to 59.1%.

The moisture content of Portion 3 was reduced to 37% causing a strength reduction as discussed subsequently.

6.5 When the soil samples were frozen as outlined in Group No.2, uniform ice segregation took place throughout the length of the sample. Photograph 6.2 shows the uniform ice segregation of sample OI-N-17-132. Horizontal and vertical cracks were filled with ice from the water removed from clay. This action is attributed to suction set up during the crystallization process (see Paragraph 5.7 and 5.8). Photograph 6.3 and 6.4 show in cross-sectional view, the ice filled cracks forming a polygonal pattern. The moisture content of the samples of Group 2 (when frozen) underwent a redistribution in the horizontal direction only. The moisture content determination of

different slices at different heights of each sample showed a deviation of moisture content of ±3% from its original uniform moisture content. This deviation was apparently due to the accumulation of ice in the vertical cracks which were filled with different thicknesses of ice.

6.6 The purpose of the tests on the third group of samples was to find out if the frost behaviour of Lake Agassiz clay would change when water was supplied parallel to the varves. In nature this would be comparable to a situation close to the river banks, lake shores, drainage ditches and grounds close to heated areas, or in areas of sporadic permafrost .

Predetermined quantities of water varying between 12 and 21 grams per sample were supplied to the samples laterally during the freezing process (see Table 6.6). The quantity of water supplied was totally absorbed by the samples in 50 to 70 hours after the samples were placed in the heat-exchange box. Photograph 6.5 shows a typical sample OC-R-27-122 for which the water was supplied laterally. The predetermined quantity of 13 grams of water was absorbed by the sample in 60 hrs. The heaving of the soil sample ceased in 450 hrs. of elapsed time. Then the sample was transferred to the freezing cell for complete freezing at $27^{o}F \pm 5^{o}F$. After 80 hrs. in the freezing cell the heave of the sample, following the transfer of the sample, had decreased by 5%,

indicating completion of ice crystallization (See Fig. 6.2).

As noted previously (Paragraph 4.6), the filter strips used to supply moisture were blocked off with nonpermeable tape so that only specified zones of the sample had access to the external water supply. In the tests, this arrangement worked very well because ice crystallization started immedidately at the lowest point of the predetermined zone that had access to water. First, 1/32 inch thick ice crystals accumulated at the upper limit of the predetermined zone. Photograph 6.7 illustrates the tearing of the filter strips due to heaving.

In the sample shown in Photograph 6.6, the water supply strip was blocked from the base to a point 1 inch above the base. Then a 1.05 inch zone was left unblocked to provide water to the sample. The water supply strip was blocked from the top of the zone to the top of the sample. The predetermined water supply of 20 grams was completely absorbed by the sample in 76 hrs., after placing the sample in the heat-exchange box. After 358 hrs. of elapsed time, the sample was removed from the heat-exchange box and transferred to the freezing cell at $27^{o}F \pm 5^{o}F$. At that time, the total heave was 26.2%. During the next 25 hrs., an additional 10% of heaving occurred. The horizontal and vertical cracks above the upper limit of the water supply zone indicate further moisture withdrawal to the freezing front from the upper layer of the soil

after the sample was removed to the freezing cell. Photographs 6.6 and 6.9 show the ice build-up in the vertical cracks beyond the water supply zone in sample OC-R-27-119. This also indicates the suction set up above the upper limit of the water supply zone to form vertical and horizontal cracks similar to the ice segregation as found in samples of Group No. 2.

In all six samples of Group No. 3, the freezing plane did not remain stationary. Although the rate of water supply was constant, the rate of cooling varied somewhat within the operational limits of the thermostat of the cooling system (See Paragraph 5.9).

The distance of the freezing front of sample OC-R-27-119 was longer than sample OC-R-27-122 (compare Photographs 6.5 and 6.6). Because of the longer distance of the freezing front of the latter sample, the heat flow given off from the freezing front and the heat loss to the surface were in equilibrium. Consequently, no additional freezing could take place in the heat-exchange box. Furthermore, moisture in the ufrozen state remained unfrozen at the top of the sample and was frozen after the sample was taken from the heat-exchange box and placed in the freezing cell.

6.7 Heaving versus time and temperature graphs of the 5 samples of Groups 1, 2 and 3 are shown in figures 6.2 and 6.3

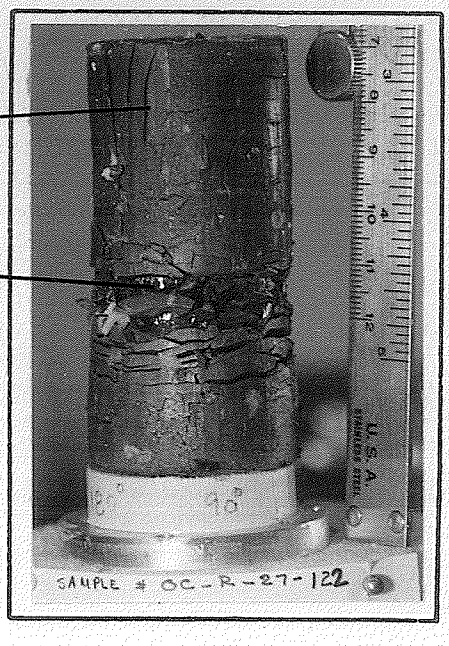

Photograph 6.5 Ice crystallization produced by external water supply during freezing process of sample OC-R-27-122

Photograph 6.6 Ice crystallization produced by external water supply during freezing process of sample OC-R-27-119

Photograph 6.7 External water supply strips disrupted during freezing

Photograph 6.8. Ice crystallization at water supply zone and ice sheet buildup in the shrinkage cracks above water supply zone of sample OC-R-27-119

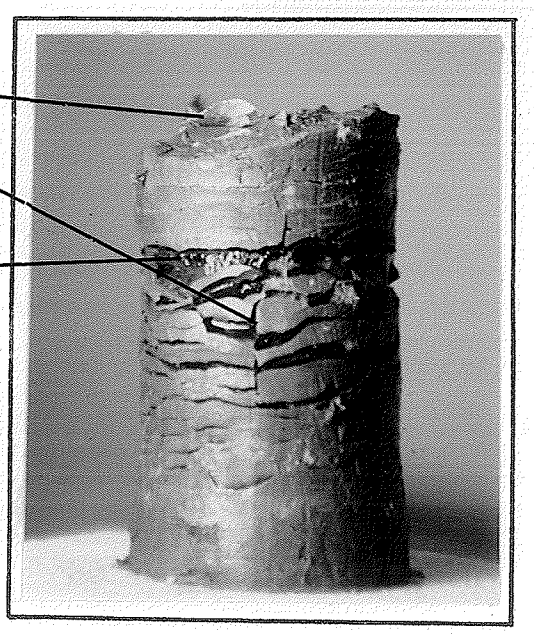

Photograph 6.9 Ice crystallization and ice sheet buildup of sample OC-R-27-119 by external water supply

6.8 The frost heave of five samples was calculated using formulas (5.1) and (5.2) and compared with experimental results (See Tables 6.1 to 6.6). Computed and observed values of heave are shown in Table 6.6. For comparison, the computed values have been expressed as ratios of the observed values. They are also shown in Table 6.6. In the samples frozen without a water supply, the ratios were found to be 0.68, 0.47, 0.65 for samples OC-N-27-116, OC-N-17-124 and OC-N-17-132, respectively. For the samples frozen with water supply, the ratios were found to be 0.93 and 1.27 for samples OC-R-27-119 and OC-R-27-122 respectively.

The calorimetric test results of P. J. Williams (18) (See graph 5.38) were used to determine the relative ice content.

6.9 Clear ice lenses were observed in samples that were frozen undisturbed and uniaxially, indicating the state of molding of samples prior to freezing. No ice lenses could be seen in soil samples that were frozen undisturbed or remolded and frozen from all-around. This agrees with Taber's findings which are summarized in Paragraph 5.11.

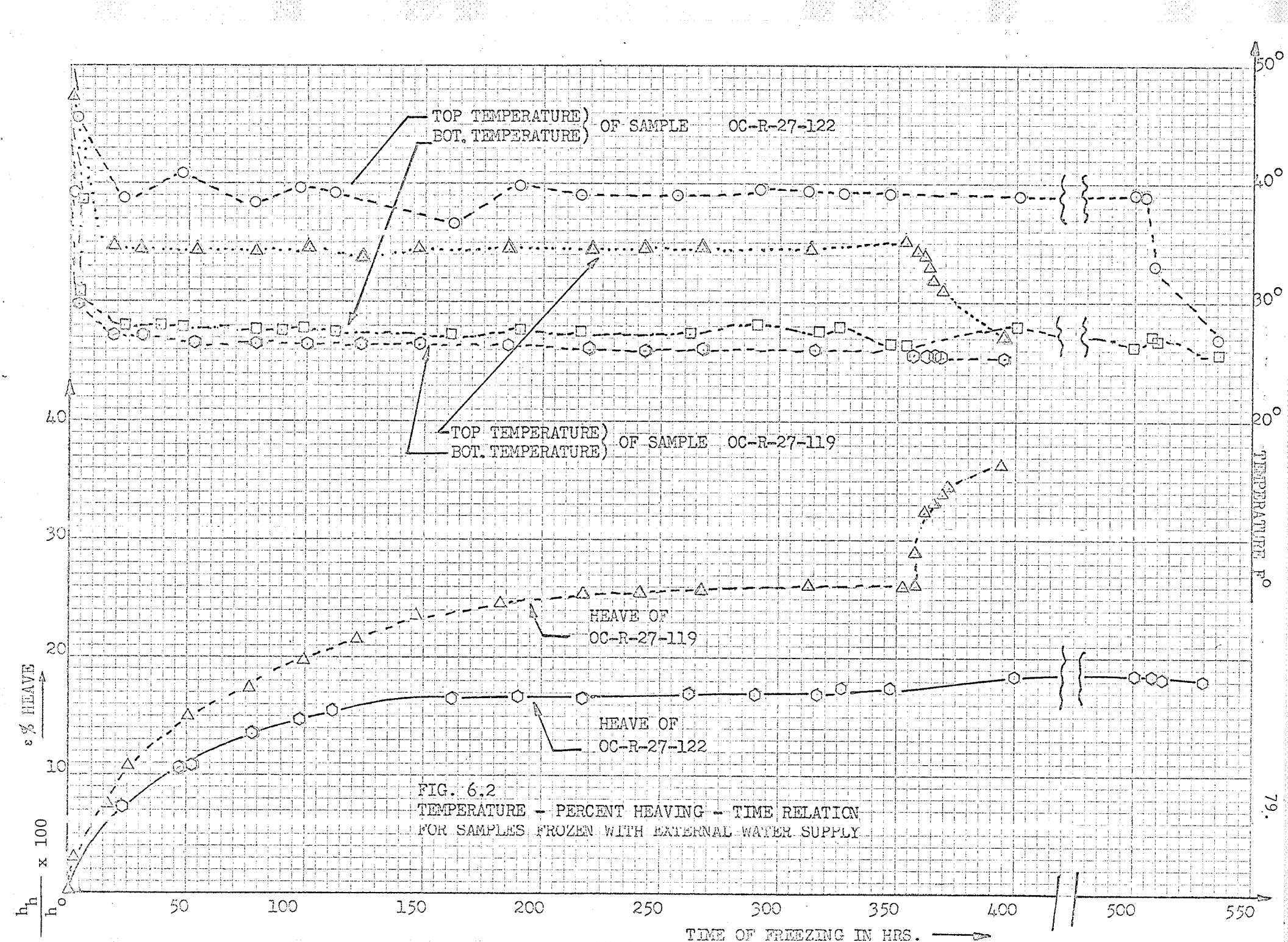

FIG. 6.2
TEMPERATURE - PERCENT HEAVING - TIME RELATION
FOR SAMPLES FROZEN WITH EXTERNAL WATER SUPPLY

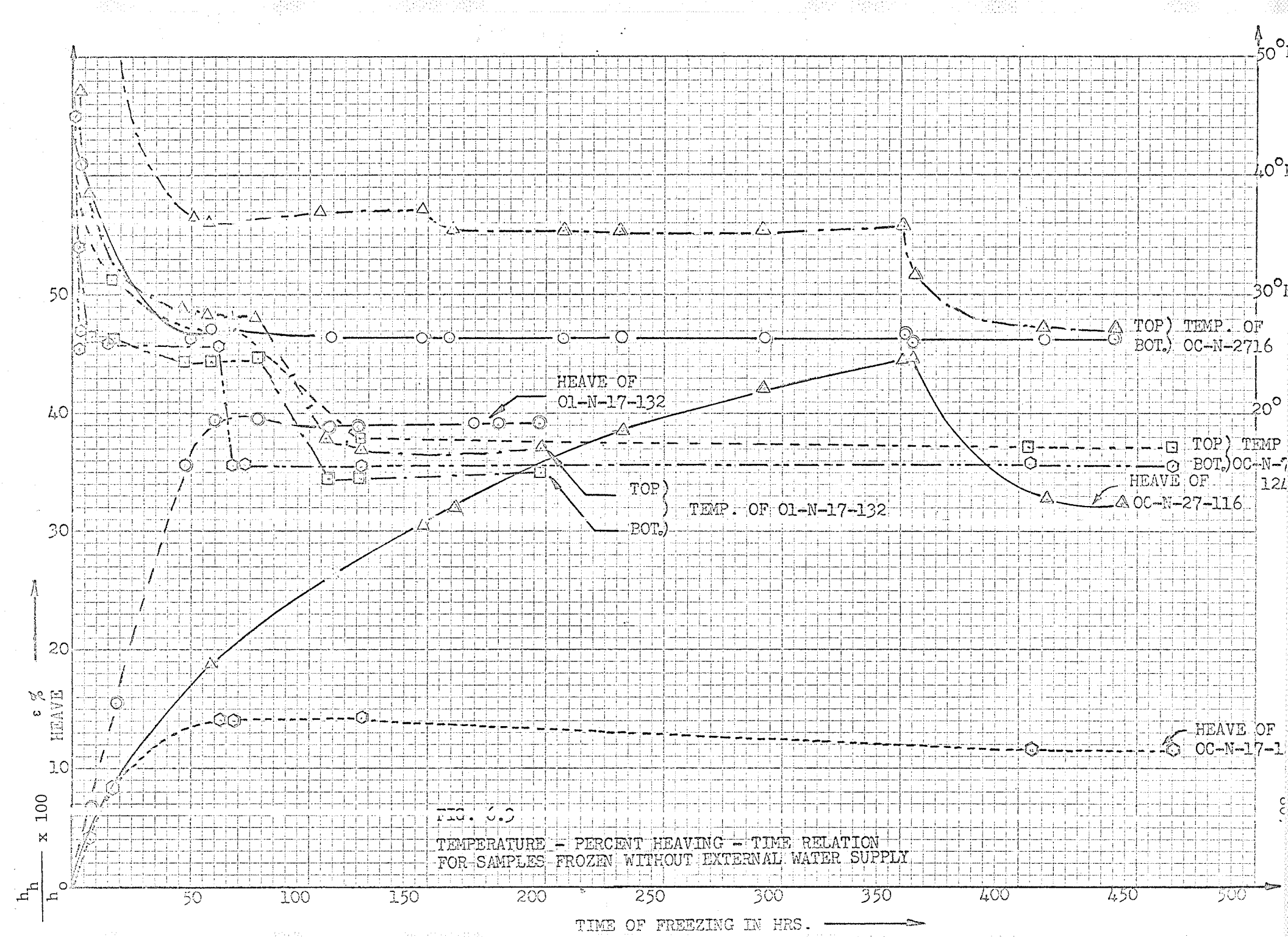

FIG. 6.3

TEMPERATURE - PERCENT HEAVING - TIME RELATION
FOR SAMPLES FROZEN WITHOUT EXTERNAL WATER SUPPLY

TABLE 6.1
HEAVE (IN PERCENT) - TIME RELATION
FOR SAMPLE OC-N-27-116 FROZEN AT 27°F
WITH NO EXTERNAL WATER SUPPLY TO THE SAMPLE

Elapsed Time in Hrs. Hr.	Min.	Temperature of sample in F° BOT.	TOP	Heave of sample in inches	Heave In Percent	Remarks
0	00	38	78	0	0	Sample placed in heat exchange box, thermostat at 27°F
1	00	32	63	.0030	0.109	
20	00	26.5	36.5	.0460	1.680	
23	55	27.0	36.0	.0520	1.890	
44	00	26.5	37.0	.0725	2.640	
58	55	26.5	37.0	.0830	3.050	
65	35	26.5	35.2	.0880	3.200	
83	20	26.5	35.2	.0960	3.450	
93	55	26.5	35.2	.1060	3.850	
117	45	26.5	35.2	.1156	4.180	
141	00	26.5	35.8	.1220	4.450	
141	00	26.5	34.5	.1220	4.450	Sample transferred to freezing cell for complete freezing
142	05	26.0	31.5	.1215	4.441	
142	30	26.0	31.0	.1205	4.438	
164	15	26.0	27.0	.0920	3.250	
176	40	26.0	27.0	.0925	3.250	

TABLE 6.2
HEAVE (IN PERCENT) - TIME RELATION
FOR SAMPLE OC-N-17-124 FROZEN AT 17°F
WITH NO EXTERNAL WATER SUPPLY TO THE SAMPLE

Elapsed time in Hrs. Hr.	Min.	Temperature of sample in F° BOT.	TOP	Heave of sample in inches	heave in percent	Remarks
0	00	45	59	0	0	Sample placed in freezing cell thermostat set at 27°F
0	15	34	57	0	0	
0	20	27	55.5	.0030	.108	
0	30	25.5	54	.0080	.288	
0	45	25.5	51.0	.0105	.362	
1	00	25.5	47.0	.0130	.468	
1	15	26.0	45.0	.0135	.486	
6	00	26.0	32.5	.0240	.865	
25	00	25.0	27.0	.0395	1.430	
27	15	15.0	27.0	.0390	1.405	Thermostat set down to 17°F
27	35	15.5	20.5	.0390	1.405	
49	30	15.5	18.0	.0390	1.405	
162	00	15.5	17.0	.0320	1.155	
186	00	15.5	17.0	.0320	1.155	

TABLE 6.3
HEAVE (IN PERCENT) - TIME RELATION
FOR SAMPLE OI-N-17-132 FROZEN AT 17°F
WITH NO EXTERNAL WATER SUPPLY TO THE SAMPLE

Elapsed time in Hrs. Hr.	Min.	Temperature of sample in F° BOT.	TOP	Heave of sample in inches	heave in percent	Remarks
0 -	00	39.5	80.0	0	0	Sample placed in freezing cell, thermostat at 27°F
-	25	35.0	72.0	0	0	
3 -	00	26.5	38.5	.0190	0.680	
7 -	10	26.5	31.5	.0440	1.585	
18 -	25	25.5	28.0	.0990	3.565	
23 -	45	25.0	27.5	.1105	3.975	
31 -	25	25.5	27.0	.1105	3.975	Thermostat set down to 17°F
31 -	35	25.3	27.0	.1105	3.890	
43 -	30	15.5	18.0	.1082	3.900	
46 -	10	15.5	18.0	.1087	3.916	
48 -	10	15.5	17.5	.1088	3.916	
50 -	30	15.5	17.5	.1088	3.916	
51 -	30	15.5	17.0	.1089	3.917	
68 -	00	15.5	17.0	.1083	3.900	
72 -	16	15.5	17.0	.1083	3.900	
78 -	32	15.5	17.0	.1085	3.915	

TABLE 6.4
HEAVE (IN PERCENT) - TIME RELATION
FOR SAMPLE OC-R-27-119 FROZEN AT 27°F
WITH EXTERNAL WATER SUPPLY

Elapsed time in Hrs. Hr.	Min.	Temperature of sample in F° BOT.	TOP	Heave of sample in inches	Heave in percent	Remarks
0 -	00	39.5	66.5	0	0	Sample placed in heat exchange box, thermostat at 27°F with provision of external water supply
17 -	20	27.0	34.5	.2125	7.650	
27 -	45	27.0	34.5	.2980	10.790	
51 -	40	26.5	34.5	.4060	14.630	
76 -	00	26.5	34.5	.4980	17.350	End of water supply
100 -	05	26.2	34.5	.5460	19.750	
123 -	05	26.2	33.8	.6038	21.780	
148 -	25	26.2	34.5	.6635	23.900	
185 -	35	26.2	34.5	.6668	24.100	
217 -	35	26.0	34.5	.6980	25.200	
242 -	10	26.0	34.5	.7150	25.850	
268 -	55	26.0	34.5	.7190	25.950	
290 -	25	26.0	34.5	.7190	25.950	
314 -	10	26.5	35.0	.7220	26.050	
353 -	45	26.0	34.0	.7250	26.100	
358 -	40	25.5	34.2	.7255	26.200	Sample transferred to the freezing cell for complete freezing
359 -	40	25.5	33.0	.8055	29.050	
363 -	10	25.2	32.0	.8555	30.820	
363 -	40	25.5	31.0	.9885	35.600	
384 -	05	25.5	27.3	1.0015	36.200	

TABLE 6.5
HEAVE (IN PERCENT) - TIME RELATION
FOR SAMPLE OC-R-27-122 FROZEN AT 27°F
WITH EXTERNAL WATER SUPPLY

Elapsed time in Hrs. Hr. - Min.	Temperature of sample in F° BOT.	TOP	Heave of sample in inches	heave in percent	Remarks
0 - 00	56.5	78.0	0	0	Sample placed in heat exchange box, thermostat at 27°F with external water supply
2 - 45	30.5	45.5	.0790	2.845	
23 - 45	28.0	38.5	.1990	7.230	
59 - 25	28.0	40.5	.2940	10.600	
52 - 15	27.5	38.0	.3765	13.700	End of water supply
97 - 45	28.0	39.5	.4030	14.620	
121 - 30	27.5	39.0	.4240	15.400	
161 - 05	27.5	37.5	.4540	16.550	
191 - 45	27.8	39.5	.4600	16.700	
217 - 55	27.5	39.0	.4610	16.750	
261 - 15	27.5	39.0	.4650	16.900	
291 - 15	28.0	39.5	.4645	16.850	
315 - 30	27.5	39.2	.4695	16.900	
327 - 45	28.0	39.0	.4769	17.320	
348 - 30	26.5	39.0	.4750	17.280	
402 - 30	28.2	39.0	.5120	18.610	
450 - 30	26.5	39.0	.5130	18.650	Sample transferred to the freezing cell for complete freezing
510 - 15	27.5	39.0	.5190	18.650	
511 - 35	27.0	33.0	.5090	18.500	
530 - 15	25.5	27.0	.4960	18.050	

TABLE 6.6
EXPERIMENTAL AND COMPUTED FROST
HEAVE RESULTS

Sample No.	% Total moisture content	Weight of dry soil grams	Volume of external water supply, cu. cm.	% Unfrozen wtr. content	Cross-sectional area sq. cms.	i_o% Relative ice cont.	Heave h_e obtained cms. experimental	Heave h_e obtained cms. computed	Ratio of computed vs. experimental
OC-N-27-116	49.3	80.4	-	25	9.95	49	0.234	0.1595	0.68
OC-N-17-124	48.5	79.5	-	25	9.90	49	0.081	0.1720	0.47
OC-N-17-132	48.6	79.0	-	25	9.72	49	0.272	0.1765	0.65
OC-R-27-119	49.25	79.6	20.18	25	9.90	49	2.545	2.3610	0.93
OC-R-27-122	49.4	80.8	13.30	25	9.95	49	1.270	1.6150	1.27

NOTES: For the computation of heave an average water content of 49.0 has been taken.

For unfrozen water content in frozen soil the test result of P.J. Williams was used see Fig. 5.6.

B. Part II - Data and Test Results of Stress-Strain-Time And Strength Behaviours

6.10 In this part of the investigation, the followings were investigated for frozen Lake Agassiz clay:

1) The effect of normal stress and temperature on the visco-elastic properties under uniaxial constant load,

2) The effect of stress release over a period of time on strained frozen soils, and

3) The unconfined strengths of thawed out soil samples following one cycle of freezing.

Because of the complex difficulties involved in obtaining direct shear strengths of frozen soils, it was decided to relate compressive stress and the coefficient of compressive viscosity to shear stress and coefficient of shearing viscosity under the following assumptions:

a - The specimens were completely saturated,

b - The volume of the specimens remains constant at all times,

c - Originally plane and parallel surfaces remain plane and parallel, and

d - The presence of friction between top and bottom plates between which the sample is placed can be neglected.

6.11 Under the assumptions made in Paragraph 6.10 [23]

(See Fig. 6.4):

For an isotropic elastic body stressed under uniaxial compression,

$$\varepsilon_z = \frac{1}{E} \cdot \sigma_z; \qquad \gamma_{12} = \frac{1}{G} \cdot \tau_{12} \qquad \ldots\ldots (6.1a)$$

For an isotropic viscous body stressed under uniaxial compression

$$\varepsilon_z^o = \frac{1}{\Psi} \cdot \sigma_z; \qquad \gamma_{12}^o = \frac{1}{\eta} \cdot \tau_{12} \qquad \ldots\ldots (6.1b)$$

Where

ε_z = compressive elastic strain,

ε_z^o = rate of compressive viscous strain,

γ_{12} = maximum elastic shearing strain,

γ_{12}^o = rate of maximum viscous shearing strain,

σ_z = compressive principal stress,

τ_{12} = maximum shearing stress,

η = coefficient of shearing viscosity,

E = Young's modulus of elasticity,

Ψ = coefficient of compressive viscosity,

G = modulus of rigidity.

Considering the volume to remain constant for a cube of sides ℓ_o being elastically or plastically transferred to a parallelepiped

with sides ℓ_1, ℓ_2, ℓ_3, after application of load we have:

$$\frac{\ell_1}{\ell_0} \cdot \frac{\ell_2}{\ell_0} \cdot \frac{\ell_3}{\ell_0} = 1 \quad . \qquad \ldots\ (6.2)$$

Consequently, the sum of natural logarithmic strains is:

$$\ell_n \left(\frac{\ell_1}{\ell_0} \right) + \ell_n \left(\frac{\ell_2}{\ell_0} \right) + \ell_n \left(\frac{\ell_3}{\ell_0} \right) = 0 \quad .$$

Writing $\bar{\varepsilon}_1 = \ell_n \left(\frac{\ell_1}{\ell_0} \right)$, $\bar{\varepsilon}_2 = \ell_n \left(\frac{\ell_2}{\ell_0} \right)$ and $\bar{\varepsilon}_3 = \ell_n \left(\frac{\ell_3}{\ell_0} \right)$,

the sum of logarithmic strains is:

$$\bar{\varepsilon}_1 + \bar{\varepsilon}_2 + \bar{\varepsilon}_3 = 0 \quad . \qquad \ldots\ (6.3)$$

For uniaxial loading in the 1 direction,

$$\bar{\varepsilon}_2 = \bar{\varepsilon}_3 = -\mu \bar{\varepsilon}_1 \quad . \qquad \ldots\ (6.4)$$

Combining (6.3) and (6.4), the Poisson's ratio for a saturated, isotropic, elastic soil with no volume change is

$$\mu = 1/2 \quad . \qquad \ldots\ (6.5)$$

From equations (6.3), (6.4) and (6.5) one obtains

$$\bar{\varepsilon}_2 = \bar{\varepsilon}_3 = -\frac{\sigma_z}{2E} \quad . \qquad \ldots\ (6.6a)$$

It follows

$$\bar{\varepsilon}^o_1 + \bar{\varepsilon}^o_2 + \bar{\varepsilon}^o_3 = 0 \quad ,$$

And

$$\bar{\varepsilon}^o_2 = \bar{\varepsilon}^o_3 = -\frac{\sigma_z}{2\Psi} \quad . \qquad \ldots\ (6.6b)$$

Where $\bar{\varepsilon}^o_1$, $\bar{\varepsilon}^o_2$ and $\bar{\varepsilon}^o_3$ are the rate of logarithmic strain in the 1, 2 and 3 directions respectively.

Reference to Fig. 6.4, for uniaxial compression in the 1 direction (z direction), $\sigma_y = 0$. The maximum shearing stress is given by

$$\tau_{12} = \frac{1}{2} (\sigma_z - \sigma_y) \quad ,$$

$$\tau_{12} = \frac{1}{2} \sigma_z \quad . \qquad \ldots\ (6.7)$$

According to (6.1a), the maximum elastic shearing strain is given by

$$\gamma_{12} = \varepsilon_z - \varepsilon_y = \frac{\tau_{12}}{G} = \frac{\sigma_z}{2G} \quad . \qquad \ldots\ (6.8a)$$

According to (6.1b), the rate of maximum viscous shearing strain is given by

$$\gamma^{o}_{12} = \varepsilon^{o}_{z} - \varepsilon^{o}_{z} = \frac{\tau_{12}}{\eta} = \frac{\sigma_z}{2\eta} \cdot \qquad \ldots\ (6.8b)$$

According to Hooke's Law:

$$\varepsilon_x = \frac{\sigma_x}{E} - \mu \frac{\sigma_y}{E} - \mu \frac{\sigma_z}{E} \quad ,$$

$$\varepsilon_y = - \mu \frac{\sigma_x}{E} + \frac{\sigma_y}{E} - \mu \frac{\sigma_z}{E} \quad ,$$

$$\varepsilon_z = - \mu \frac{\sigma_x}{E} - \mu \frac{\sigma_y}{E} + \frac{\sigma_z}{E} \cdot$$

Hence

$$\varepsilon_z - \varepsilon_y = \frac{1}{E}[\sigma_z + \mu\sigma_z - \sigma_y - \mu\sigma_y] = \frac{1 + \mu}{E} (\sigma_z - \sigma_y) \quad ,$$

For uniaxial compression in the z direction $\sigma_y = o$

Therefore

$$\varepsilon_z - \varepsilon_y = \frac{1 + \mu}{E} \sigma_z \cdot \qquad \ldots\ (6.9a)$$

It follows

$$\varepsilon^{o}_{z} - \varepsilon^{o}_{y} = \frac{1 + \mu}{\Psi} \sigma_z \cdot \qquad \ldots\ (6.9b)$$

Substituting (6.9a) in (6.8a)

$$\frac{1}{2G} = \frac{1 + \mu}{E} \quad \text{or} \quad G = \frac{E}{2\ (1 + \mu)} \cdot \qquad \ldots\ (6.10)$$

Using (6.5)

$$G = \frac{E}{3} \quad . \qquad \ldots\ (6.11a)$$

Substituting(6.9b) in (6.8b) and using (6.5)

$$\frac{1}{2\eta} = \frac{1 + \mu}{\Psi} \quad \text{or} \quad \eta = \frac{\Psi}{2\ (1 + \mu)} = \frac{\Psi}{3} \ . \qquad \ldots\ (6.11b)$$

Combining (6.8a) and (6.11a), one obtains

$$\gamma_{12} = \frac{\sigma_z}{2G} = \frac{3}{2} \cdot \frac{\sigma_z}{E} \ . \qquad \ldots\ (6.12a)$$

Combining (6.8b) and (6.11b), one obtains

$$\gamma^{o}_{12} = \frac{\sigma_z}{2\eta} = \frac{3}{2} \cdot \frac{\sigma_z}{\Psi} \ . \qquad \ldots\ (6.12b)$$

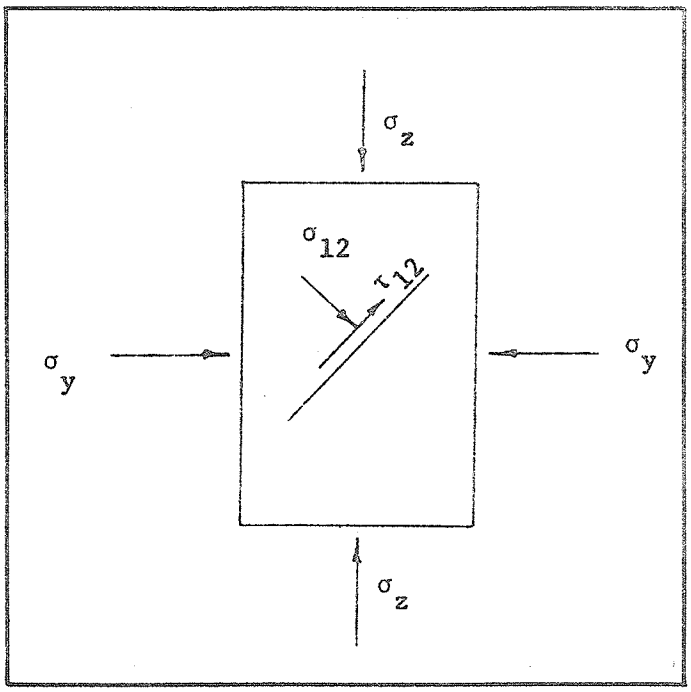

Figure 6.4 Maximum shearing stress in terms of principal compressive stress for elastic and/or viscous body.

6.12 Tables 6.7, 6.8, and 6.9 show the program undertaken to establish the strain-time relation under constant nominal axial stress. The actual axial stress includes a correction, for changes in cross-sectional area (as the sample deformed) based on the assumption of constant volume and maintenance of cylindrical form. The corrected area was obtained from the relationship:

$$A_c = A_o \frac{h_o}{h} \quad \ldots\ldots (6.13)$$

Where A_c = corrected area at the time of deformation at any stage,

A_o = the original area before application of load,

h_o = the height of the specimen before application of stress,

h = the height of the specimen after application of stress at the time of deformation at any stage.

The strain was then adjusted to constant stress using a triaxial co-ordinate system or "block diagram".

6.13 The samples shown in Table 6.7 of Program No. I were subjected to a relatively slow uniaxial freeze by controlling the temperature of top and bottom of the samples as indicated.

6.14 The samples in Table 6.8 of Program II were subjected to

relatively rapid uniaxial freezing. In both cases mentioned in Tables 6.7 and 6.8, no external water supply was provided.

6.15 Table 6.9 shows Program III undertaken for specimens tested when a source of external water was available during initial uniaxial slow freezing.

6.16 Table 6.10 shows Program IV undertaken for different purposes listed herein. In this program samples were subjected to a relatively rapid uniaxial or extra rapid all around freezing. Some of them were subjected to relaxation or strength tests in frozen condition whilst others were subjected to strength tests, after having been thawed following first cycle of freezing as described in subsequent paragraphs.

6.17 Figures 6.5 to 6.14 illustrate the stress-strain-time relationships of Test Programs I, II and III.

The strain-time relations obtained from test Programs I, II and III exhibited similar modes of deformation consisted of elastic and plastic strain caused by constant stresses applied.

The deformations investigated in the present work were found to consist of three segments, as follows:

a) the first segment was an instantaneous deformation obeying Hooke's law. (see Fig. 5.3)

b) the second segment was a time-dependent deformation at a decreasing rate of strain. (see Fig. 5.3)

TABLE 6.7
PROGRAM NO. I FOR TESTING SAMPLE FOR STRAIN-TIME RELATIONSHIP AT CONSTANT AXIAL COMPRESSIVE STRESS, SLOW FREEZE CONDITION, NO EXTERNAL WATER SUPPLY, UNIAXIAL FREEZE AND UNDISTURBED SAMPLES

Sample No.	Initial freeze condition	Final freeze condition	Nominal axial stress psi
OC-N-27-114	140 Hrs. top of sample at 36 $\pm 0.5^{o}$F	Rapid freezing of entire sample at 27 $\pm 0.5^{o}$F	25
OC-N-27-115	Bottom of sample at 27 $\pm 0.5^{o}$F		50
OC-N-27-116			75

TABLE 6.8
PROGRAM NO. II FOR TESTING SAMPLES FOR STRAIN-TIME RELATIONSHIP AT CONSTANT AXIAL COMPRESSIVE STRESS, RAPID FREEZE CONDITIONS, NO EXTERNAL WATER SUPPLY, UNIAXIAL FREEZE AND UNDISTURBED SOIL SAMPLES

Sample No.	Rapid freeze conditions in temp. of	Nominal axial stress psi	Set up for freezing
OC-N-27-128A	27 ±0.5	25	Rapid freezing thermostat set up at 27°F
OC-N-27-128B	27 ±0.5	50	
OC-N-27-128C	27 ±0.5	75	Initial step 27° ±0.5 after equilibrium thermostat set down to 17°F
OC-N-17-124A	17 ±0.5	25	
OC-N-17-124B	17 ±0.5	50	
OC-N-17-124C	17 ±0.5	75	Initial step thermostat set up at 27 F° following equilibrium thermostat lowered to 17 F° following equilibrium thermostat set down to 7°F
OC-N- 7-125A	7 ±0.5	25	
OC-N- 7-125B	7 ±0.5	50	
OC-N- 7-125C	7 ±0.5	75	

TABLE 6.9 PROGRAM NO. III FOR TESTING SAMPLES FOR STRAIN-TIME RELATIONSHIP AT CONSTANT COMPRESSIVE AXIAL STRESS, SLOW FREEZE CONDITIONS, EXTERNAL WATER SUPPLY, UNIAXIAL FREEZE AND UNDISTURBED SAMPLES

Sample No.	Initial freeze	Final freeze	Nominal stress psi
OC-R-27-118	350 to 450 hrs., top of sample at 34° to 37°F, bottom of the sample 27 +0.5°F, 11 to 13, grams water supplied through side filter	Entire sample cooled rapidly to 27°F	25
OC-4-27-123			50
OC-R-27-121			75

TABLE 6.10

PROGRAM NO. IV FOR OBSERVATION OF FREEZING AND OBTAINING STRENGTH IN THAWED CONDITION AFTER FIRST CYCLE OF FREEZING FROM ALL DIRECTIONS AND STUDY OF STRESS RELAXATION IN FROZEN CONDITION

Sample No.	Type of freezing	Freezing rate	Temperature of freezing	Condition of sample when frozen	Purpose of test	Conditions in which the samples tested
OM-N-31.5-126	Uniaxial	Rapid	31.5°F	Undisturbed	Strength	In frozen condition
OC-N-(-40)-33	All around	"	-40°F	"	"	not frozen condition
OC-N-(-40)-34	" "	"	"	"	"	Thawed out following first cycle of freezing
OC-N-(-40)-35	" "	"	"	Remolded	"	Not frozen
OC-N-(-40)-36	" "	"	"	"	"	Thawed out following first cycle of freezing
OM-N-27-127	Uniaxial	"	27°F	Undisturbed	Relaxation	In frozen condition
OM-N-17-131	"	"	17°F	"	"	" "
O1-N-17-132	"	"	17°F	"	Observation	" " than thawed

c) The third segment was a time-dependent deformation at a constant rate of strain (See Fig. 5.3).

d) A fourth segment, known as a deformation at accelerating rate of strain that leads generally to total failure, was not included in this study.

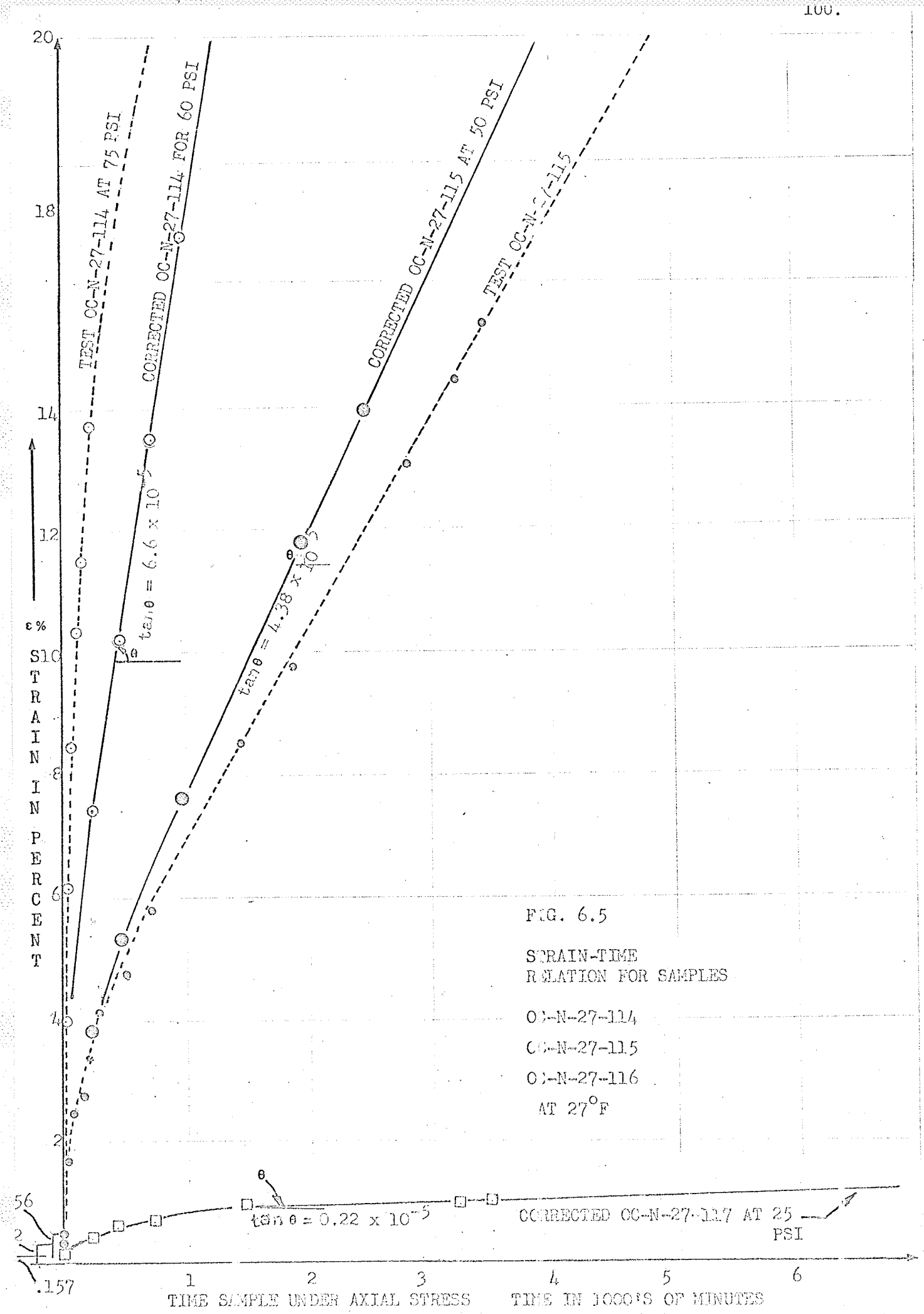

FIG. 6.5

STRAIN-TIME
RELATION FOR SAMPLES

OC-N-27-114

OC-N-27-115

OC-N-27-116

AT 27°F

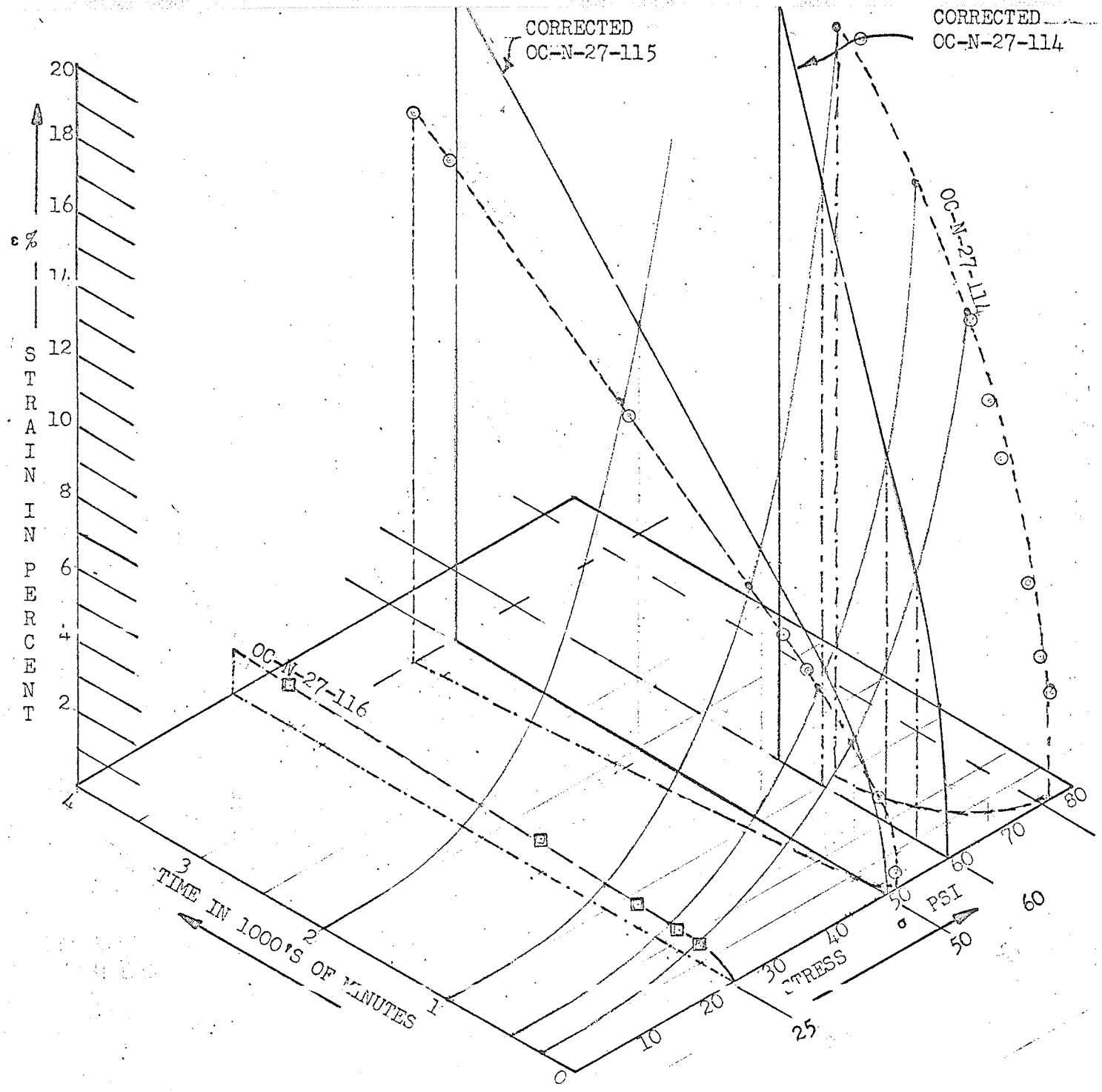

FIG. 6.6

TRIAXIAL DIAGRAM OF STRESS-TIME-STRAIN RELATION FOR SAMPLES

OC-N-27-114
OC-N-27-115
OC-N-27-116
At 27°F

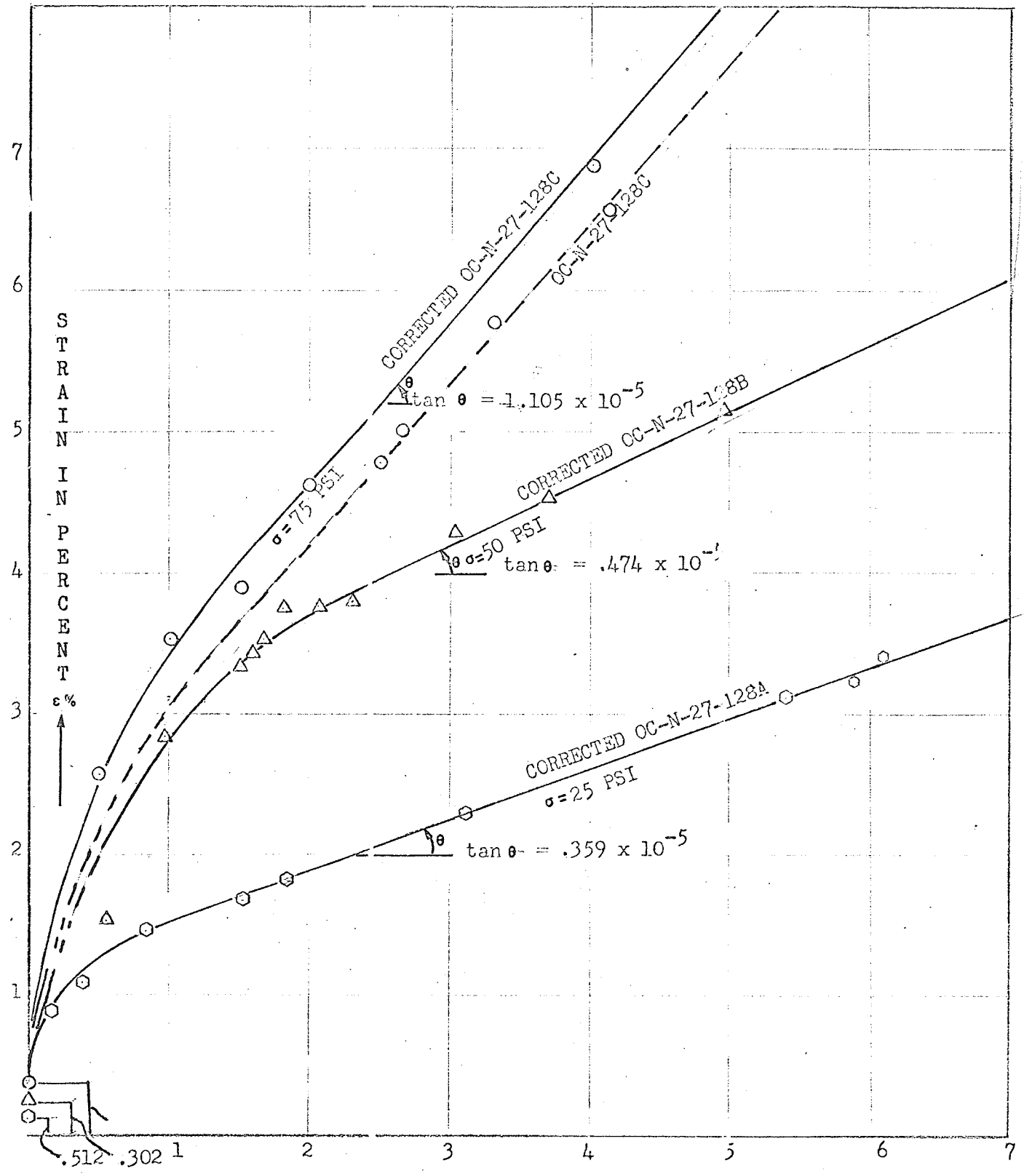

TIME SAMPLE UNDER AXIAL STRESS

FIG. 6.7

STRESS-TIME-STRAIN RELATION FOR SAMPLES

OC-N-27-128A
OC-N-27-128B
OC-N-27-128C
AT 27°F

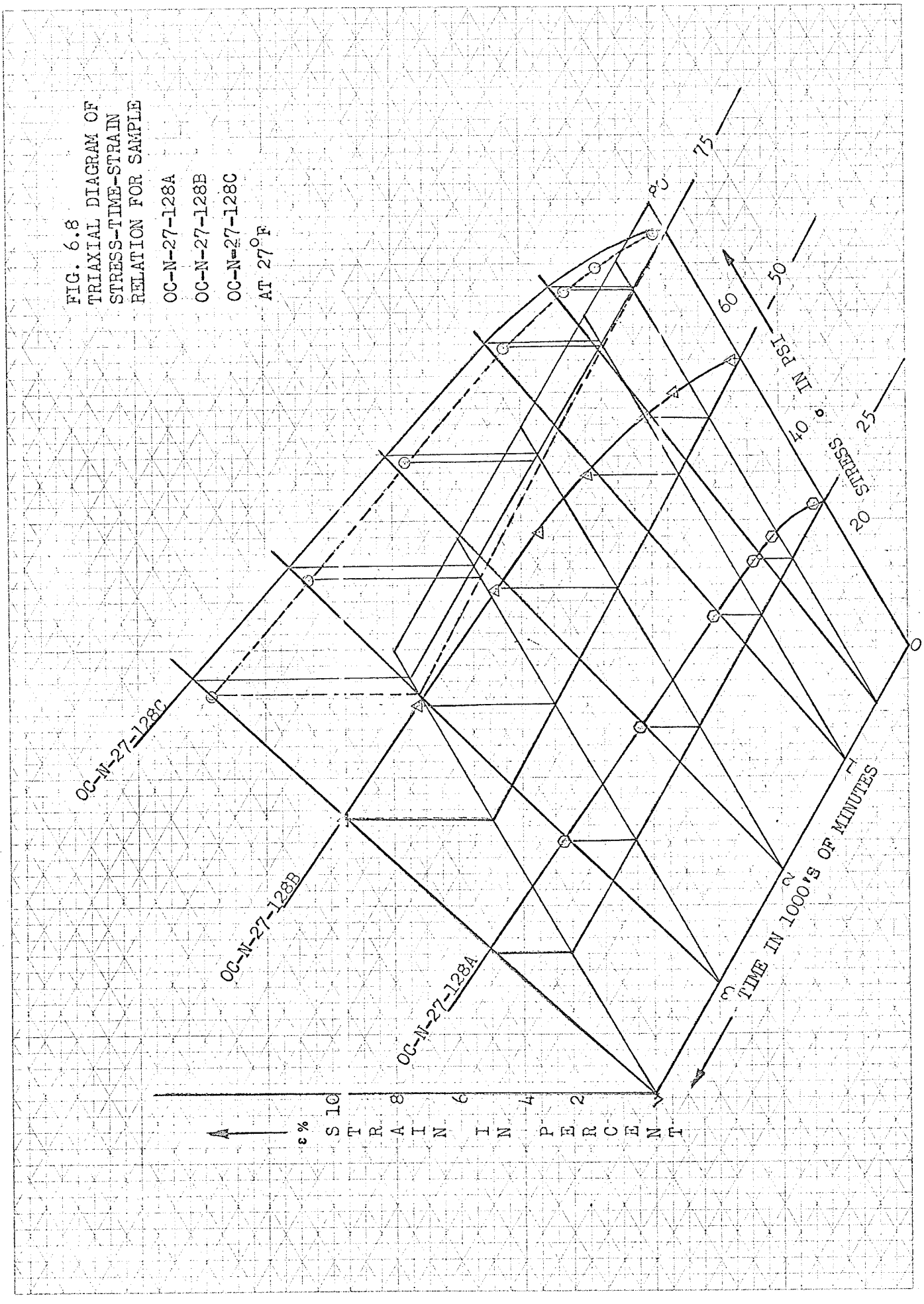

FIG. 6.8
TRIAXIAL DIAGRAM OF
STRESS-TIME-STRAIN
RELATION FOR SAMPLE

OC-N-27-128A
OC-N-27-128B
OC-N-27-128C
AT 27°F

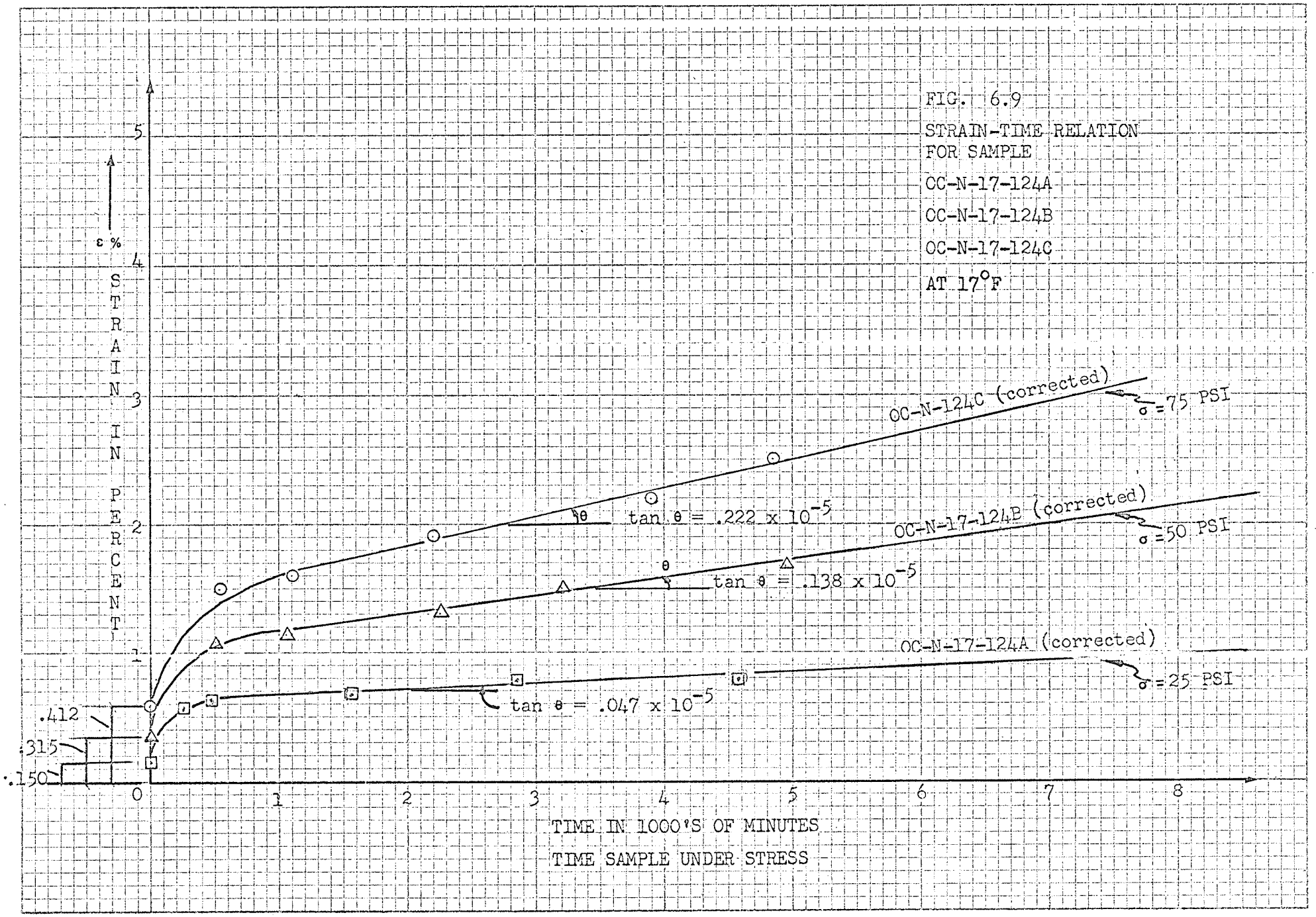
FIG. 6.9
STRAIN-TIME RELATION
FOR SAMPLE
CC-N-17-124A
CC-N-17-124B
CC-N-17-124C
AT 17°F
STRAIN IN PERCENT
ε %
OC-N-124C (corrected)
σ = 75 PSI
tan θ = .222 x 10^-5
OC-N-17-124B (corrected)
σ = 50 PSI
tan θ = .138 x 10^-5
OC-N-17-124A (corrected)
σ = 25 PSI
tan θ = .047 x 10^-5
.412
.315
.150
0
1
2
3
4
5
6
7
8
TIME IN 1000'S OF MINUTES
TIME SAMPLE UNDER STRESS

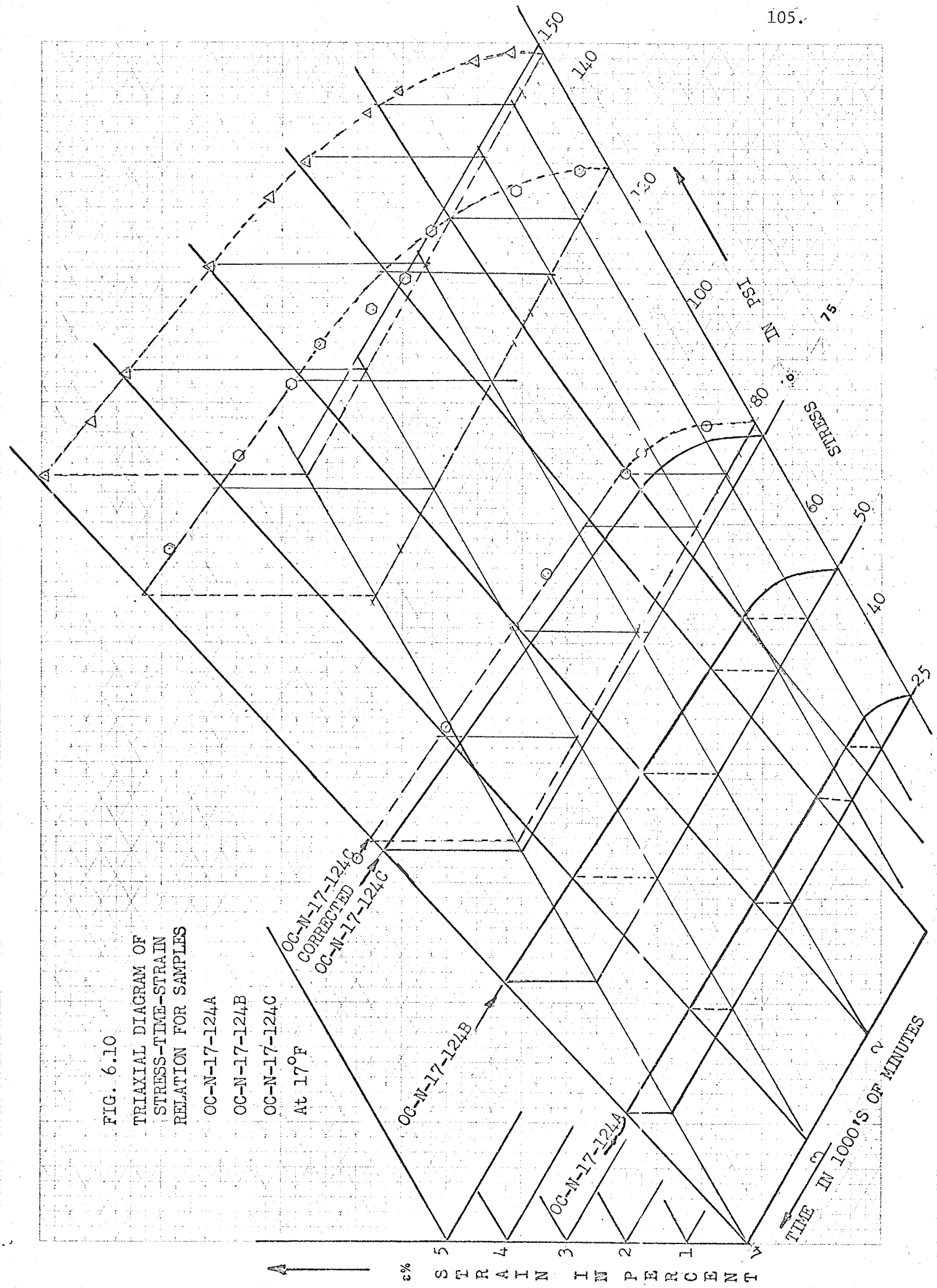

FIG. 6.10
TRIAXIAL DIAGRAM OF
STRESS-TIME-STRAIN
RELATION FOR SAMPLES
OC-N-17-124A
OC-N-17-124B
OC-N-17-124C
At 17°F

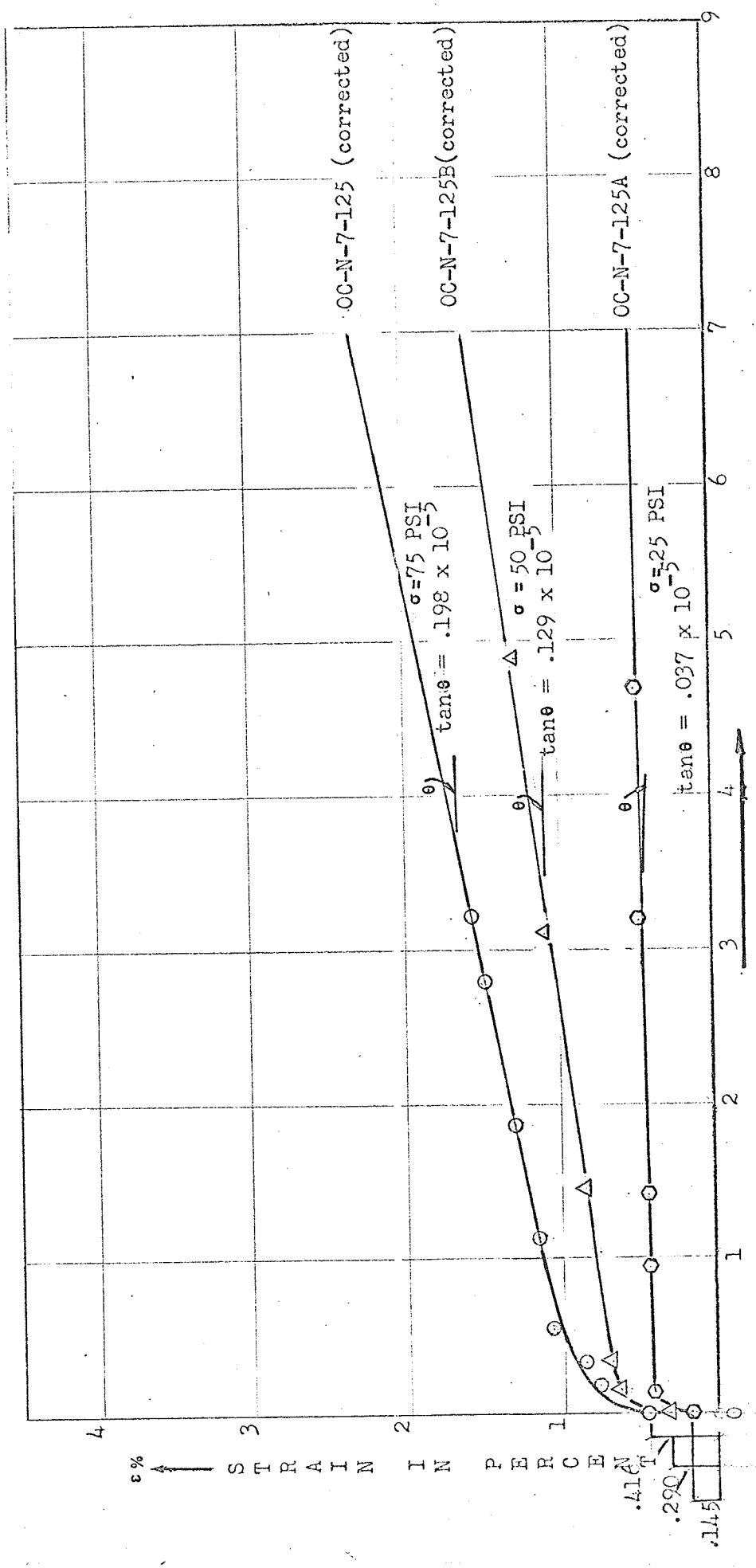

FIG. 6.11

STRAIN-TIME RELATION
UNDER SUSTAIN LOAD
FOR SAMPLE

OC-N-7-125A

OC-N-7-125B

OC-N-7-125C

At $7^{\circ}F$

FIG. 6.12

TRIAXIAL DIAGRAM OF STRESS-TIME-STRAIN RELATION FOR SAMPLE

OC-N-7-125A

OC-N-7-125B

OC-N-7-125C

At 7°F

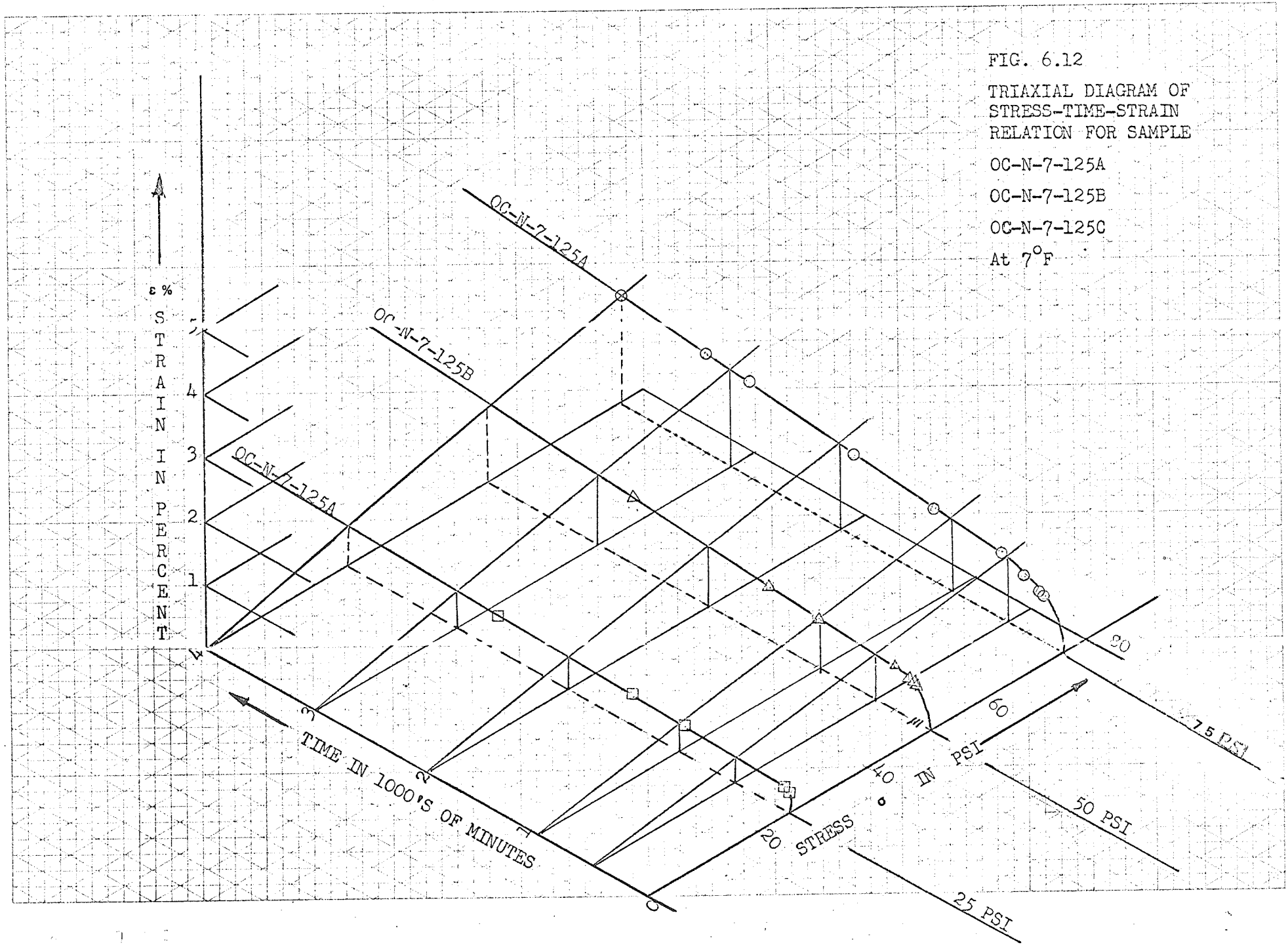

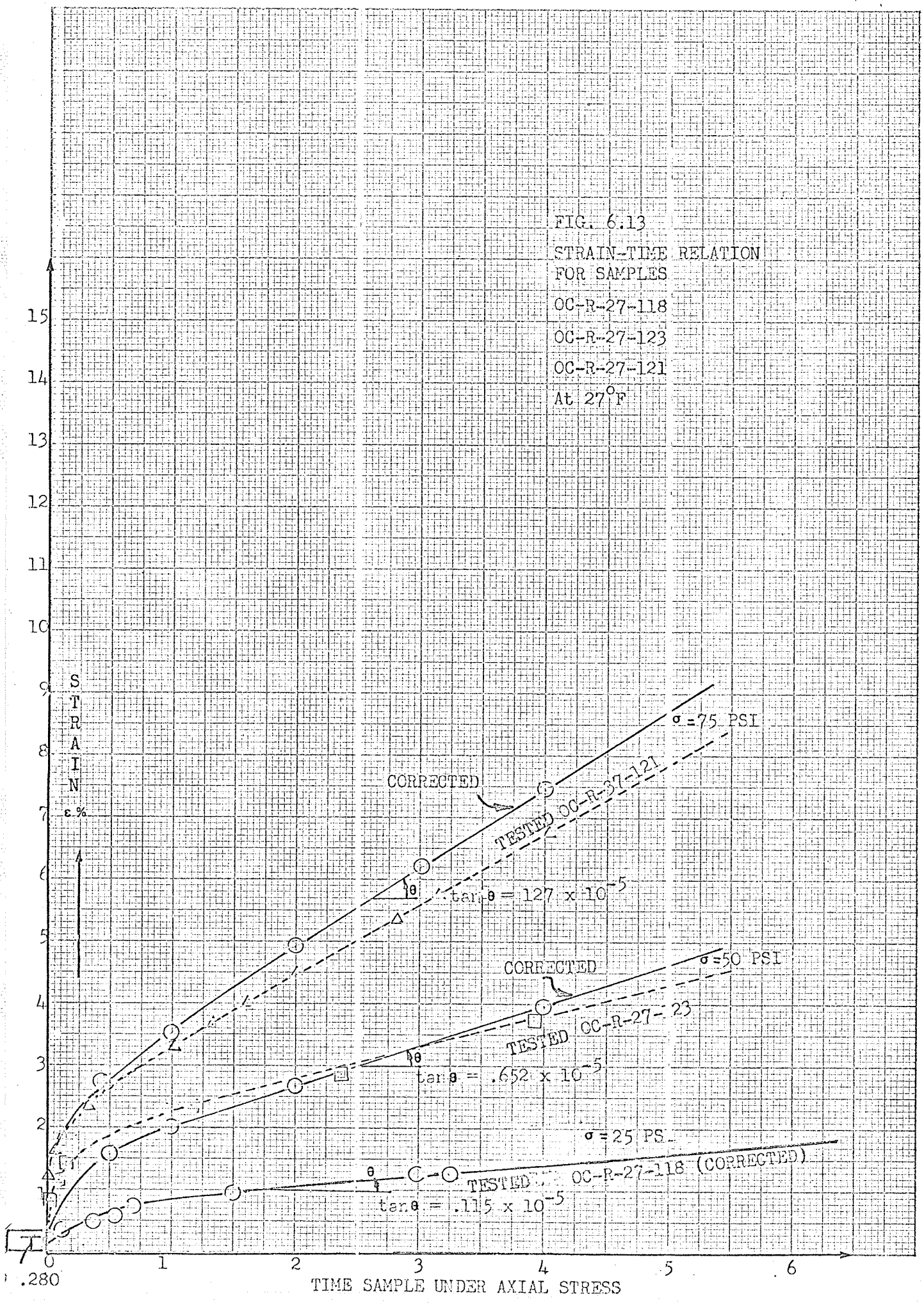

FIG. 6.13
STRAIN-TIME RELATION
FOR SAMPLES
OC-R-27-118
OC-R-27-123
OC-R-27-121
At 27°F

FIG. 6.14
STRESS-TIME-STRAIN
RELATION FOR SAMPLE
OC-R-27-118
OC-R-27-123
OC-R-27-121
AT 27°F

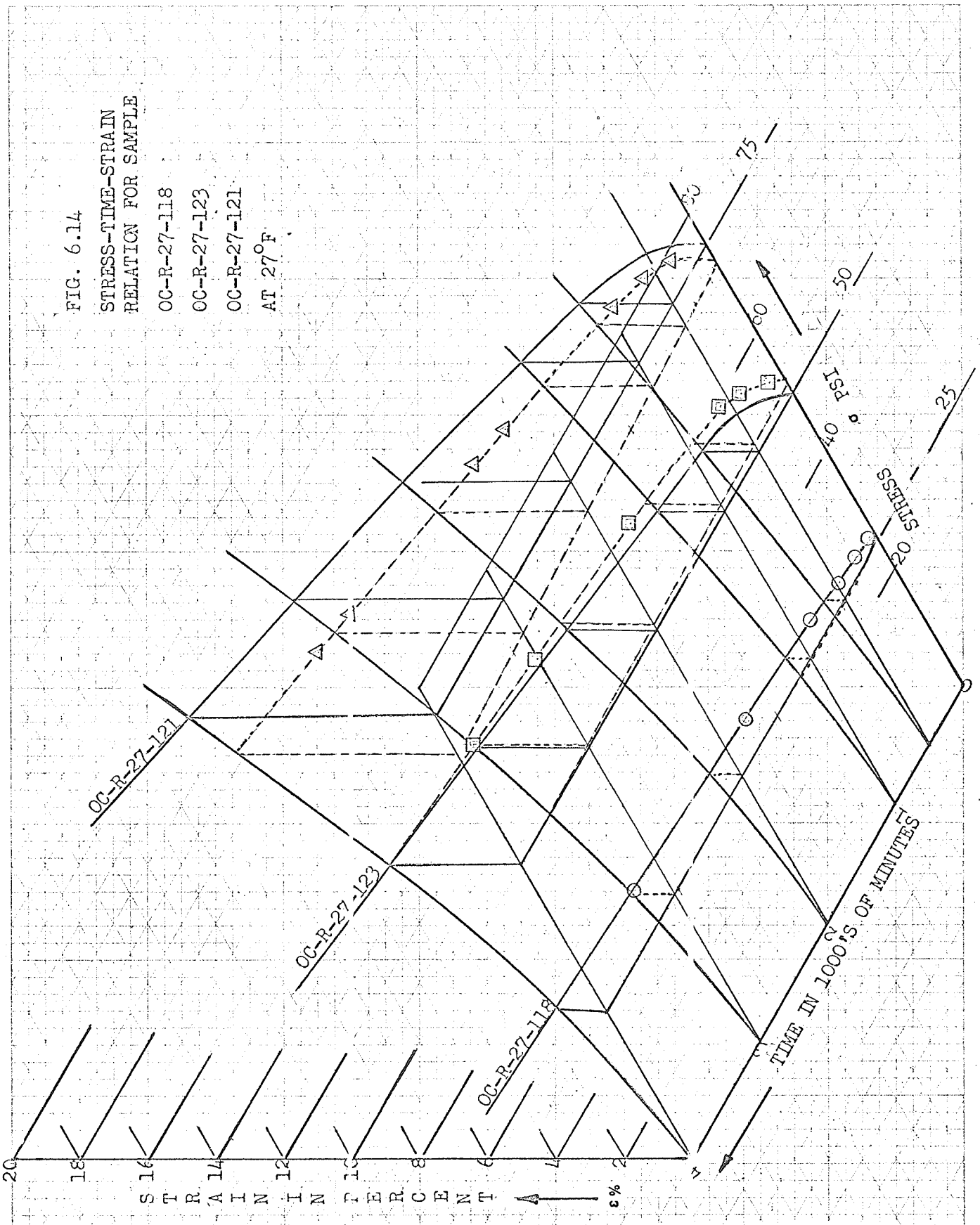

Test results for the different segments of each of the three groups are shown in Table 6.11.

The total deformation process may be expressed as follows:

$$\varepsilon = \varepsilon_o + \varepsilon_{(t)} = \varepsilon_o + \varepsilon_1 + \varepsilon_2 \quad \text{.... (6.14)}$$

Where

ε = total strain,

ε_o = instantaneous strain,

ε_t = total time dependent strain = $\varepsilon_1 + \varepsilon_2$,

ε_1 = strain at decelerated strain rate,

ε_2 = strain at constant strain rate.

6.18 It was verified that the first segment ε_o is completely and instantaneously recovered upon removal of the applied load and may be expressed as follows:

$$\varepsilon_o = \frac{\sigma}{E_o}$$

Where

σ = applied stress psi,

E_o = Young's Modulus psi.

TABLE 6.11
YOUNG'S MODULUS, DURATION OF STRAIN AT DECELERATING STRAIN RATE
AND SLOPE OF CONSTANT STRAIN-TIME

Sample	Freezing temperature F^{o}	Applied constant stress psi	Instantaneous deformation ε^{o}% inch per inch x 100	Modulus of elasticity E psi	Inch per inch x 100 per min. $\tan\theta = \frac{\varepsilon}{t} \times 10^{-5}$	Duration of strain at decelerated strain rate in min.
OC-N-27-116	27	25	0.157	150×10^{2}	0.22×10^{-5}	
OC-N-27-115	27	50	0.312	100.5×10^{2}	4.38×10^{-5}	650
OC-N-27-114	27	60	0.356	158×10^{2}	6.60×10^{-5}	1500
OC-N-27-128A	27	25	0.152	166×10^{2}	0.35×10^{-5}	800
OC-N-27-128B	27	50	0.302	166×10^{2}	0.47×10^{-5}	1680
OC-N-27-128C	27	75	0.410	187×10^{2}	1.105×10^{-5}	2001
OC-N-17-124A	17	25	0.150	166×10^{2}	0.222×10^{-5}	390
OC-N-17-124B	17	50	0.315	159×10^{2}	0.138×10^{-5}	800
OC-N-17-124C	17	75	0.412	182×10^{2}	0.047×10^{-5}	1420
OC-N- 7-125C	7	25	0.145	172×10^{2}	0.037×10^{-5}	240
OC-N- 7-125B	7	50	0.290	173×10^{2}	0.129×10^{-5}	410
OC-N- 7-125C	7	75	0.416	179.5×10^{2}	0.198×10^{-5}	610
OC-R-27-118	27	25	0.152	164.5×10^{2}	0.175×10^{-5}	1085
OC-R-27-123	27	50	0.280	178×10^{2}	0.652×10^{-5}	1300
OC-R-27-121	27	75	0.429	175×10^{2}	1.270×10^{-5}	1685

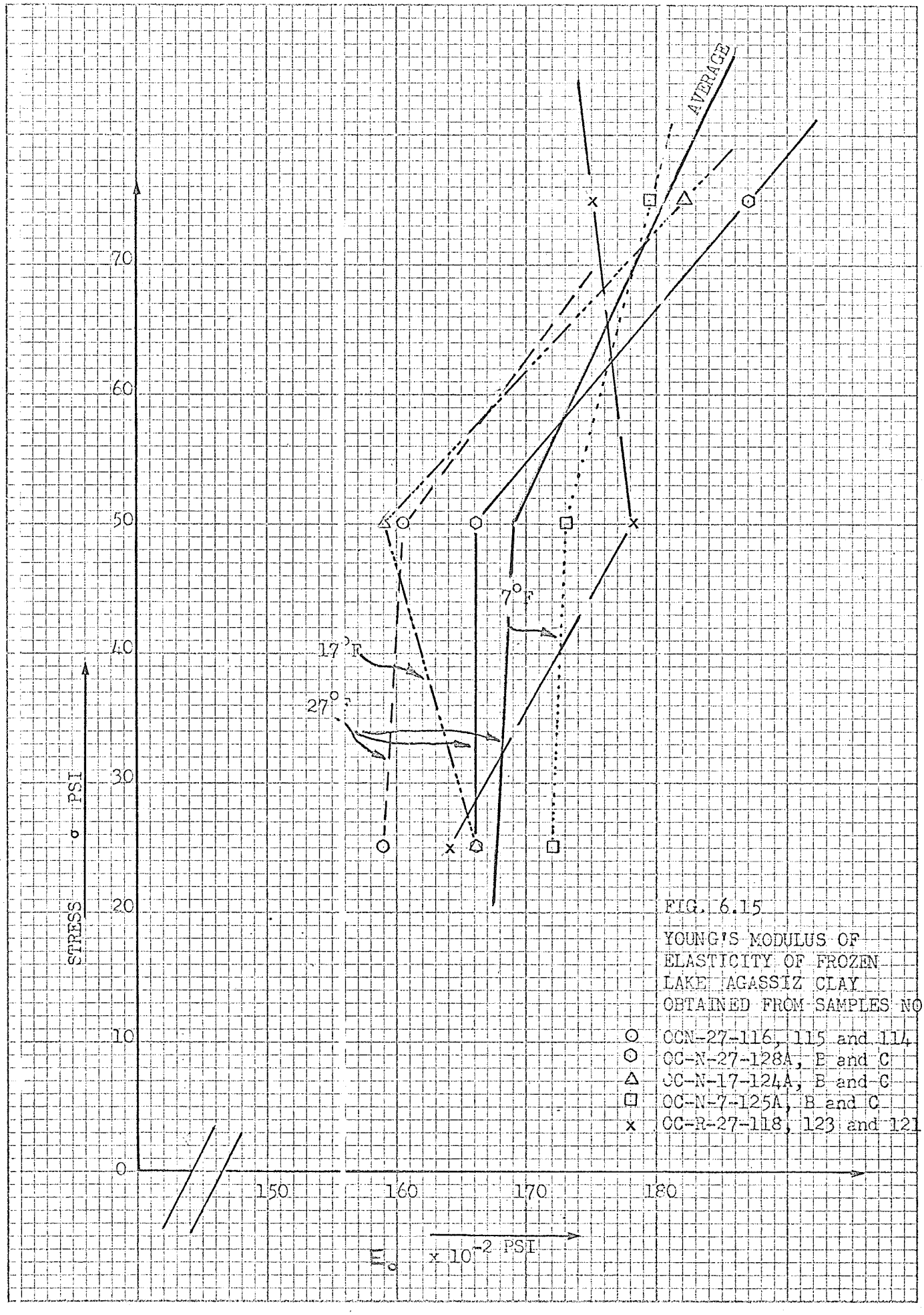

FIG. 6.15
YOUNG'S MODULUS OF ELASTICITY OF FROZEN LAKE AGASSIZ CLAY OBTAINED FROM SAMPLES NO.

- ○ CCN-27-116, 115 and 114
- ⊙ CC-N-27-128A, B and C
- △ CC-N-17-124A, B and C
- □ CC-N-7-125A, B and C
- x CC-R-27-118, 123 and 121

This instantaneous deformation was found to be independent of temperature, approximately proportional to the applied stress and ranged (see fig. 6.15):

$$E_o = 165 \times 10^2 \text{ to } 180 \times 10^2 \text{ psi} . \quad \ldots\ldots (6.15)$$

The deformation in this stage is due to elastic changes in ice crystal, minerals, and elastic compression of water and entrapped air (See Paragraph 5.27) without causing any melting of ice.

6.19 It was not verified in the present work that ε_1 was recoverable with time upon removal of the applied load. However, the duration of deformation at decelerating strain rate was found to be not constant for varying stress, as the theory states (See Paragraph 5.34). Figure 6.17 illustrates the relationship of duration of deformation at decelerating strain rate versus temperature of samples OC-N-7-124 A, B and C, OC-N-17-125 A, B and C and OC-N-27-128 A, B and C. According to Figure 6.17, the duration of deformation at declerating strain rate decreases linearly with the lowering of freezing temperature. However, the duration of ε_1 increases in nonlinear proportion with increasing stress, indicating a decrease of coefficient of viscosity with increase of the applied stress.

6.20 Figure 6.18 illustrates the relationship of ε_1 versus temperature at various stress levels. According

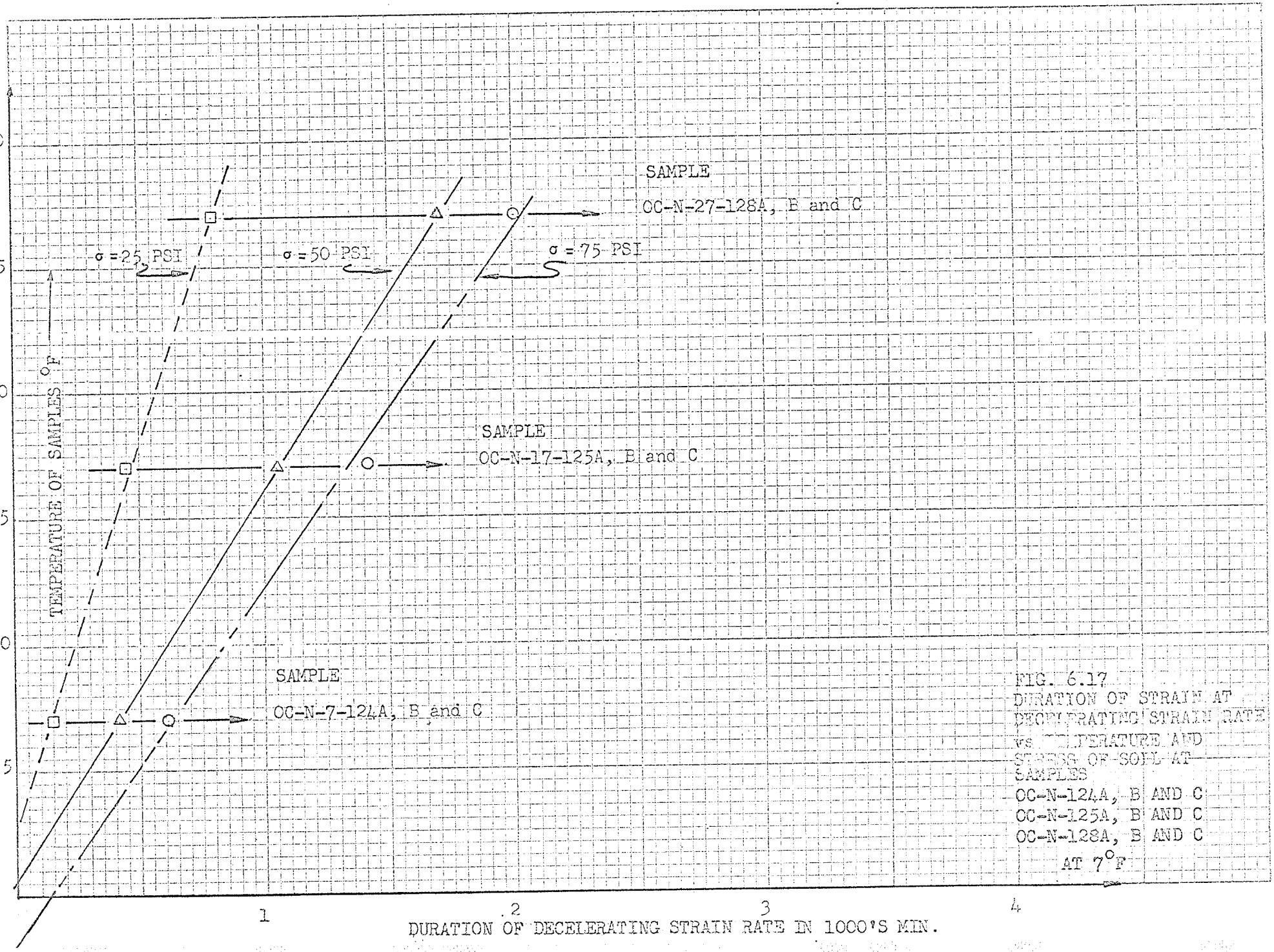

FIG. 6.17
DURATION OF STRAIN AT
DECELERATING STRAIN RATE
vs TEMPERATURE AND
STRESS OF SOIL AT
SAMPLES
OC-N-124A, B AND C
OC-N-125A, B AND C
OC-N-128A, B AND C
AT 7°F

to this figure, the magnitude of ε_1 at lower temperatures approaches zero in a non-linear fashion.

6.21 Figure 6.19 illustrates the relationship of strain rate versus temperature of the third segment (i.e. time dependent deformation at constant rate of strain, see Paragraph 5.27) obtained from the series of tests conducted. According to Figure 6.19, the constant rate of strain for each magnitude of stress applied, decreases sharply in non-linear fashion as the temperature was lowered.

6.22 The decrease of constant rate of strain with a lowering of temperature is believed to be caused by a decrease of non-frozen water in the frozen soil thus increasing the cementing force of ice crystals. On the other hand, the constant rate of strain increases rapidly with increasing temperature.

6.23 When the temperature of the frozen soil increased from $27^{o}F$ to $31.5^{o}F$, the strength of the soil was found to approach that of unfrozen soils. Figure 6.20 illustrates the behaviour of sample OM-N-31.5-126, which was subjected to a triaxial compression test for 1090 minutes. Then, in order to expedite the test, the strain rate was increased to 68×10^{-6} inches per minute, and this caused the soil to fail at 23.5 psi at a total strain of $\varepsilon = 9.3\%$ after 2780 minutes from the start of the test. Failure occurred along a slip plane as shown in Photo-

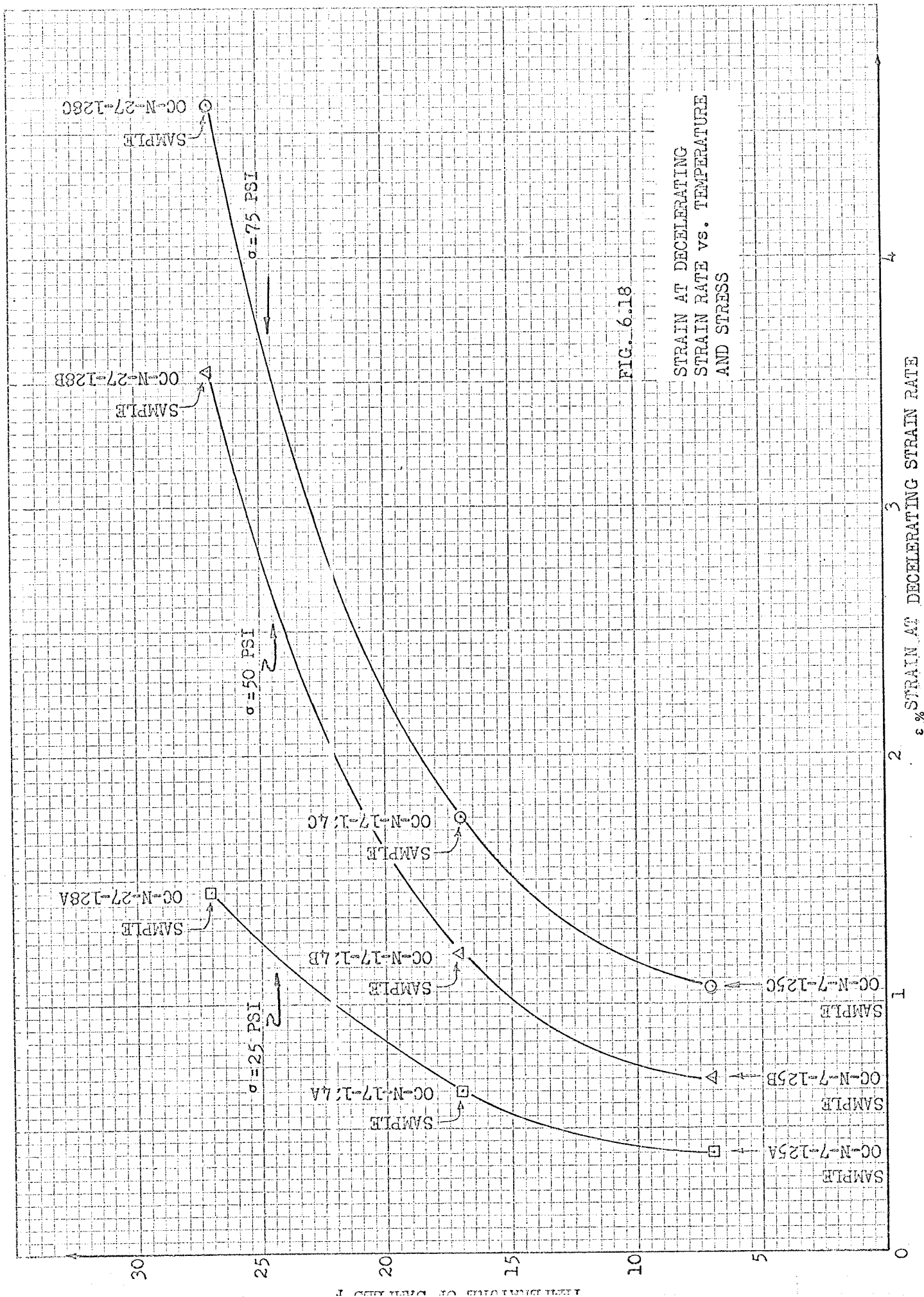
FIG. 6.18
STRAIN AT DECELERATING
STRAIN RATE vs. TEMPERATURE
AND STRESS
ε_1% STRAIN AT DECELERATING STRAIN RATE
0
1
2
3
4
5
10
15
20
25
30
σ=75 PSI
σ=50 PSI
σ=25 PSI
OC-N-7-125C
SAMPLE
OC-N-7-125B
SAMPLE
OC-N-7-125A
SAMPLE
OC-N-17-1;4C
SAMPLE
OC-N-17-1;4B
SAMPLE
OC-N-17-1;4A
SAMPLE
OC-N-27-128C
SAMPLE
OC-N-27-128B
SAMPLE
OC-N-27-128A
SAMPLE

graphs No. 6.10, 6.11 and 6.12. The strength weakening of the soil, frozen at 31.5°F, is assumed to be caused by the presence of approximately 45% of nonfrozen water in the frozen soil (see Paragraph 5.38 and Figure 5.10) accompanied by partial or total destruction of the soil fabric and redistribution of the original moisture content. This destruction is due to the expansion of microscopic and macroscopic ice crystals which were formed during the freezing process between the soil particles.

Photograph 6.10 shows sample OC-N-27-126 after failure. Photograph 6.11 and 6.12 show characteristic freezing in this sample namely, the horizontal and vertical polygonal cracks which were filled with ice during the freezing process.

Chapter III of the book Basic Mechanics of Freezing, Frozen and Thawing Soils, p. 21 by N. A. Tsytowich (16) reports on the high compressibility of "clay loam" and "sandy loam" as follows:

> "... compressibility of frozen clay loam and sandy loam at -.3°C (31.5°F) and especially at 0.1°C (31.8°F) is considerable. .... At this temperature, the compressibility of frozen clay soils is close to that of unfrozen soils showing little plasticity; such soils may undergo differential settlement with time."

This agrees with the results of the present tests. Figure 6.21 illustrates the results of another series of tests carried out on "never" frozen soil, i.e. soils which have not been frozen since the

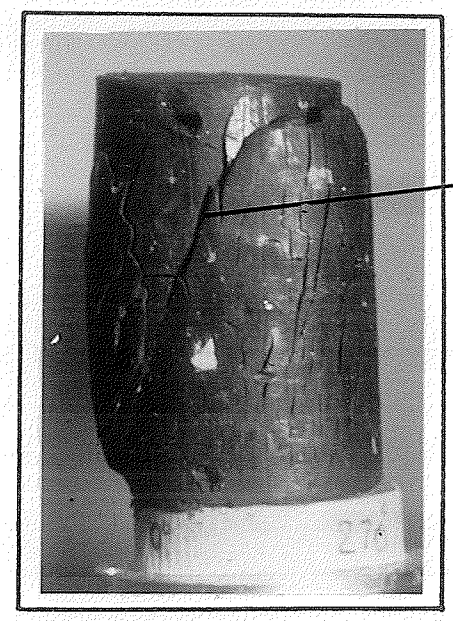

Photograph 6.10

Sample after failure of sample CC-N-27-126 at 31.5°F

Photograph 6.11

Failure plane and ice crystals of sample CC-N-27-126 at 31.5°F

Photograph 6.12

Ice buildup in the vertical shrinkage cracks of sample CC-N-27-126 at 31.5°C.

end of the last glacial period (see Paragraph 3.1). In these tests, instead of uniaxial freezing, the samples were frozen from all directions in both undisturbed and remolded condition. Following one freezing cycle, and thawing, unconfined compression strengths were determined.

In the case of the undisturbed samples, the thawed strength at failure was 43.5% of the original undisturbed and non frozen strength.

In the case of the remolded samples, the thawed strength at failure was 76.6% of the original strength of remolded and non frozen samples.

6.24 Figure 6.22 shows the stress-strain-time relations of soil samples of Group No. I (slow freeze condition - see Paragraph 6.13). Figures 6.23, 6.24 and 6.25 illustrate the stress-strain-time relations of soil samples of Group No. II (rapid freeze condition - see Paragraph 6.14). Figure 6.26 illustrates the stress-strain relations of soil samples of Group No. III (slow freeze condition with external water supply - see Paragraph 6.15) for different time intervals. These illustrations indicate that the stress and strain curves obtained are nonlinear at any stress level at any given time. The slopes of the stress-strain curves obtained from the samples of Groups No. I and No. III are decreasing with increasing

strain while the slopes of the stress-strain curves in Group No. II are increasing for the same intervals of time and stress condition. It is believed that the decrease of the slopes of the curves with increased strain shown in Figure 6.26 of Group No. 1 is due to withdrawal of pore water from the upper layers of the sample during the freezing period causing higher porosity and less ice cementing force with consequent lower strength that leads to higher rate of strain.

The increase of the slope of the curves with increasing strain shown in Figure 6.23, 6.24 and 6.25 of Group No. II has been related to a relatively uniform distribution of ice lenses which reduces the thickness of the water film between the mineral particles and ice crystals. This results in an increase of the interparticle bonding force causing strengthening of the soils of Group No. II with a consequent lowering of strain rate. However, introducing the large amounts of ice in thick layers contributed by the external water supplied to the samples in Group No. III caused a drop in strength because of the cohesion of ice being lower than that of a uniform mixture of fine ice crystals and mineral particles.

6.25 Figure 6.27 illustrates the stress relaxation in Sample OM-N-27-127 which was frozen at $27^{o}F$. The sample was stressed up to 112.85 psi in the triaxial compression machine and the strain locked. During the relaxation time of T = 1535 minutes, the stress was relaxed to 62.8 psi.

Figure 6.28 illustrates the stress relaxation of sample OM-N-17-131. This time the sample was stressed and subjected to six cycles of loading and relaxation. The relaxation times were found to vary, up to the fifth cycle, between 1008 and 1520 minutes while the magnitude of the relaxed stresses varied between 80.11 psi and 106.6 psi. During the sixth cycle, the relaxed stress was 105.5 psi while the relaxation time reached a value of 1994 minutes (see table 6.12). This was an increase of about 65 percent over the average relaxation time noted in the previous five cycles and 98 percent over the first relaxation time cycle . In view of the fact that, theoretically, all relaxation times for any stress or cycle of stresses should be equal (see Paragraphs 5.34 and 5.35), it was interesting to note, that an examination of the sample after the test revealed an ice buildup on the surface of the sample (see Photograph 6.12). It is believed (see also Paragraph 5.23) that this buildup of surface ice was due to a squeezing-out of ice (in liquid form) as a result of stress concentrations at the contacts between mineral particles and ice crystals (see Paragraphs 5.23 and 5.24). Movement of ice away from the regions of stress concentration towards the surface of the sample (where stress is minimum) produces further densification resulting in increased viscosity and longer relaxation time.

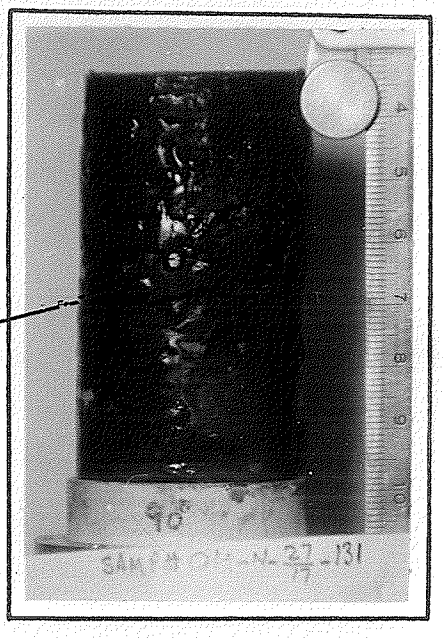

Photograph 6.13

Squeezing out of ice to the free surface of the sample due to application of cyclic stress to frozen soil specimen

TABLE 6.12
RELAXATION AND RELEASED STRESS DUE TO CYCLING STRAINS APPLIED TO SAMPLE OM-N-17-131 AT 17°F

Cycle of strain	Relaxation time	Released stress psi	% Strain required to increase stress	Ratio of cycled relaxation time to the initial time	Ratio of last relaxation time to the area cycled relaxation time
1	1008	85.9	Initial	1	
2	1470	80.1	0.478	1.41	
3	1413	99.5	0.794	1.28	
4	1520	84.9	0.599	1.51	0.65
5	1447	106.6	0.470	1.46	
6	1994	105.5	0.521	1.98	

FIG. 6.19
STRAIN-RATE-TEMPERATURE RELATION

$$\frac{1/\psi\,\sigma}{t} = \frac{\varepsilon}{t} = \tan\theta$$

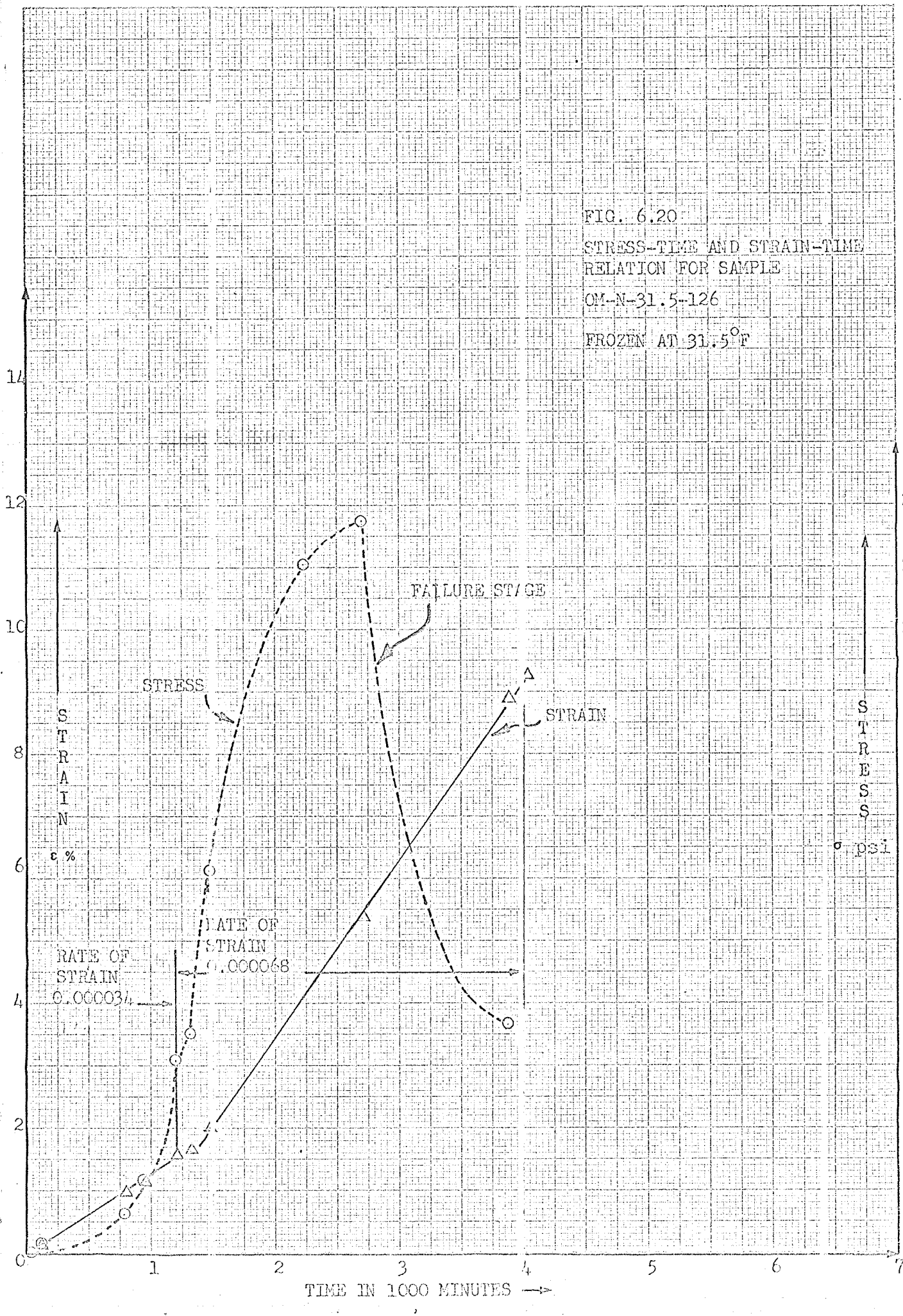
FIG. 6.20
STRESS-TIME AND STRAIN-TIME RELATION FOR SAMPLE
CM-N-31.5-126
FROZEN AT 31.5°F
FAILURE STAGE
STRESS
STRAIN
RATE OF STRAIN 0.000068
RATE OF STRAIN 0.000034
STRAIN ε %
STRESS σ psi
TIME IN 1000 MINUTES →
0
1
2
3
4
5
6
7
2
4
6
8
10
12
14
16
18
20
22
24

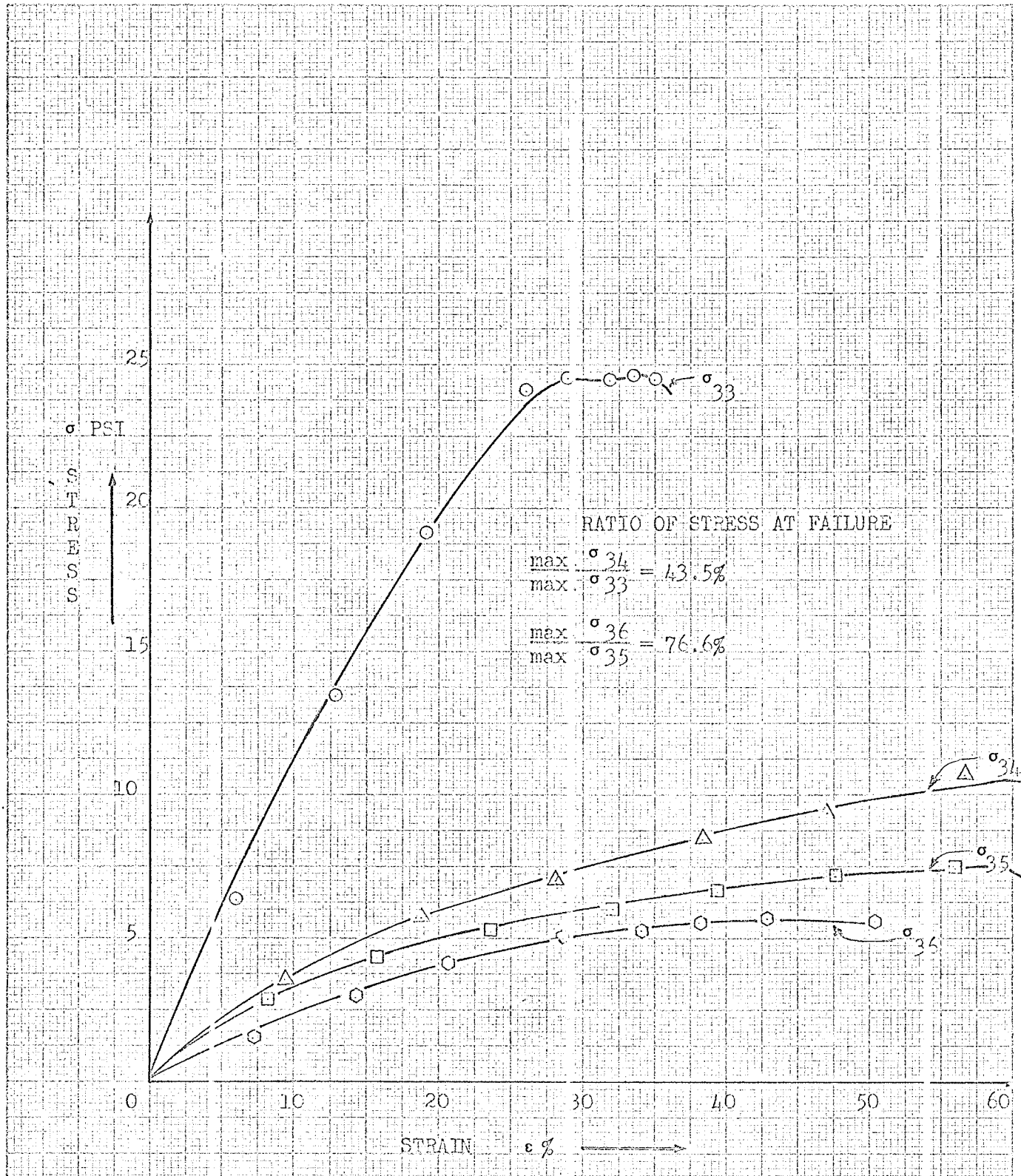

FIG. 6 .21 UNCONFINED COMPRESSIVE STRENGTH OF

SAMPLE ⊙ OC-N-(-40)-33 : Never frozen undisturbed soil sample

SAMPLE △ CC-N-(-40)-34 : " " " " " thawed following the first cycle of all around freezing at -40°F.

SAMPLE □ OC-N-(-40)-35 : Never frozen remolded soil, sample.

SAMPLE ⬡ OC-N-(-40)-36 : " " " " " , thawed following the first cycle of all around freezing at -40°F.

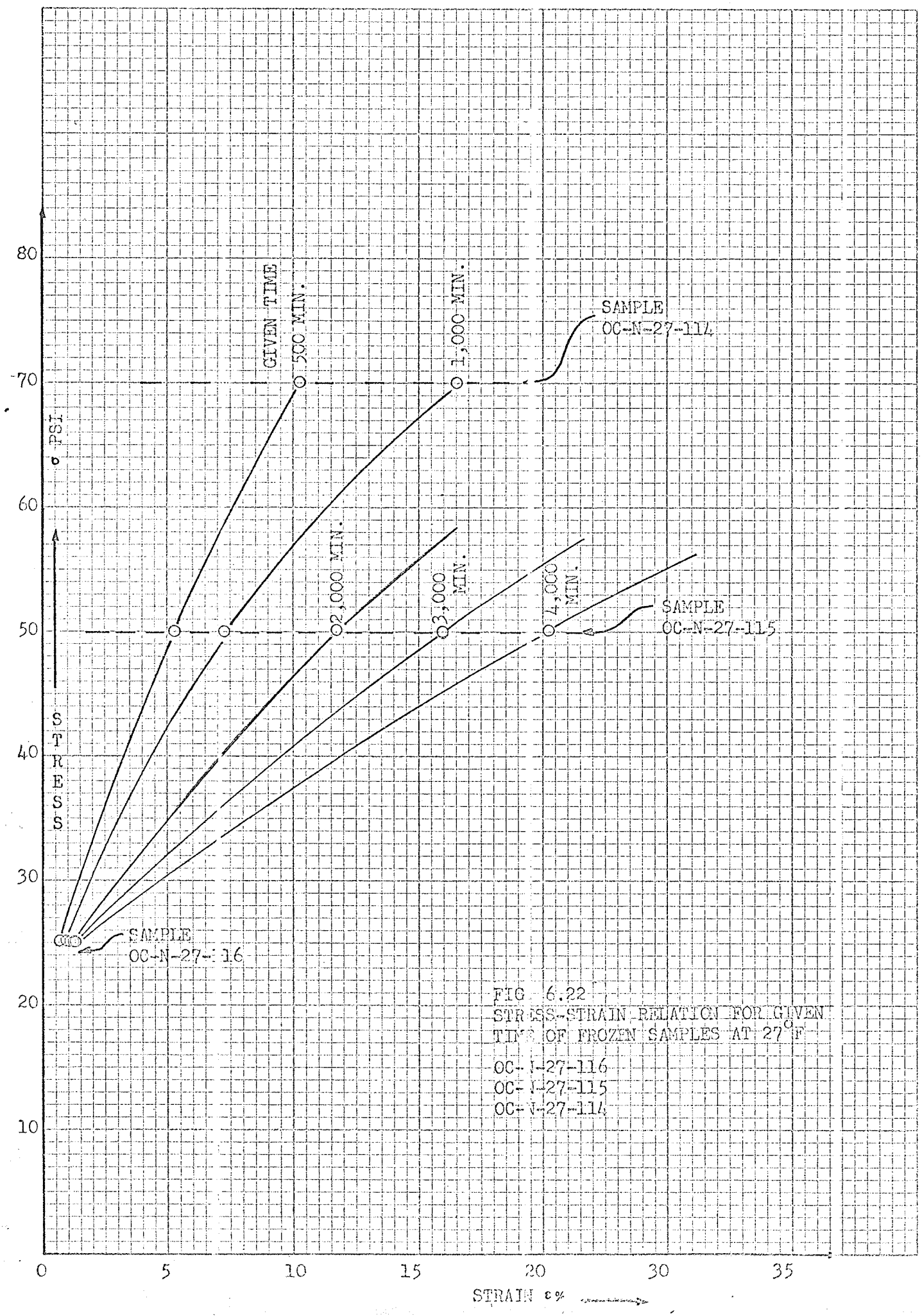

FIG 6.22
STRESS-STRAIN RELATION FOR GIVEN TIME OF FROZEN SAMPLES AT 27°F

OC-N-27-116
OC-N-27-115
OC-N-27-114

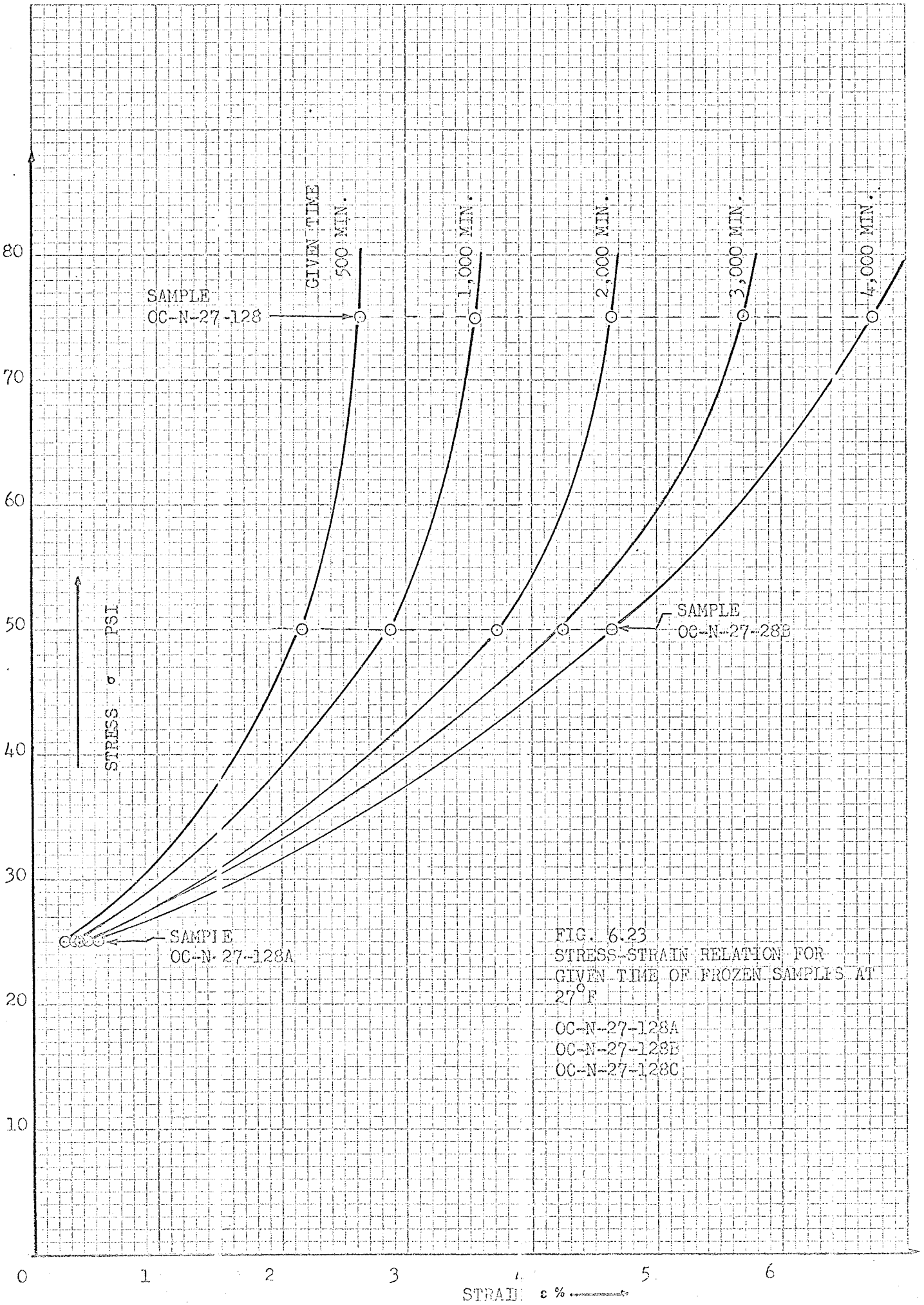

FIG. 6.23
STRESS-STRAIN RELATION FOR GIVEN TIME OF FROZEN SAMPLES AT 27°F

OC-N-27-128A
OC-N-27-128B
OC-N-27-128C

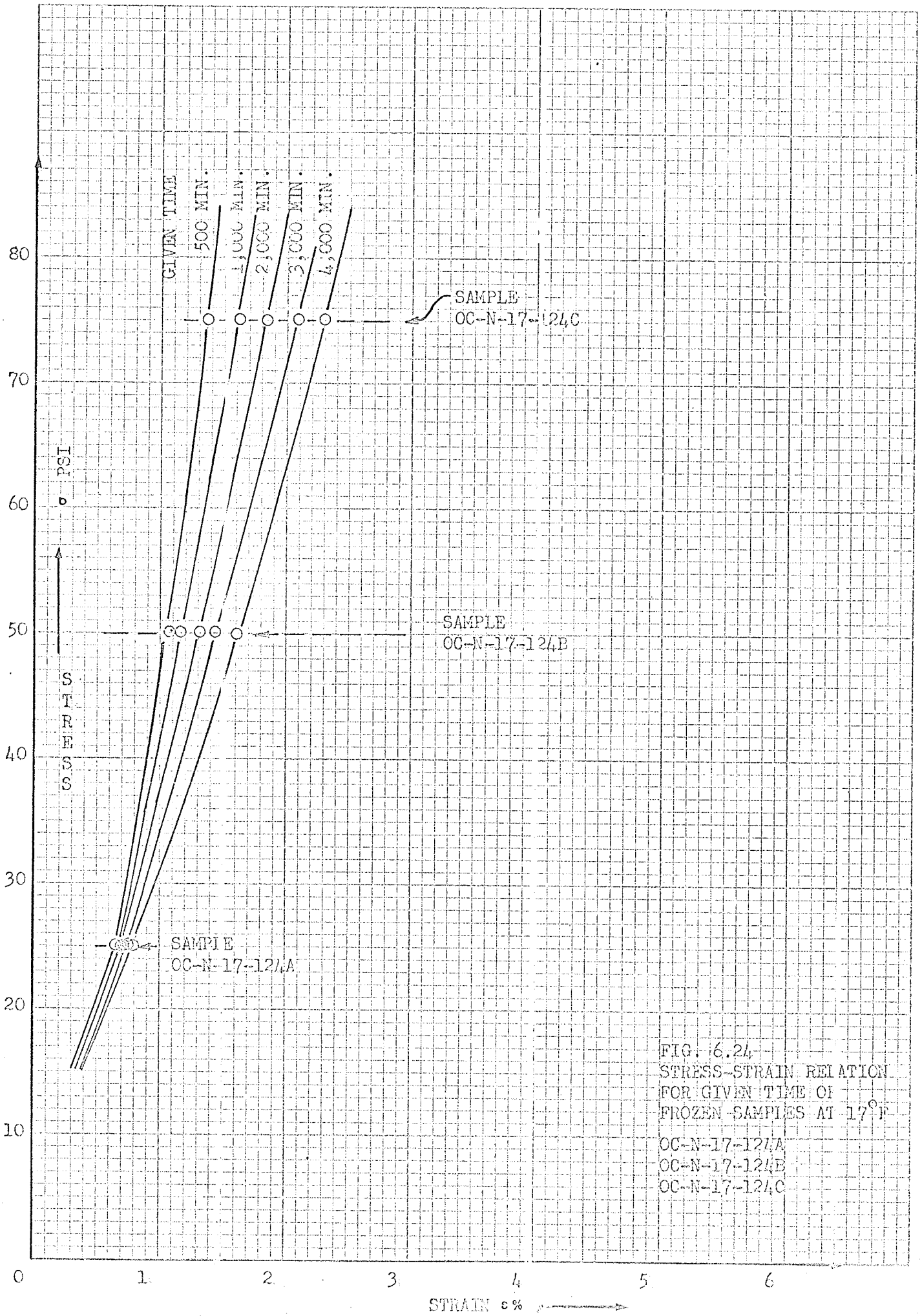

FIG. 6.24
STRESS-STRAIN RELATION FOR GIVEN TIME OF FROZEN SAMPLES AT 17°F

OC-N-17-124A
OC-N-17-124B
OC-N-17-124C

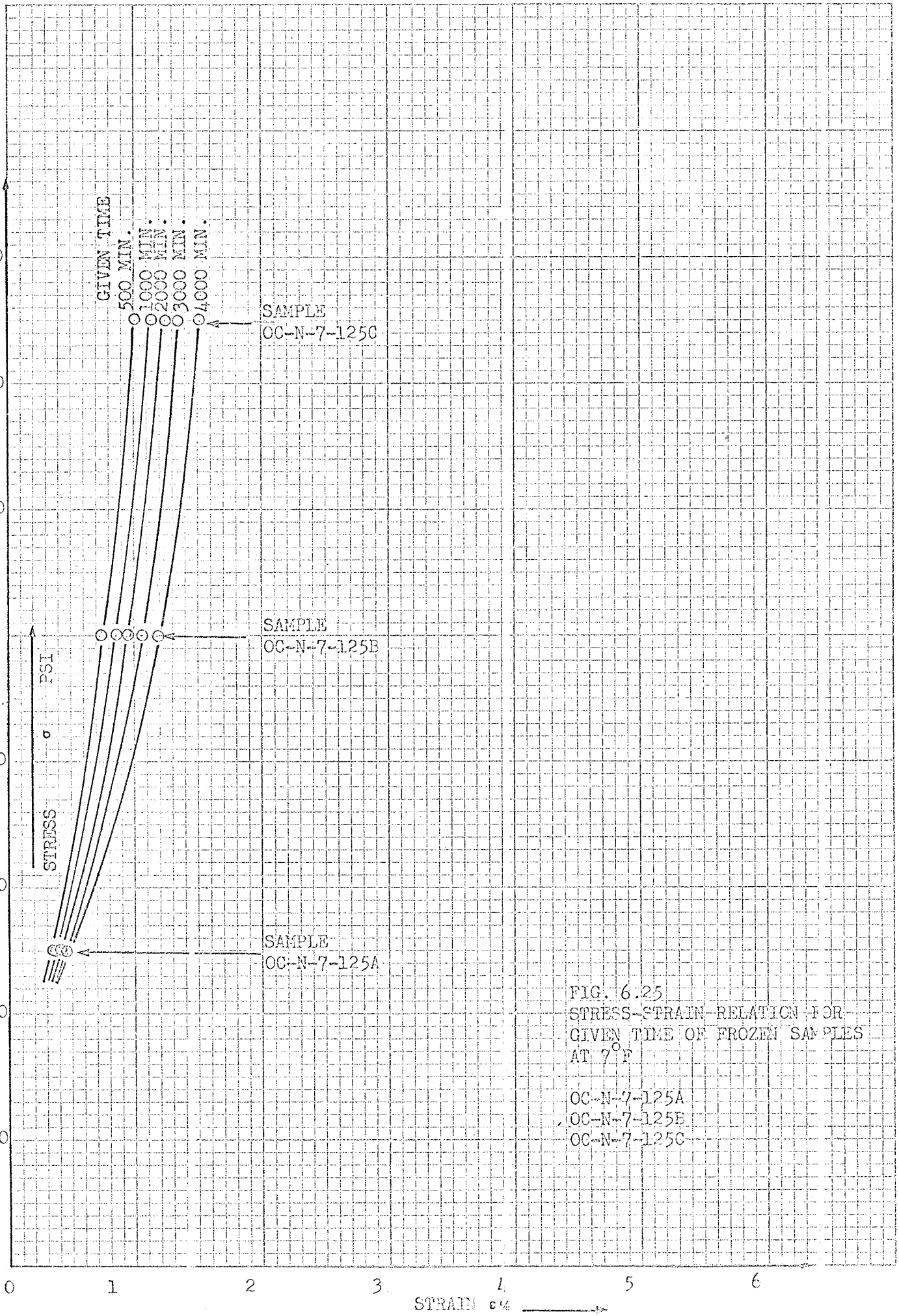

FIG. 6.25
STRESS-STRAIN RELATION FOR GIVEN TIME OF FROZEN SAMPLES AT 7° F

OC-N-7-125A
OC-N-7-125B
OC-N-7-125C

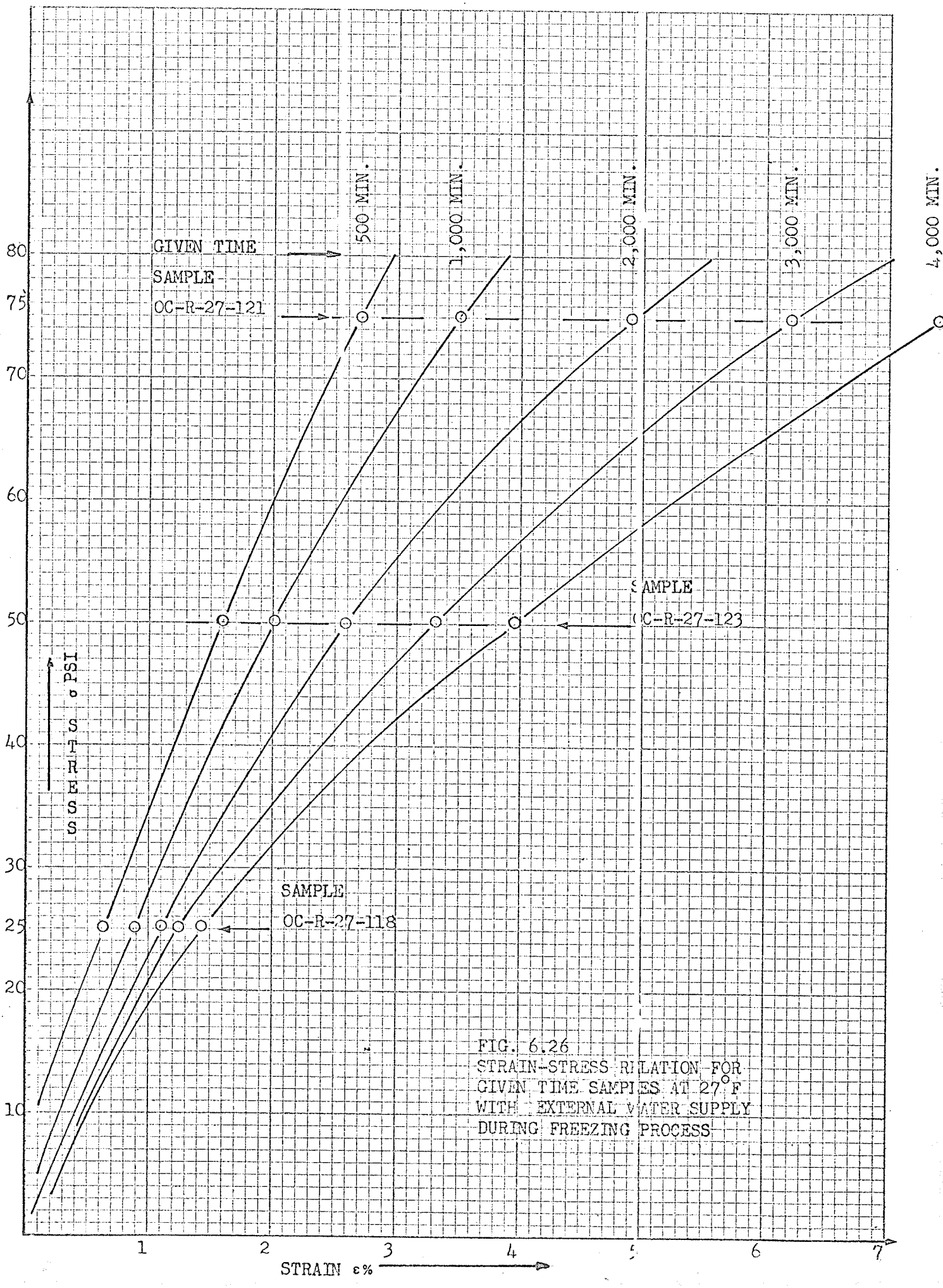

FIG. 6.26
STRAIN-STRESS RELATION FOR GIVEN TIME SAMPLES AT 27°F WITH EXTERNAL WATER SUPPLY DURING FREEZING PROCESS

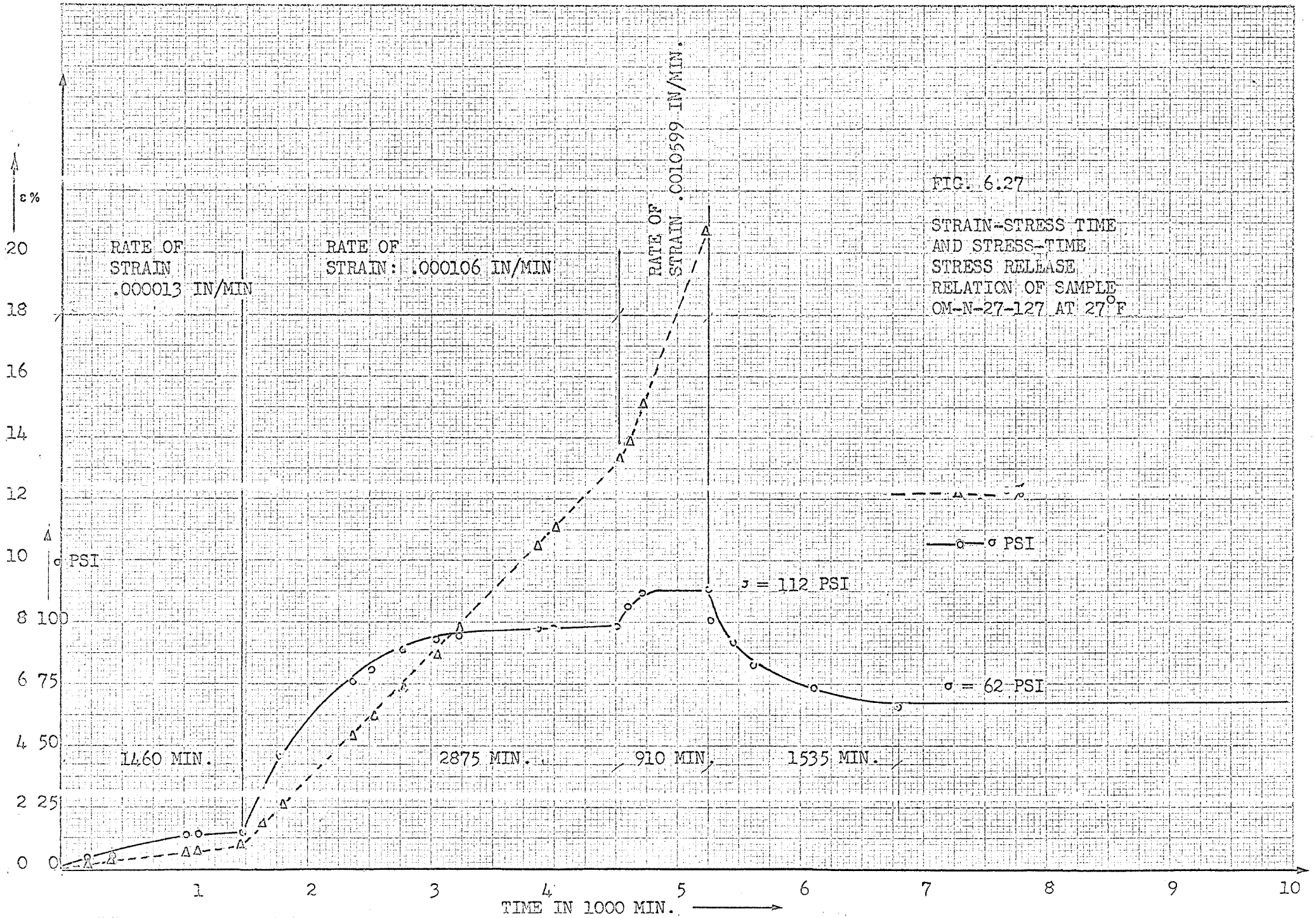
FIG. 6.27
STRAIN-STRESS TIME AND STRESS-TIME STRESS RELEASE RELATION OF SAMPLE OM-N-27-127 AT 27°F
RATE OF STRAIN .000013 IN/MIN
RATE OF STRAIN : .000106 IN/MIN
RATE OF STRAIN .0010599 IN/MIN.
ε%
σ PSI
σ = 112 PSI
σ = 62 PSI
1460 MIN.
2875 MIN.
910 MIN.
1535 MIN.
TIME IN 1000 MIN.
0
2 25
4 50
6 75
8 100
10
12
14
16
18
20
1
2
3
4
5
6
7
8
9
10

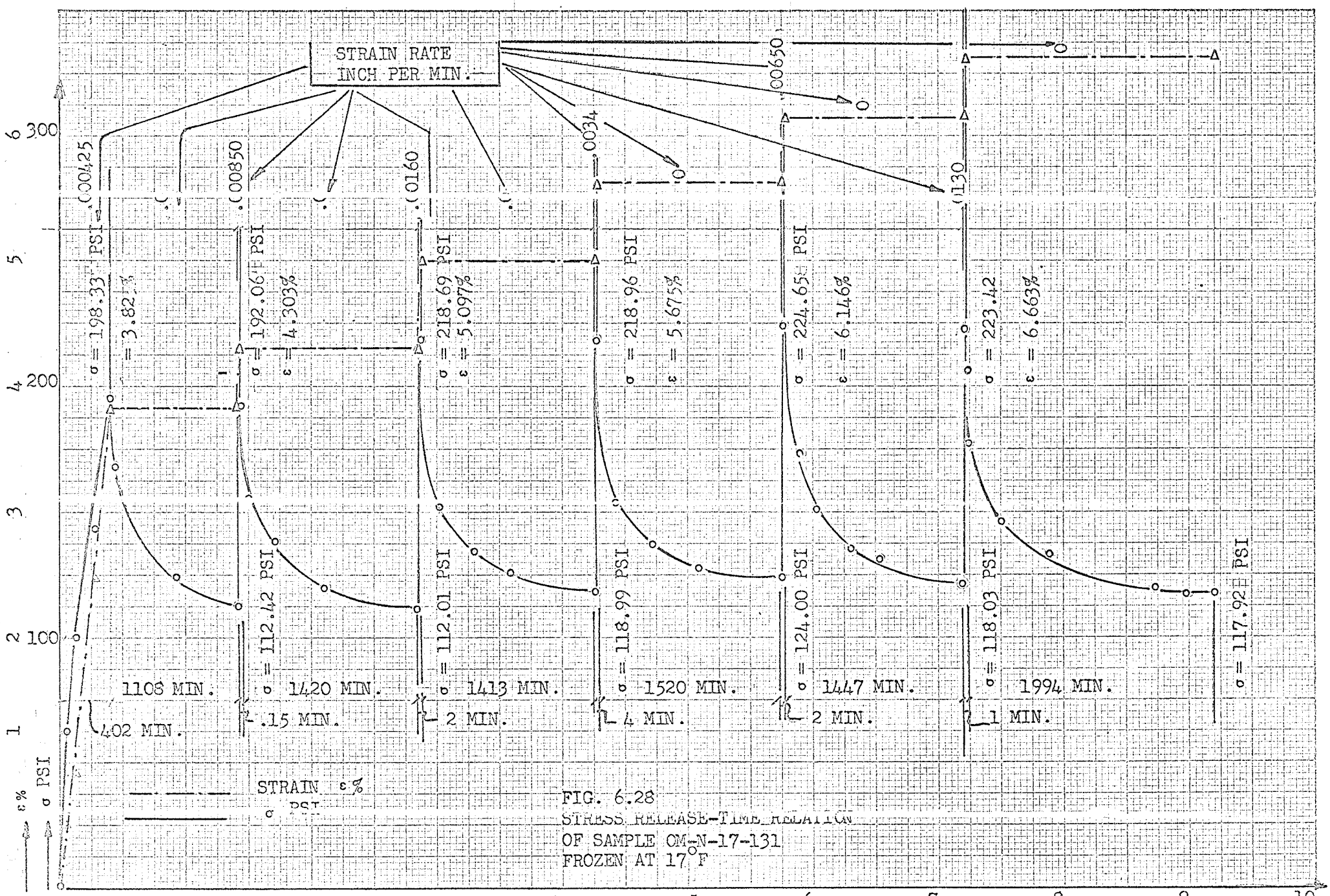

FIG. 6.28
STRESS RELEASE-TIME RELATION
OF SAMPLE OM-N-17-131
FROZEN AT 17°F

6.26 Finally for answers to the questions:

1) Had the freezing and subsequent thawing altered the properties of the clay and in what manner?

2) Did freezing alter the structure of clay?

3) What is the cause of loss of strength?

The conclusions reached will apply to the freezing and loading conditions and dimensions of soil samples used in this investigation only. Further research should be carried out to determine the validity of these results for samples of any other dimensions and for any other freezing and loading conditions.

The experiments have definitely shown that withdrawal or redistribution of moisture produces layers of ice which crystallize perpendicular to the heat flow direction and columnar ice sheets parallel to the heat flow direction, when the soil samples are uniaxially frozen. This ice segregation leads to further densification of soil particles causing cohesional strengthening, (see paragraphs 5.2, 5.8). When the sample is thawed, the ice lenses and ice layers in horizontal and vertical directions (see Photograph 6.2), turn to free water between the colony of densified mineral particles, thus causing total loss of strength. If the freezing is, however, applied from all directions, the soil is forced to expand not only in one direction, as was the case with uniaxial freeze. It will expand in three directions or six fronts,

that is, two fronts in each of the X, Y and Z directions. The samples will completely freeze much more rapidly.

The expansion of frozen soil in X, Y and Z directions is not restricted during the initial freezing period. The samples at this stage could expand in the direction of heat flow (see paragraph 5.2). However, as the freezing penetrates deeper a rigid zone of frozen soil is built up, thus restricting the inner zone from expanding (see Fig. 6.29).

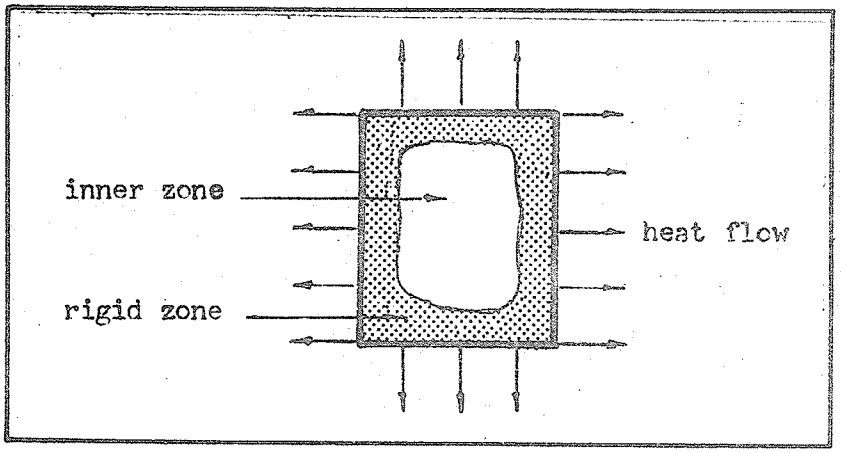

Fig. 6.29 Rigid zone buildup by allaround freezing.

The strength of both undisturbed and remolded thawed soil specimens, following all around freezing has shown values approximately equal to unfrozen remolded soil strengths (see Paragraph 6.23). The extra rapid freezing caused by application of all around freezing and the buildup of a rigid envelope around the soil specimen allows the sample to freeze with restricted change in volume and with limited moisture redistribution or ice segregation.

Consequently there is little if any change in density. The strength weakening of thawed soil could be explained by Terzaghi's (22) phenomenon of loss of strength (see paragraph 5.39) as follows: The pore water has partially frozen and ice crystals have formed, with their optical axes oriented parallel to the direction of the heat flow. The expansion due to the crystallization was large enough to destroy the binding effect between soil particles resulting in a wider separation of particles and loss of strength (see figure 5.11 b and c).

CHAPTER VII

CONCLUSIONS

CHAPTER VII

CONCLUSIONS

A. EQUIPMENT AND INSTRUMENTATION

7.1 The heat exchange box and freezing cell fabricated for this work have performed well. Uniaxial freezing was achieved with or without external water supply to the sample being frozen.

Use of the heat exchange box and freezing cell allows one to alter the freezing temperature in a few hours, as compared with a walk-in cold room which takes at least two days to establish equilibrium in addition to the following disadvantages:

(a) Expensive to build in comparison with the equipment designed for this work.

(b) Variation of the thermostatically controlled temperature of walk-in cold room is $-1^{o}F$ as compared with $-0.5^{o}F$ in the present work (See 7.2).

(c) Personal observation of some walk-in cold rooms reveals a loss of efficiency due to icing conditions not only in the cold room but in the freezing unit component as well. The efficiency drops in one week and the entire unit becomes inoperative after two weeks and requires defrosting. Thus test times are severely limited to a maximum of two weeks.

By using vapor barriers inside and around the freezing cell it was possible to operate this system for any length of time.

(d) At small expense one can fabricate several freezing cells and operate them at a variety of temperature. A variety of tests under various temperatures can be conducted simultaneously.

(e) Uniaxial freezing and thawing could be obtained without removing the sample from the freezing cell or changing the position of the sample for any number of cycles of freezing and thawing.

Also, temperatures down to $-92^{o}F$ were attained and soil samples were frozen to $-92^{o}F$ by the writer, using dry ice in addition to the mechanical freezing unit.

7.2 Installing thermostats with greater sensitivity would minimize temperature fluctuation intervals and provide an opportunity to study the freezing phenomena when temperatures of frozen soils are set up very close to $32^{o}F$.

B. FREEZING AND MECHANICAL BEHAVIOR OF FROZEN LAKE AGASSIZ CLAY

7.3 Lake Agassiz clay is frost susceptible when water is supplied parallel to the varves. The varves provide a more permeable path for water to reach the freezing front.

7.4 Soil frozen at a slow freezing rate was found to have a greater rate of deformation under constant load than soil frozen at a higher rate of freezing where all other conditions such as moisture content, temperature and stress are equal.

7.5 In comparing samples frozen with:

(a) external water supplied

(b) no external water supplied,

it was found that (a) gave thicker, non-uniformly distributed ice lenses, whereas (b) gave more uniformly distributed thinner ice lenses. Under equal temperature and stress conditions, (a) gave higher strain rates.

7.6 At 31.5^{o}F the strength of soils tested was found to be approximately the same as unfrozen soil.

7.7 The strength of "never" frozen, undisturbed soil when frozen from all directions was reduced when thawed to approximately 43% of its original undisturbed strength following one cycle of freezing. The strength of "never" frozen remolded (to its original density and moisture content) soils when frozen from all around was reduced to approximately 76 per cent, when thawed following the first freezing cycle.

The uniaxially frozen soils, however, failed to show any strength following the thaw-out after the first cycle of freezing.

7.8 Young's modulus for the unfrozen soils tested was approximately constant. It was independent of temperature and ice content in the ranges tested. The value of Young's modulus of frozen soil tested was found to be

$$E = 165 \times 10^{-2} \text{ to } 180 \times 10^{-2} \text{ psi.}$$

7.9 The duration of deformation at decelerating rate of strain (retarded strain) of frozen soil tested increased linearly with increasing temperature at a given stress level (Fig. 6.17). The strain rate decreases with lower temperatures, and appears to become zero in a non-linear fashion. (Fig. 6.19)

7.10 The constant rate of strain of frozen soils decreases sharply with the lowering of temperature.

7.11 The internal ice content of frozen soil subject to cycled stress or strain decreased as ice formed on the surface. This surface ice buildup is due to a squeezing out of ice in liquid form as a result of stress concentration at the contacts between mineral particles and ice crystals. The movement of ice away from the regions of stress concentration toward the surface of the sample (where stress is minimum) produces further densification of frozen soils resulting in increased viscosity and consequently increase of relaxation time.

BIBLIOGRAPHY

BIBLIOGRAPHY

1. Johnston, W.A. 1934. "Surface Deposits and Ground Water Supply of Winnipeg Map Area, Manitoba." Canada Department of Mines, Bureau of Economic Geology, Geological Survey, Memoir 174, pp. 2.

2. Ehrlich, W.A., Poyser, E.A., Pratt, L.E., and Ellis, J.H. 1953. "Report Reconnaissance Soil Survey of Winnipeg and Morris Map Sheet Area." Manitoba Soil Survey, Soil Report No. 5, pp. 3 & 4.

3. Riddell, W.F. 1949. "Foundation Conditions in Winnipeg and Immediate Vicinity." Proceedings of 1949 Civilian Soil Mechanics Conference, Lethbridge, Alberta. Technical Memorandum No. 17, pp. 3-9. National Research Council, Ottawa, Canada.

4. Baracos, A. 1960. "The Stability of River Banks in the Metropolitan Winnipeg Area". Proc. 14th Canadian Soil Mechanics Conference, Niagara Falls, Ontario, October, 1960 (NRC Technical Memorandum No. 69)

5. "Procedure for Testing Soils, 1964." American Society for Testing and Materials. 1916 Race Street, Philadelphia 3., Pa., U.S.A.

6. Penner, E. 1959. "The Mechanics of Frost Heaving in Soils." Research Paper No. 87 of Division of Building Research. National Research Council, Ottawa, Canada.

7. Nielsen and Rauschenberger. 1962. "Frost and Foundations". Technical Translation 1021. National Research Council of Canada. Ottawa, Canada.

8. Taber, S. 1929. "Frost Heaving." Journal of Geology. University of Chicago Press. Chicago, U.S.A.

9. Terzaghi, C. 1925. "Principles of Soil Mechanics". Engineering News. Vol. XCV, pp. 796-800.

10. Penner. 1962. "Frost Heave." Canadian Building Digest. National Research Council. D.B.R., CBC. 26. Ottawa, Canada.

11. Taber, S. 1930. "The Mechanics of Frost Heaving." Journal of Geology. University of Chicago Press. Chicago, U.S.A.

12. Osler, J.C. McGill University, Montreal, 1967. "The Influence of Depth of Frost Penetration on the Frost Susceptibility of Soils." Canadian Geotechnical Journal, Vol. IV, No. 3, pp. 340. National Research Council and Geotechnical Engineering Institute of Canada.

13. Schaible, Lothar. 1955. "Die Bautechnik." 31(9), pp. 28-292-2954. National Research Council of Canada, Technical Translation. No. 568. Ottawa, Canada.

14. Kachurin, S.P. 1964. National Research Council Technical Translation No. 1157, pp. 5.

15. Terzaghi, K. and Pede, R.B. 1948. "Soil Mechanics in Engineering Practice." pp. 132. New York, John Wiley and Sons, Inc. U.S.A.

16. Tsytovich, et al. National Research Council, Technical Translation. No. 1239. Ottawa, Canada.

17. Proceedings Permafrost International Conference No. 1963, pp. 231 & 317. Publication No. 1287. National Academy of Science, National Research Council. Washington, D.C. 20418, U.S.A.

18. Williams, P.J. 1964. Specific heat and unfrozen water content of frozen soils. Geotechnique, Volume XIV, No. 3. The Institution of Civil Engineering. Great George Street, London, S.W. 1, Great Britain.

19. Yong, R. 1962. Research of fundamental properties and characteristics of frozen soils. First Canadian Conference on Permafrost. Technical Memorandum No. 76, pp. 84. National Research Council of Canada. Ottawa, January, 1963.

20. Condon, E.U., Odishaw, H., and Reiner, M. "Handbook of Physics." McGraw - Hill Book Co., Inc., New York, Toronto, London, pp. 3 - 42.

21. Parsons, R.C. and Hedley, G.F. 1967. "The Analysis of the Viscous Property of Rocks for Classification." Reprinted from Int. J. Rock Mech. Min. Sci. Vol. 3, pp. 325-335. Queen's Printer and Controller of Stationery. Ottawa, Canada.

22. Taylor, D.W. 1962. "Fundamentals of Soil Mechanics." John Wiley and Sons, Inc. New York, London, pp. 63.

23. Polakowsky, N.H. and Ripling, E.J. 1966. "Strength and Structure of Engineering Materials." Englewood, Cliffs, New Jersey.